



UNIL | Université de Lausanne

Unicentre

CH-1015 Lausanne

<http://serval.unil.ch>

Year : 2019

Identification and characterization of mediators of fluconazole tolerance in *Candida albicans*

Delarze Eric

Delarze Eric, 2019, Identification and characterization of mediators of fluconazole tolerance in *Candida albicans*

Originally published at : Thesis, University of Lausanne

Posted at the University of Lausanne Open Archive <http://serval.unil.ch>

Document URN : urn:nbn:ch:serval-BIB_8F7CFB67F3DF9

Droits d'auteur

L'Université de Lausanne attire expressément l'attention des utilisateurs sur le fait que tous les documents publiés dans l'Archive SERVAL sont protégés par le droit d'auteur, conformément à la loi fédérale sur le droit d'auteur et les droits voisins (LDA). A ce titre, il est indispensable d'obtenir le consentement préalable de l'auteur et/ou de l'éditeur avant toute utilisation d'une oeuvre ou d'une partie d'une oeuvre ne relevant pas d'une utilisation à des fins personnelles au sens de la LDA (art. 19, al. 1 lettre a). A défaut, tout contrevenant s'expose aux sanctions prévues par cette loi. Nous déclinons toute responsabilité en la matière.

Copyright

The University of Lausanne expressly draws the attention of users to the fact that all documents published in the SERVAL Archive are protected by copyright in accordance with federal law on copyright and similar rights (LDA). Accordingly it is indispensable to obtain prior consent from the author and/or publisher before any use of a work or part of a work for purposes other than personal use within the meaning of LDA (art. 19, para. 1 letter a). Failure to do so will expose offenders to the sanctions laid down by this law. We accept no liability in this respect.



UNIL | Université de Lausanne

Faculté de biologie
et de médecine

Institute of Microbiology, University of Lausanne and University Hospital of
Lausanne, Switzerland

Identification and characterization of mediators of fluconazole tolerance in *Candida albicans*

Thèse de doctorat ès sciences de la vie (PhD)

présentée à la

Faculté de biologie et de médecine
de l'Université de Lausanne

par

Eric DELARZE

Master de l'Université de Lausanne

Jury

Prof. Thierry Pedrazzini, President
Prof. Dominique Sanglard, Thesis Director
Prof. Murielle Cornet, Expert
Prof. Maurizio Sanguinetti, Expert

Lausanne
2019



UNIL | Université de Lausanne

Faculté de biologie
et de médecine

Institute of Microbiology, University of Lausanne and University Hospital of
Lausanne, Switzerland

Identification and characterization of mediators of fluconazole tolerance in *Candida albicans*

Thèse de doctorat ès sciences de la vie (PhD)

présentée à la

Faculté de biologie et de médecine
de l'Université de Lausanne

par

Eric DELARZE

Master de l'Université de Lausanne

Jury

Prof. Thierry Pedrazzini, President
Prof. Dominique Sanglard, Thesis Director
Prof. Murielle Cornet, Expert
Prof. Maurizio Sanguinetti, Expert

Lausanne
2019

Imprimatur

Vu le rapport présenté par le jury d'examen, composé de

Président·e	Monsieur	Prof.	Thierry	Pedrazzini
Directeur·trice de thèse	Monsieur	Prof.	Dominique	Sanglard
Expert·e·s	Madame	Prof.	Murielle	Cornet
	Monsieur	Prof.	Maurizio	Sanguinetti

le Conseil de Faculté autorise l'impression de la thèse de

Monsieur Eric Delarze

Master en sciences moléculaires du vivant, Université de Lausanne

intitulée

**Identification and characterization of mediators of
fluconazole tolerance in *Candida albicans***

Lausanne, le 28 juin 2019

pour le Doyen
de la Faculté de biologie et de médecine

Prof.  Thierry Pedrazzini

Acknowledgements

I would like to thank first the Swiss National Foundation for the financial support of this project.

I also thank Dominique for accepting me into his laboratory and for his support during the project and his proactivity during the redaction of this thesis.

I also want to thank some people for their support and role in this work:

First of all, the Team Tolerance for their investment in the project with, in order of slavery service:

- Fabio who did a tremendous work and, even if he was much older than myself, was like a son to me.
- Claire and Laetitia who had the chance to share my benevolence and tried to bribe me to know who my favorite was.
- And finally, Ludivine who, despite my absence due to the redaction of this thesis, did a great work and help to conclude this project.

The old Sanglard's team with Stéphane, Luís, and more especially my two mommies Alix and Françoise and my lab-sister Sara, who taught me everything I know and for their support and counsels at the beginning of this thesis and after.

The two other Master students at that time, Marion P. and Tiia who made Fabio and me discover great music... and who shared the burden of taking care of our beloved *Galleria*. Extra thank to Marion who wrote the script for the enrichment analysis that I would never have been able to do by myself.

The new team fungus with Sanne, Abhilash, Ludivine, Margot, Emilie, Danielle and Marion A., not only for their support during this project, but also and mainly for the good times, the trips to Lyon, Barcelona and Iceland, and more locally, the visit of Gruyères, the Celtic Festival, the murder party and the open cellars among others. I wish all of them all the best for their future.

Additional thank to Marion A., who made me understand that there is no shame to engulf 40 sushi pieces all alone, for the psychological follow-up since she arrived and for the drink and food support for a poor jobless PhD student. There will always be a special place in my heart for you.

Amanda and Luca who made me discover and love many whiskies and rums. But also, for their good music taste, the concerts, the hikes, the dinners, the beers and all the good times passed together. And, of course, for giving me the occasion to practice lucha libre with a senile cat during an amazing cat-sitting.

Laetitia, who was able to motivate me to do sport... for a time... For the hikes full of marmots, for both the 5 a.m. and midnight runs, for her love of the mountain and her amazing "sense of humor". May you find the light in Bern.

Claire, who made me realize that nice people exist in Valais, who was always elegant, even while playing bowling and who made me understand that there are never enough perfumed candles in one's life. I wish you all the best dealing with your new room-mate.

Aurélië, who sold me her sister in exchange of good treatment, who shares my love of cooking and for sticking together against the adversity at the student association.

Aline, Nathalie, Jessica, Alain and Thomas from the Biologist Team, who can bear me since the Bachelor and with whom I had memorable nights.

Of course, my family who, even if I was not present a lot for them during these past few years, support me until the end, despite not really understanding what I was doing with my life.

And finally, a few special thanks. First to Claire, Laëticia and Marion A. for their support in difficult times and second to Aline and Carmen who accepted me when I was deskless and without whom I wouldn't have been able to finish writing this thesis.

Abstract

Candida spp. are major human pathogens and a major issue in intensive care units around the world. *Candida* infections have a high mortality rate despite the use of antifungal treatments. One cause of these therapeutic failures is the acquisition of mutations in the fungus leading to antifungal resistance. In the case of the fungistatic azole drug fluconazole (FLC), the mechanisms of resistance have been extensively studied in the past. However, some clinical isolates are known to be able to survive at high FLC concentrations without acquiring resistance mutations. This phenomenon is attributed to antifungal tolerance. Mechanisms behind FLC tolerance are still understudied, mainly due to the lack of proper way to identify and quantify tolerance between isolates. In this study, we first attempted to better define and characterize antifungal tolerance in *Candida albicans* by establishing a convenient quantification method and proposing thresholds allowing a better discrimination of tolerance between isolates. Next, we implemented this method and definition in order to identify mediators of tolerance using a collection of approximately 580 doxycycline-dependent overexpression (OE) *C. albicans* strains, each of which overexpressing a specific *C. albicans* gene. By pooling the whole collection and maintenance under FLC pressure, we were able to enrich the pool in FLC-tolerant strains which were further characterized. Among tested strains, three of them, overexpressing either *CRZ1*, *GZF3* or *YCK2* resulted in an increased FLC tolerance in presence of doxycycline. However, only the *CRZ1* and *GZF3* OE strains reached the threshold of tolerance. These two genes were further confirmed to be involved in FLC tolerance as their deletion in known tolerant clinical isolates resulted in a decrease of tolerance. Furthermore, we showed that Gzf3 was likely acting downstream of Crz1 since *CRZ1* OE in absence of *GZF3* resulted in an increased tolerance, which was not the case of *GZF3* OE in absence of *CRZ1*. In addition, using a transcriptomic approach, we showed that *CRZ1* might play a role in the tolerance of clinical isolates as it was overexpressed as compared to the wild type susceptible strain SC5314 in presence of FLC. Overall, this study allowed a better definition of tolerance and gave new insights of the mechanisms behind this phenomenon. This study established novel approaches for the identification of genetic mediators of tolerance as well as a convenient testing of tolerance in large strain collections.

Résumé

Les espèces *Candida* sont des pathogènes humains importants et un problème majeur dans les unités de soins intensifs du monde entier. Les infections à *Candida* possèdent un taux de mortalité élevé malgré la présence de traitements antifongiques. L'une des causes de ces échecs thérapeutiques est l'acquisition de mutations conduisant à une résistance aux antifongiques. Dans le cas du fluconazole (FLC), les mécanismes de résistance ont été largement étudiés dans le passé. Cependant, certains isolats cliniques sont capables de survivre à des concentrations élevées de FLC sans acquérir ou développer de résistance ; un phénomène connu sous le nom de tolérance. Les mécanismes à l'origine de la tolérance au FLC sont encore peu étudiés, principalement en raison de l'absence de méthode appropriée pour identifier et quantifier la tolérance. Dans cette étude, nous avons d'abord essayé de mieux définir et caractériser la tolérance en proposant une méthode de quantification et des seuils appropriés permettant une meilleure discrimination entre isolats. Puis, nous avons utilisé cette méthode et définition afin d'identifier de nouveaux médiateurs de la tolérance à l'aide d'une collection d'environ 580 souches, chacune surexprimant un gène spécifique en présence de doxycycline (Dox). En regroupant la totalité de la collection en une seule population et en maintenant une sélection en présence de FLC, nous avons pu enrichir la population en souches résistantes et/ou tolérantes. Après analyse de ces dernières, trois d'entre elles, surexprimant *CRZ1*, *GZF3* et *YCK2*, respectivement, ont montré une tolérance accrue en présence de Dox et de FLC. Cependant, seules les souches surexprimant *CRZ1* et *GZF3* ont atteint notre limite inférieure de tolérance. En délétant ces gènes dans des isolats cliniques tolérants, nous avons pu confirmer leurs rôles dans ce phénotype, démontrer par la perte de tolérance découlant de ces délétions. *Gzf3* fût aussi déterminé comme se trouvant en aval de *Crz1* dans la réponse au FLC, comme la surexpression de *CRZ1* en l'absence de *GZF3* entraînait une augmentation de la tolérance, ce qui n'était pas le cas de *GZF3* en l'absence de *CRZ1*. Finalement, utilisant une approche transcriptomique, nous avons démontré que *CRZ1* pouvait jouer un rôle dans la tolérance des isolats cliniques, celui-ci étant surexprimé par rapport à la souche sauvage SC5314 en présence de FLC. En résumé, cette étude a permis de donner une meilleure définition au phénomène de tolérance, tout en proposant de nouveaux médiateurs de cette réponse au FLC. Cette étude a aussi permis le développement de nouvelles approches, tant pour l'identification de médiateurs génétiques de la tolérance que pour l'identification de souches tolérantes en utilisant de larges collections de souches.

Table of Contents

ACKNOWLEDGEMENTS	I
ABSTRACT	III
RÉSUMÉ	V
TABLE OF CONTENTS	VII
LIST OF ABBREVIATIONS.....	X
LIST OF FIGURES	XI
LIST OF TABLES	XII
LIST OF SUPPLEMENTARY ELEMENTS	XIII
LIST OF SUPPLEMENTARY FIGURES	XIII
LIST OF SUPPLEMENTARY TABLES	XIII
LIST OF SUPPLEMENTARY FILES	XIII
GENERAL INTRODUCTION	1
<i>CANDIDA</i> SPP. AND THEIR RELEVANCE AS HUMAN PATHOGENS	1
<i>CANDIDA ALBICANS</i>	5
AVAILABILITY AND LIMITATIONS OF CURRENT ANTIFUNGAL THERAPIES	9
<i>Inhibitors of nucleic acid synthesis</i>	12
<i>Fungal membrane disruptors</i>	14
<i>Inhibitors of fungal cell wall synthesis</i>	16
<i>Inhibitors of ergosterol biosynthesis</i>	19
<i>Resistance mechanisms to azoles</i>	23
ANTIFUNGAL SUSCEPTIBILITY ASSAYS.....	27
ANTIFUNGAL TOLERANCE: DEFINITIONS, RELEVANCE AND KNOWN MECHANISMS	32
DEFINITION OF TOLERANCE TO ANTIFUNGALS.....	32
KNOWN MECHANISMS INVOLVED IN FLC TOLERANCE IN <i>C. ALBICANS</i>	34
AIMS OF THIS WORK	37
SUMMARY OF MAIN FINDINGS	38
PART ONE: IMPLEMENTATION OF A TOLERANCE INDEX FOR THE STUDY AND QUANTIFICATION OF TOLERANCE TO FLUCONAZOLE IN <i>CANDIDA ALBICANS</i>.	40
ABSTRACT	40
INTRODUCTION	41
MATERIAL AND METHODS	43
<i>Strains used in this study</i>	43
<i>Media and growth conditions</i>	44
<i>FLC susceptibility and tolerance assays</i>	44
<i>Growth curve</i>	45
<i>Software and statistical analysis</i>	46
RESULTS.....	47
<i>Determination of optimal culture condition for FLC tolerance identification</i>	47
<i>Establishment of a tolerance index and tolerance thresholds</i>	49
<i>Selection of culture conditions for the identification of tolerance</i>	50
<i>Application of the tolerance assay for the identification of tolerant strains</i>	52
CONCLUSIONS.....	55

PART TWO: IDENTIFICATION AND CHARACTERIZATION OF THE TRANSCRIPTION FACTORS *CRZ1* AND *GZF3* AS MEDIATORS OF TOLERANCE TO FLUCONAZOLE IN *C. ALBICANS*. 59

ABSTRACT	59
INTRODUCTION	60
MATERIAL AND METHODS	61
<i>Strains used in this study</i>	61
<i>Media and growth conditions</i>	67
<i>Primers and plasmids</i>	67
<i>Yeast transformation</i>	68
<i>Construction of Deletion Mutants and Revertant Strains</i>	68
<i>Determination of optimal Dox concentration for OE</i>	70
<i>Iron compensation of the FLC-Dox synergistic effect</i>	70
<i>FLC susceptibility and tolerance assays</i>	71
<i>Calcium induction of tolerance</i>	72
<i>Pool enrichment in tolerant/resistant strains</i>	72
<i>Genomic DNA extraction</i>	73
<i>Amplification of the barcodes</i>	74
<i>Library preparation and sequencing</i>	74
<i>Barcode quantification</i>	74
<i>Software and statistical analysis</i>	75
RESULTS	76
<i>Identification of optimal OE culture conditions</i>	76
<i>Enrichment in resistant/tolerant OE strains in pool assay</i>	79
<i>Single strain FLC tolerance profiling</i>	84
<i>Putative negative regulators of tolerance</i>	86
<i>Putative positive regulators of tolerance</i>	93
CONCLUSIONS	104

PART THREE: TRANSCRIPTOMIC IMPRINTS OF FLUCONAZOLE RESPONSE IN THE WILD TYPE STRAIN SC5314 AND TOLERANT CLINICAL ISOLATES. 110

ABSTRACT	110
INTRODUCTION	112
MATERIAL AND METHODS	114
<i>Strains used in this study</i>	114
<i>Media and growth conditions</i>	114
<i>RNA extraction</i>	115
<i>DNase treatment</i>	116
<i>Determination of RNA quality</i>	116
<i>RNA sequencing and RNAseq data mining</i>	116
RESULTS	118
<i>Transcriptional profile of SC5314 in the presence of FLC</i>	118
<i>Transcriptional profiles of clinical strains in the presence of FLC</i>	125
CONCLUSIONS	132

GENERAL DISCUSSION AND FUTURE PERSPECTIVES: 135

DEFINING FLC TOLERANCE	135
DISCOVERY OF NOVEL FLC TOLERANCE MEDIATORS	136
NEXT STEPS IN UNDERSTANDING OF FLC TOLERANCE	137
TRANSCRIPTOMIC IMPRINTS OF FLC RESPONSE IN TOLERANT CLINICAL ISOLATES	138

BIBLIOGRAPHY	140
---------------------------	------------

List of Abbreviations

5-FC	Flucytosine	ICU	Intensive Care Unit
5-FU	5-Fluorouracil	IE	Insufficient Evidences
5-FUMP	5-Fluorodeoxyuridine Monophosphate	ITC	Itraconazole
5-FUTP	5-Fluorodeoxyuridine Triphosphate	IV	Intravenous
ABC	ATP-Binding Cassette	LOH	Loss of Heterozygosity
AFG	Anidulafungin	MFG	Micafungin
AIDS	Acquired Immune Deficiency Syndrome	MIC	Minimum Inhibitory Concentration
AMB	Amphotericin B	MLST	Multi Locus Sequence Typing
AMPR	Ampicillin Resistance	MOPS	3-(N-Morpholino) Propanesulfonic Acid
BC	Barcode	NAM	North America
BSI	Blood Stream Infection	NOUR	Nourseothricin
CAMR	Chloramphenicol Resistance	O/N	Overnight
CAS	Caspofungin	OD	Optical Density
CBP	Clinical Breakpoints	OE	Overexpression
CI	Confidence Interval	PBS	Phosphate Buffered Solution
CLSI	Clinical & Laboratory Standards Institute	PO	Per Os
CSM	Complete Supplement Mixture	PSZ	Posaconazole
CTZ	Coelenterazine	PVC	Pre-Vacuolar Compartment
DEPC	Diethyl pyrocarbonate	RIN	RNA Integrity Number
DN	Downregulated	RNA	Ribonucleic Acid
DNA	Deoxyribonucleic Acid	ROS	Reactive Oxygen Species
DOX/D	Doxycycline	RPM	Revolution Per Minute
EDTA	Ethylenediaminetetraacetic acid	RPMI	Roswell Park Memorial Institute Medium
ETOH	Ethanol	RT	Room Temperature
EU	Europe	RV	Reverse
EUCAST	European Committee on Antimicrobial Susceptibility Testing	SDS	Sodium Dodecyl Sulfate
FDR	False Discovery Rate	SSI	Statens Serum Institute
FLC/F	Fluconazole	STDEV	Standard Deviation
FOA	5-Fluoro-Orotic Acid	TE	Tris-EDTA
FWD	Forward	TET	Tetracycline
GC	Growth Control	TF	Transcription Factor
GI	Gastro Intestinal	TI	Tolerance Index
GO	Gene Ontology	TR	Tolerance Ratio
GOI	Gene of Interest	UMP	Uracil Monophosphate
GSEA	Gene Set Enrichment Analysis	UP	Upregulated
GTP	Guanosine Triphosphate	URA	Uracil
GTW	Gateway	VCZ	Voriconazole
HAART	Highly Active Antiretroviral Therapy	WT	Wild type
		YEP	Yeast Extract Peptone
		YEPD	Yeast Extract Peptone Dextrose
		YNB	Yeast Nitrogen Base

List of Figures

FIGURE 1: <i>CANDIDA</i> SPP. DISTRIBUTION OVER THE LAST DECADES.	2
FIGURE 2: ROLE OF ANTIFUNGAL PROPHYLAXIS UPON <i>CANDIDA</i> SPP. DISTRIBUTION.	4
FIGURE 3: MORPHOLOGICAL FORMS OF <i>C. ALBICANS</i>	5
FIGURE 4: ROUTES OF <i>CANDIDA</i> INFECTION AND DISSEMINATION.	7
FIGURE 5: <i>C. ALBICANS</i> CELL AND THE FIVE MAJOR ANTIFUNGAL CLASSES WITH THEIR RESPECTIVE TARGETS.	9
FIGURE 6: GENERAL GUIDELINES FOR CANDIDEMIA TREATMENT.	12
FIGURE 7: PYRIMIDINE ANALOGS.	13
FIGURE 8: POLYENES.	15
FIGURE 9: ERGOSTEROL PATHWAY IN <i>C. ALBICANS</i>	16
FIGURE 10: ECHINOCANDINS.	18
FIGURE 11: ALLYLAMINES.	19
FIGURE 12: WORLDWIDE FLC AVAILABILITY AND PRICING IN US \$.	21
FIGURE 13: AZOLES.	22
FIGURE 14: RESISTANCE MECHANISMS OF AZOLES AND POLYENES.	24
FIGURE 15: DISTRIBUTION OF FLC MIC VALUES IN <i>C. ALBICANS</i>	30
FIGURE 16: SUSCEPTIBILITY PROFILES TO FLC ON ETEST.	33
FIGURE 17: SUSCEPTIBILITY PROFILES TO FLC IN MICRODILUTIONS ASSAY.	33
FIGURE 18: COMPARISON OF EUCAST AND CLSI CONDITIONS FOR THE IDENTIFICATION OF TOLERANT <i>C. ALBICANS</i> ISOLATES USING FLC SUSCEPTIBILITY ASSAYS.	48
FIGURE 19: IDENTIFICATION OF TOLERANT STRAINS AND DEFINITION OF TOLERANCE INDEX (TI).	50
FIGURE 20: COMPARISON OF CLSI AND EUCAST PROTOCOLS FOR THE IDENTIFICATION OF TOLERANT ISOLATES.	51
FIGURE 21: SCREENING OF CLINICAL ISOLATES AND TI DETERMINATION.	53
FIGURE 22: TOLERANCE SCREEN OF 159 <i>C. ALBICANS</i> STRAIN.	55
FIGURE 23: DOXYCYCLINE-DEPENDENT OVEREXPRESSION SYSTEM.	76
FIGURE 24: DOX EFFICIENCY AND CELL VIABILITY.	79
FIGURE 25: SUMMARIZED POOL ENRICHMENT PRINCIPLE.	80
FIGURE 26: COMPARISONS OF THE POPULATION OF THE 579-TET-INDUCIBLE OE STRAINS COLLECTION POOL AFTER 5 DAYS OF ENRICHMENT.	82
FIGURE 27: SINGLE STRAIN TOLERANCE PROFILING.	84
FIGURE 28: CALCIUM INDUCTION OF THE <i>ZPR1</i> -OE STRAIN FLC TOLERANCE.	87
FIGURE 29: SUSCEPTIBILITY PROFILES OF THE <i>ZPR1</i> -OE STRAIN.	88
FIGURE 30: TOLERANCE PROFILES OF PUTATIVE NEGATIVE REGULATORS OF FLC TOLERANCE.	89
FIGURE 31: TOLERANCE OF SELECTED CLINICAL ISOLATES.	90
FIGURE 32: TOLERANCE RATIO OF SELECTED TET-INDUCIBLE CLINICAL ISOLATES.	92
FIGURE 33: SUSCEPTIBILITY PROFILES OF SELECTED TET-INDUCIBLE STRAINS IN THE PRESENCE DOX.	94
FIGURE 34: SUSCEPTIBILITY PROFILE OF THE <i>CRZ1</i> AND <i>GZF3</i> MUTANTS OVEREXPRESSING EITHER <i>CRZ1</i> , <i>GZF3</i>	97
FIGURE 35: FLUCONAZOLE SUSCEPTIBILITY PROFILES OF THE CLINICAL ISOLATES AND THEIR RESPECTIVE DELETION MUTANTS AND REVERTANT FOR <i>CRZ1</i> AND <i>GZF3</i>	99
FIGURE 36: TOLERANCE LEVELS OF THE DIFFERENT DELETIONS MUTANTS FOR BOTH <i>CRZ1</i> AND <i>GZF3</i> IN THE DSY2110 (A), DSY4454 (B), DSY4754 (C) AND DSY4588 (D) GENETIC BACKGROUNDS.	103
FIGURE 37: SCHEMATIC REPRESENTATION OF GO TERMS ENRICHED IN GENES UP- (LEFT PANEL) AND DOWN-REGULATED (RIGHT PANEL) BY FLC IN <i>C. ALBICANS</i>	119
FIGURE 38: GSEA ENRICHMENT MAP OF FLC REGULATED GENES IN <i>C. ALBICANS</i> SC5314.	123
FIGURE 39: VENN DIAGRAM OF FLC-REGULATED GENES IN <i>C. ALBICANS</i>	124
FIGURE 40: VENN DIAGRAM OF GENES WITHIN THE CALCINEURIN- <i>CRZ1</i> CLUSTER OF THE GSEA.	124
FIGURE 41: TOLERANCE PROFILE OF THE <i>C. ALBICANS</i> CLINICAL ISOLATES.	125
FIGURE 42: GSEA ENRICHMENT MAP OF FLC REGULATED GENES IN CLINICAL ISOLATES.	131

List of Tables

TABLE 1: KNOWN RISK FACTORS FAVORING <i>CANDIDA</i> SPP. INFECTIONS.	3
TABLE 2: EPIDEMIOLOGY OF <i>CANDIDA</i> SPP.	8
TABLE 3: OVERVIEW ON THE ACTIVITY OF ANTIFUNGAL AGENTS IN SEVERAL PATHOGENIC <i>CANDIDA</i> SPECIES.	10
TABLE 4: RESISTANCE MECHANISMS OF MAJOR ANTIFUNGAL DRUGS.	11
TABLE 5: KNOWN MECHANISMS OF RESISTANCE TO AZOLES.	26
TABLE 6: REFERENCE DIAGNOSTIC METHODS AVAILABLE FOR ANTIFUNGAL SUSCEPTIBILITY PROFILING.....	28
TABLE 7: ECOFF AND CBP OF DIFFERENT ANTIFUNGAL AGENTS AND <i>CANDIDA</i> SPECIES.	31
TABLE 8: STRAINS AND CLINICAL ISOLATES USED IN THIS STUDY.	43
TABLE 9: AMINO ACID SUBSTITUTIONS IN CEC STRAINS RESISTANT TO FLC.	58
TABLE 10: REFERENCE STRAINS AND CLINICAL ISOLATES USED IN THIS STUDY.	62
TABLE 11: PARENTAL STRAINS OF THE OE COLLECTION AND DERIVATIVE.	63
TABLE 12: CLINICAL ISOLATES AND DERIVATIVES USED FOR THE OE OF PUTATIVE NEGATIVE REGULATORS OF TOLERANCE.	63
TABLE 13: <i>CRZ1</i> AND <i>GZF3</i> MUTANT STRAINS USED FOR THE OE OF EITHER <i>CRZ1</i> OR <i>GZF3</i>	64
TABLE 14: <i>CRZ1</i> AND <i>GZF3</i> DELETION MUTANTS IN TOLERANT CLINICAL ISOLATES.	66
TABLE 15: TOP 10 ENRICHED AND DEPLETED STRAINS AFTER 5 DAYS OF SUBCULTURE.	83
TABLE 16: HIGHLIGHT OF THE 10 TOP-HIT STRAINS SHOWING THE HIGHEST AND LOWEST GROWTH RATIO OF THE SINGLE STRAIN ASSAY.	85
TABLE 17: CLINICAL ISOLATES USED FOR RNASEQ WITH THEIR MIC VALUES FOR DIFFERENT ANTIFUNGAL DRUGS.	114
TABLE 18: DETAILS ON THE ENDOCARDITIS PATIENT AND THE COLLECTED ISOLATES.	126
TABLE 19: GENES REGULATED BY FLC IN THE CLINICAL STRAINS.	127

List of Supplementary Elements

All Supplementary Files and documents can be found at:

<https://www.dropbox.com/sh/vmffsquq28kwtbt/AAD0Dkn4lL5eXsA71wpGDUoxa?dl=0>

List of Supplementary Figures

Supplementary Figure 1: Map of the plasmids used in this study

Supplementary Figure 2: Figure 34 with respective strain names

Supplementary Figure 3: Figure 36 with respective strain names

Supplementary Figure 4: Verification of *CRZ1* complementation by spotting on SDS plates

List of Supplementary Tables

Supplementary Table 1: List of strains overexpressing putative negative regulators in tolerant clinical isolates backgrounds

Supplementary Table 2: List of strains overexpressing *CRZ1* or *GZF3* in deletion mutants with complete genotypes

Supplementary Table 3: Plasmids used in this study

Supplementary Table 4: Primers used in this study

List of Supplementary Files

Supplementary File 1: List of CEC clinical isolates

Supplementary File 2: P_{TET}-OE strain collection and Enrichment results

Supplementary File 3: Script and pipeline for BC quantification

Supplementary File 4: Single strain tolerance assay results

Supplementary File 5: RNAseq data and results

Supplementary File 6: GSEA conditions and analysis

Supplementary File 7: GSEA comparisons

Supplementary File 8: Multi Locus Sequence Typing of endocarditis clinical isolates

Supplementary File 9: Transcriptome comparisons between endocarditis clinical isolates

General introduction

***Candida* spp. and their relevance as human pathogens**

Fungal pathogens are challenging organisms that can cause a wide range of diseases, from mild to life-threatening infections. They are a major issue in hospital, especially in neonates and Intensive Care Units (ICUs) and the number of cases of sepsis caused by such pathogens is increasing since the early 1990s [1].

Among all human fungal pathogens, *Candida* species represent the most common cause of invasive infections [1]. It is estimated that, without considering dermatophytes infections, around 300 million people are affected by fungal infections worldwide. Among them, invasive candidiasis affects more than 250'000 people each year and is the cause of more than 50'000 deaths despite antifungal therapy [2].

It has been estimated that *Candida* spp. are the 4th most commonly isolated human pathogen causing bloodstream infections (BSIs) in ICUs [3]. However, outside of ICUs, candidemia has been established as the 7th to 10th most common cause of BSIs [2]. It is important to take in account that the distribution of *Candida* spp. responsible for invasive candidiasis varies depending of the geographical areas, the affected population, but also on a prophylaxis-based manner (Figure 1) [1, 2].

Among the 17 and more *Candida* spp. responsible for candidemia, it is estimated that five of them (*C. albicans*, *C. glabrata*, *C. parapsilosis*, *C. tropicalis* and *C. krusei*) account for 92 % of all cases of candidemia, with *C. albicans* being responsible for more than 60 % of all the cases worldwide (Figure 1 A and B) [1, 4].

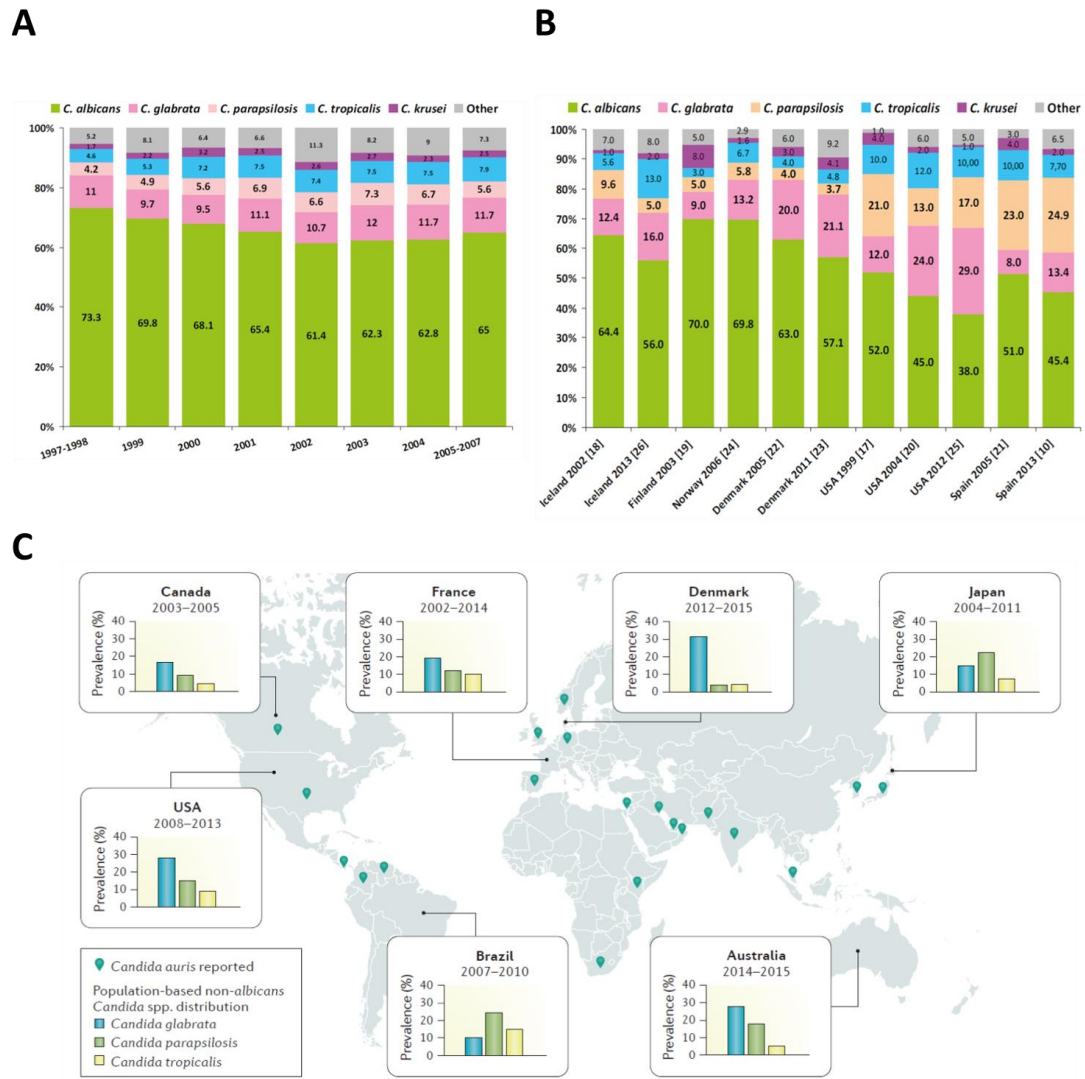


Figure 1: *Candida* spp. distribution over the last decades. (A), in European countries and USA (B) and the major non-*albicans* *Candida* spp. prevalence worldwide (C). Adapted from Guinea [1] and Pappas *et al.* [5].

The frequency at which each *Candida* species occurs varies depending on the geographical area, but, globally, *C. albicans* remains the prominent species (Figure 1 B) [1]. The main diversity in frequencies is observed between *C. glabrata* and *C. parapsilosis*. Indeed, in Northern Europe and the USA, *C. glabrata* is responsible for 10-30 % of candidemia events, and *C. parapsilosis* for 5-20 % (Figure 1B and C). However, it is reported that *C. parapsilosis* is more prevalent over *C. glabrata* in Spain, Brazil and Japan, representing 25 % of all cases against 8-14 % for *C. glabrata* (Figure 1B and C) [1, 5].

In addition to geographical diversity, it has also been observed that, along the last decades, a global shift in *Candida* spp. distribution is occurring, with an overall decrease in *C. albicans* frequency in favor

of non-*albicans* species (Figure 1A) [1]. Lately, a newly emerging species *C. auris* was reported. *C. auris* cases are spreading worldwide since first appearance in Japan in 2009. The *C. auris* infection rate increase is probably to the prophylactic use of FLC and selection of azole-resistant strains. Since its first isolation in Japan, *C. auris* has been isolated and identified in multiple countries on five continents. *C. auris* is a major human-health concern due to its resistance to multiple antifungal classes (Figure 1 C) [6].

Table 1: Known risk factors favoring *Candida* spp. infections. Adapted from Kullberg and Arendrup [2].

Risk factors	Comments
Critical illness	Especially for long-term ICU patients
Abdominal surgery	Especially in case of anastomotic leakage or repeat laparotomies
Acute necrotizing pancreatitis	
Hematologic malignant disease	
Solid-organ transplantation	
Solid-organ tumors	
Neonates	Especially low birth weight and preterm infants
Broad-spectrum antibiotics therapy	
Central vascular catheter / total parenteral nutrition	
Hemodialysis	
Glucocorticoid / chemotherapy for cancer	
<i>Candida</i> colonization	Especially if multifocal

Another factor involved in *Candida* spp. distribution is the affected population. Indeed, the age of the patient plays an important role. *C. albicans* is more frequent in neonates and young adults, while *C. parapsilosis* frequency decreases with the age of the patient and, conversely, *C. glabrata* frequency increases in older patients [1].

The condition of the patients is also important for the distribution of *Candida* spp. Indeed, several conditions (listed in Table 1) are known risk factors for the development of candidemia, with each factor determining which *Candida* spp. will be favored. For instance, *C. glabrata* and *C. krusei* are relevant pathogens commonly isolated in stem cells recipient patients, while patients receiving solid organ transplantation are more often infected by *C. albicans* and *C. glabrata* [1].

A last factor playing a major role is the use of a specific antifungal and the duration of the treatment. Logically, the type of antifungal used in prophylaxis will select for *Candida* spp. more resistant to the used agent (Figure 2 B), and the longer the treatment, the more susceptible species will be replaced by more resistant ones (Figure 2A) [1, 2].

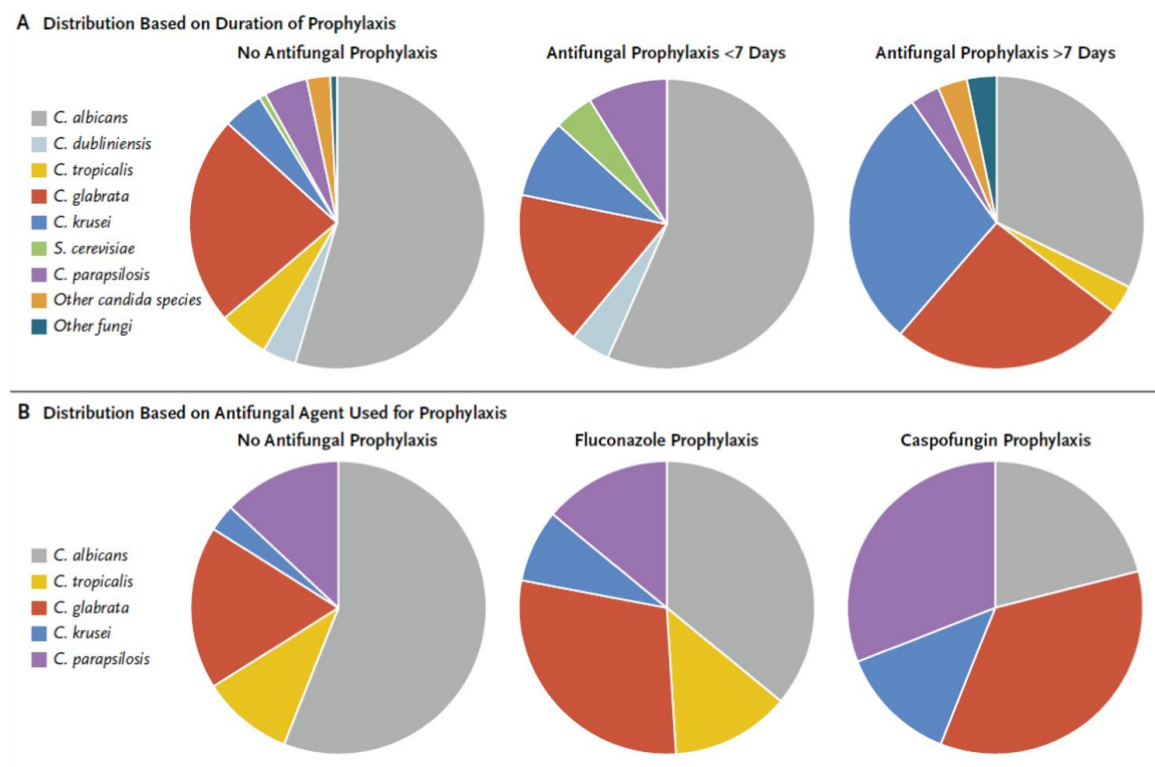


Figure 2: Role of antifungal prophylaxis upon *Candida* spp. distribution.[2]

Candida albicans

Due to the role of *C. albicans* in invasive candidiasis worldwide, a major focus is given to this species. *C. albicans* is a polymorphic yeast, belonging to the Ascomycota phylum, which can grow as budding yeast cells, pseudohyphae or true hyphae depending on the environmental conditions to which it is exposed, with each form playing a role in pathogenicity (Figure 3) [7]. Indeed, *C. albicans* strains blocked in either the yeast form or the hyphal form are known to show decreased virulence compared to a wild type (WT) strain, highlighting the necessity of a complete phenotypic morphogenesis switch for successful infection [7].

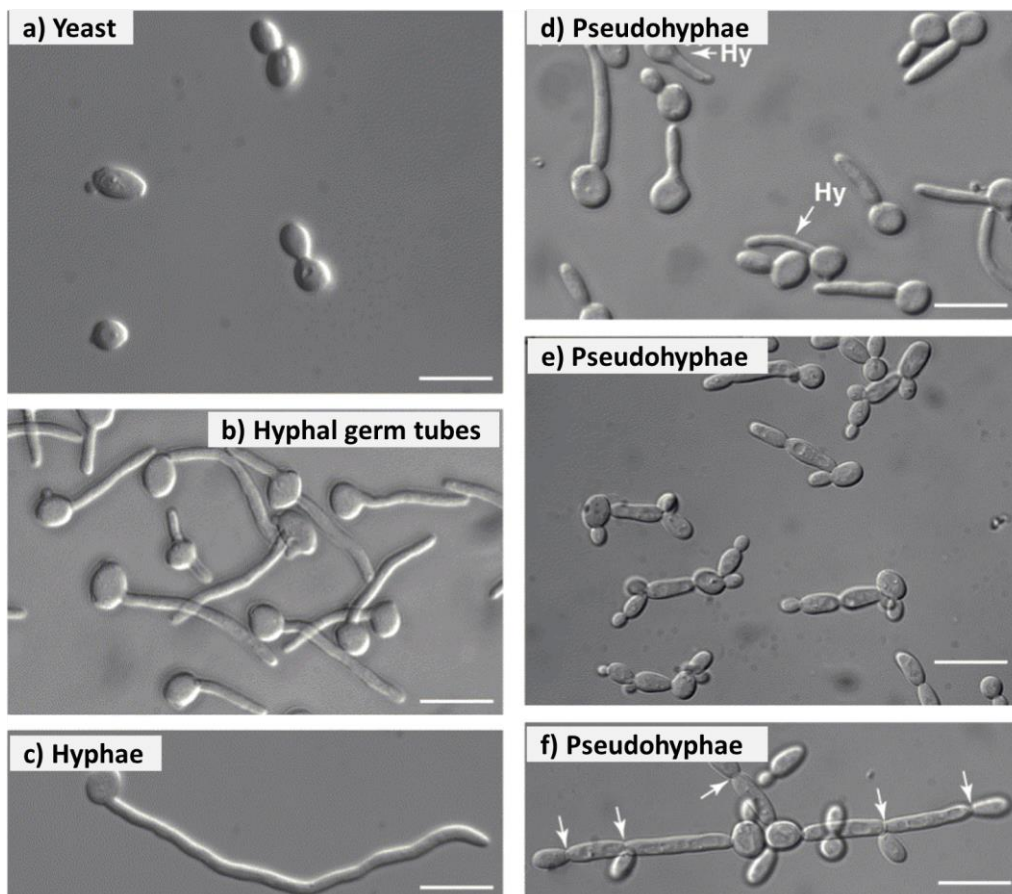


Figure 3: Morphological forms of *C. albicans*. Adapted from Sudbery *et al.* [8].

Candida spp. can be found in healthy individuals as harmless members of the commensal microbiota present on their skin, oral and vaginal mucosa and in the gastrointestinal tract [4, 9, 10]. However, following hormonal fluctuation due to menopause or to the use of hormonal treatment such as oral contraceptives [11], when the microbiota is disturbed by the use of broad spectrum antibiotics and when the host's immune defenses are weakened (*i.e.* AIDS patients), *Candida* spp. can cause superficial

infections such as oral and vaginal infections (also known as thrush). These infections are characterized by the apparition of white spots on the surface of the mucosae which are constituted of fungal colonies [12, 13]. It has been estimated that approximately 75 % of all women will suffer from superficial candidiasis at least once in their lifetime (vulvovaginal candidiasis) [14]. On a more life-threatening side, it has been reported in most large national surveys in the US that 3-5 out of 100,000 persons in the population and 1-2 % of ICU patients will face candidemia [5]. This incidence, however, varies due to geographical and epidemiological local population factors among others.

As stated above, *C. albicans* lives as a commensal of the mucosal surface of humans. However, when the mucosal microbiota equilibrium is altered, or the host immune defenses are reduced, *C. albicans* can switch from a commensal to an opportunistic lifestyle with the activation of different virulence factors. Indeed, when patients undergo strong immunosuppression such as neutropenic patients under highly active antiretroviral therapy (HAART), chemotherapy or organ transplantation, *Candida* spp. can cross the epithelial barrier, penetrate into the bloodstream and, from there, spread throughout the body and colonize internal organs such as the brain, the liver, the kidneys and the spleen (Figure 4). These infections are known as systemic or disseminated candidiasis [4, 12–15]. Risks of infections are increased by the use of catheters favoring biofilm formation, direct infection through the wound, or the use of broad-range spectrum antibiotics [4] (Figure 4). While superficial candidiasis is frequent and non-lethal, systemic candidiasis is associated with high mortality rates [14]. *Candida* spp. are found to be the seventh cause of health-care associated infections [16], and the fourth most common cause of nosocomial bloodstream infections in the USA and are associated with a crude mortality of 39.2 % despite antifungal therapies that are available (Table 2) [3, 17].

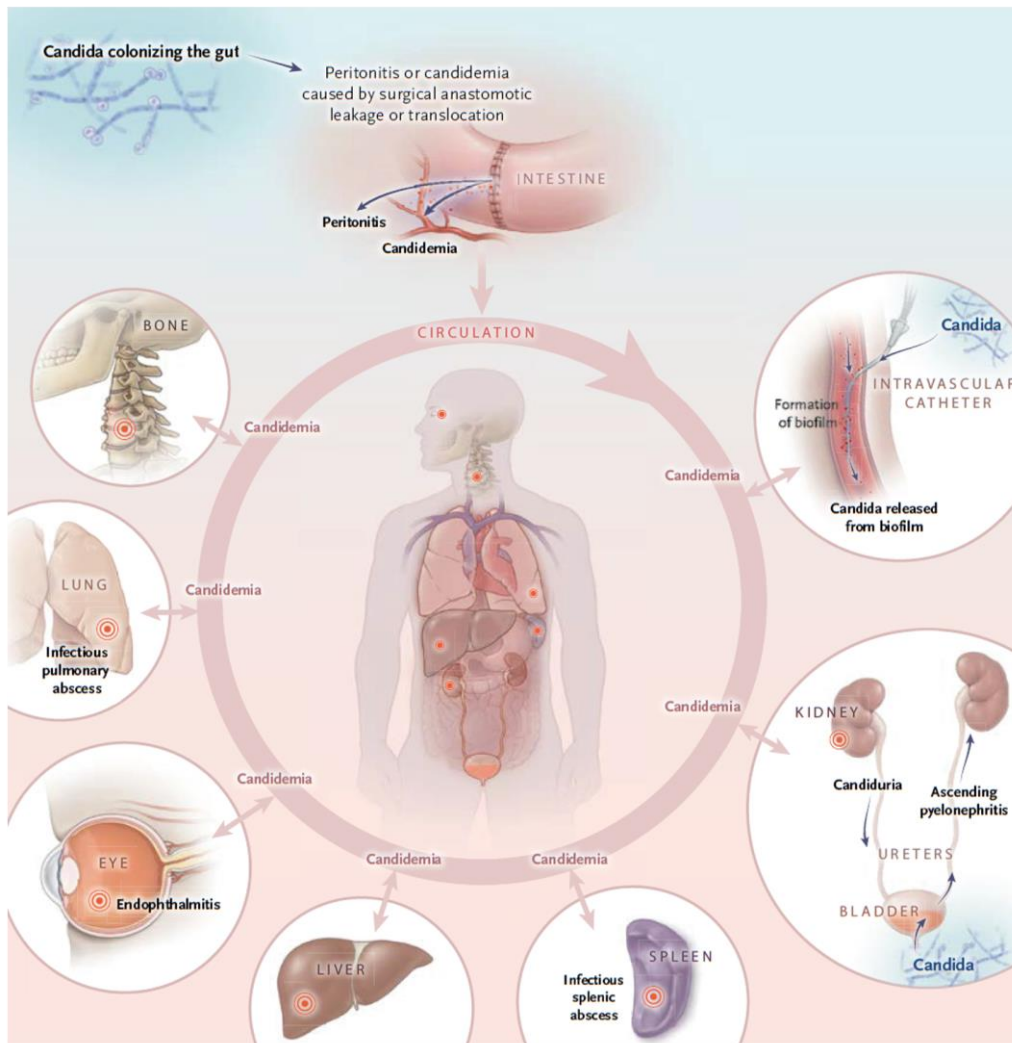


Figure 4: Routes of *Candida* infection and dissemination. *Candida* cells penetrate the organism via crossing of the gastrointestinal epithelium barrier or directly into the bloodstream via biofilm formation on intravascular catheters. Once in the bloodstream, *Candida* can disseminate throughout the body and colonize most of the organs and body parts. Adapted from Kullberg and Arendrup [2].

Table 2: Epidemiology of *Candida* spp. Incidence rate and distribution of pathogen most commonly isolated from nosocomial bloodstream infections (BSIs) (A). Incidence of most commonly isolated *Candida* spp. in BSI in Europe (EU) and North America (NAM) (B). Adapted from Wisplinghoff *et al.* [3] and Pfaller *et al.* [15].

A

Pathogen	BSIs per 10,000 admissions	% of BSIs (rank) n = 20,978	% of crude mortality (rank)
Coagulase-negative <i>Staphylococcus</i> spp.	15.8	31.3 (1)	20.7 (8)
<i>Staphylococcus aureus</i>	10.3	20.2 (2)	25.4 (6)
<i>Enterococcus</i> spp.	4.8	9.4 (3)	33.9 (3)
<i>Candida</i> spp.	4.6	9.0 (4)	39.2 (1)
<i>Escherichia coli</i>	2.8	5.6 (5)	22.4 (7)
<i>Klebsiella</i> spp.	2.4	4.8 (6)	27.6 (4)
<i>Pseudomonas aeruginosa</i>	2.1	4.3 (7)	38.7 (2)
<i>Enterobacter</i> spp.	1.9	3.9 (6)	26.7 (5)

B

Organism	Total <i>Candida</i> isolates (%) n = 256,882	EU isolates (%) n = 109,643	NAM isolates (%) n = 11,682
<i>C. albicans</i>	65.3	67.9	48.9
<i>C. glabrata</i>	11.3	11.3	21.1
<i>C. tropicalis</i>	7.2	4.9	7.3
<i>C. parapsilosis</i>	6.0	4.2	13.6
<i>C. krusei</i>	2.4	3.4	3.1
Other <i>Candida</i> spp.	7.8	8.3	5.2

Availability and limitations of current antifungal therapies

The high mortality rate of systemic candidiasis can partially be explained by the apparition of antifungal resistance which rapidly limits the option of alternative treatments due to the few classes of available drugs (summarized in Figure 5) [19, 20]. Due to the high functional similarity between fungi and human cells, which are both eukaryotic organisms, only a few cellular processes are fungal-specific and can thus be targeted by antifungals. The development of antifungal agents is therefore more challenging due to the shared potential drug targets existing in fungi and their hosts [19]. Currently, only five categories of antifungals are available against *Candida* spp. which can be classified based on their targets (Figure 5). Despite acting on a defined target, an antifungal may have a different effect, or no effect at all, depending on the involved fungal species (Table 3) [20]. In the case of invasive candidiasis, the current treatment guidelines are well established with echinocandins prophylaxis (due to their broad efficacy spectrum) until the proper identification of the species is carried out (Figure 6). In the following sections, the characteristics of major antifungal agents will be summarized.

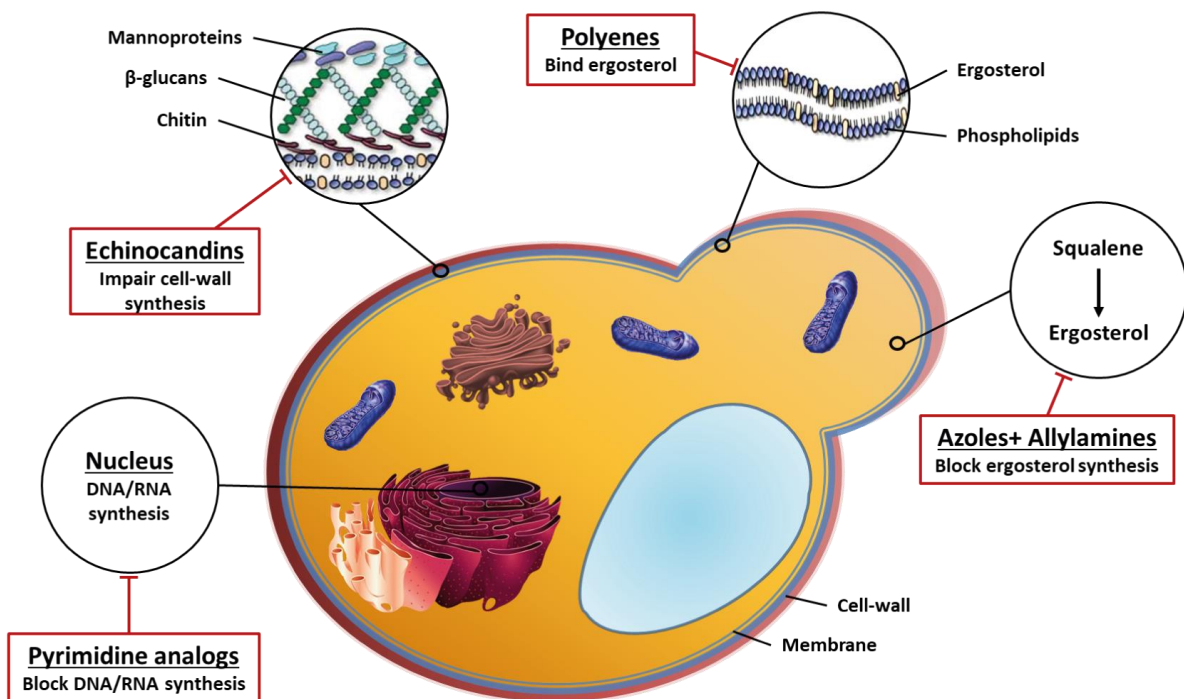


Figure 5: *C. albicans* cell and the five major antifungal classes with their respective targets.

Table 3: Overview on the activity of antifungal agents in several pathogenic *Candida* species. Adapted from Delarze and Sanglard [20].

Organism	Antifungal agent								
	AMB ¹	FLC	ITC	VCZ	PSZ	AFG	CAS	MFG	5-FC
<i>C. albicans</i>	+ ²	+	+	+	+	+	+	+	± ²
<i>C. glabrata</i>	+	±	±	±	±	+	+	+	±
<i>C. krusei</i>	+	- ²	±	+	+	+	+	+	-
<i>C. lusitaniae</i>	-	+	+	+	+	+	+	+	+
<i>C. parapsilosis</i>	+	+	+	+	+	±	±	±	+
<i>C. tropicalis</i>	+	+	+	+	+	+	+	+	+

¹ (AMB) Amphotericin B, (FLC) Fluconazole, (ITC) Itraconazole, (VCZ) Voriconazole, (PSZ) Posaconazole, (AFG) Anidulafungin, (CAS) Caspofungin, (MFG) Micafungin and (5-FC) Flucytosine.

² Drugs with activity (+), no activity (-) and variable activities (±) against the specified organisms.

Table 4: resistance mechanisms of major antifungal drugs. Adapted from Spampinato and Leonardi [21].

Antifungal class	Genetic basis for resistance	Functional basis for resistance
Azoles	<ul style="list-style-type: none"> - Upregulation of <i>CDR1/CDR2</i> and <i>MDR1</i> by point mutations in <i>TAC1</i> and <i>MRR1</i> transcription factors - Point mutations in <i>ERG11</i> - Upregulation of <i>ERG11</i> by gene duplication and transcription factor regulation - Point mutations in <i>ERG3</i> 	<ul style="list-style-type: none"> - Upregulation of drug transporters¹ - Decreased lanosterol 14-α-demethylase binding affinity for the drug² - Increased lanosterol 14-α-demethylase concentration³ - Alterations in the ergosterol pathways by C5 sterol desaturase inactivation³
Echinocandins	<ul style="list-style-type: none"> - Point mutations in <i>FKS1</i> and <i>FKS2</i> 	<ul style="list-style-type: none"> - Decreased glucan synthase processivity for the drug²
Polyenes	<ul style="list-style-type: none"> - Point mutations in <i>ERG3</i> and <i>ERG6</i> 	<ul style="list-style-type: none"> - Decreased ergosterol content in cells³
Nucleoside analogs	<ul style="list-style-type: none"> - Point mutations in <i>FCY2</i> - Point mutations in <i>FCY1</i> - Point mutations in <i>FUR1</i> 	<ul style="list-style-type: none"> - Inactivation of cytosine permease affecting drug uptake¹ - Alterations in 5-fluorocytosine metabolism by cytosine deaminase or uracil phosphorybosyl transferase inactivation³

¹ Reduced intracellular drug concentration

² decreased target affinity/processivity for the drug

³ counteraction of the drug effect

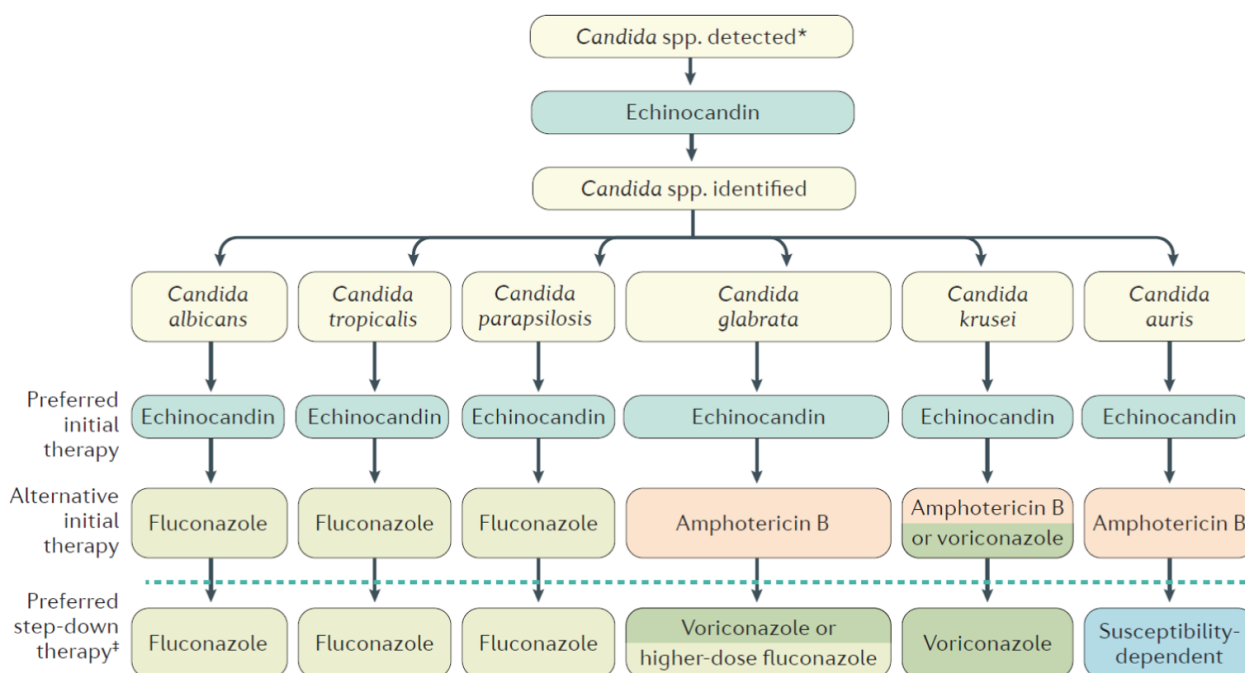


Figure 6: General guidelines for candidemia treatment. Adapted from Pappas *et al.* [5].

Inhibitors of nucleic acid synthesis

Pyrimidine analogues

5-fluorocytosine (5-FC), also known as 5-flucytosine, is a fluorinated pyrimidine analog (Figure 7A) that interferes with pyrimidine metabolism, protein synthesis and DNA/RNA biosynthesis (Figure 7B). This compound is actively transported into the fungal cells via a cytosine permease and, once in the cytoplasm, is deaminated by a cytosine deaminase in 5-fluorouracil (5-FU) (Figure 7B). Uracil monophosphate (UMP) pyrophosphorylase then converts 5-FU into 5-fluorouridine monophosphate (5-FUMP), which can be phosphorylated in 5-fluorouridine triphosphate (5-FUTP) and inhibits protein synthesis by the integration of 5-FUTP into fungal RNA in place of UTP (Figure 7B) [19]. In addition, the conversion of 5-FUMP in 5-fluorodeoxyuridine monophosphate (5-FdUMP), an inhibitor of the thymidylate synthase by uridine monophosphate pyrophosphorylase blocks DNA synthesis and cell division by inhibition of thymidylate synthase, a key enzyme in the DNA synthesis (Figure 7B) [19, 22].

5-FC does not show direct toxicity against mammalian cells as they lack the cytosine deaminase enzyme. However, 5-FC can be converted to 5-FU by the intestinal bacterial microflora thus causing adverse effects such as nausea, diarrhea, vomiting and diffuse abdominal pain [22].

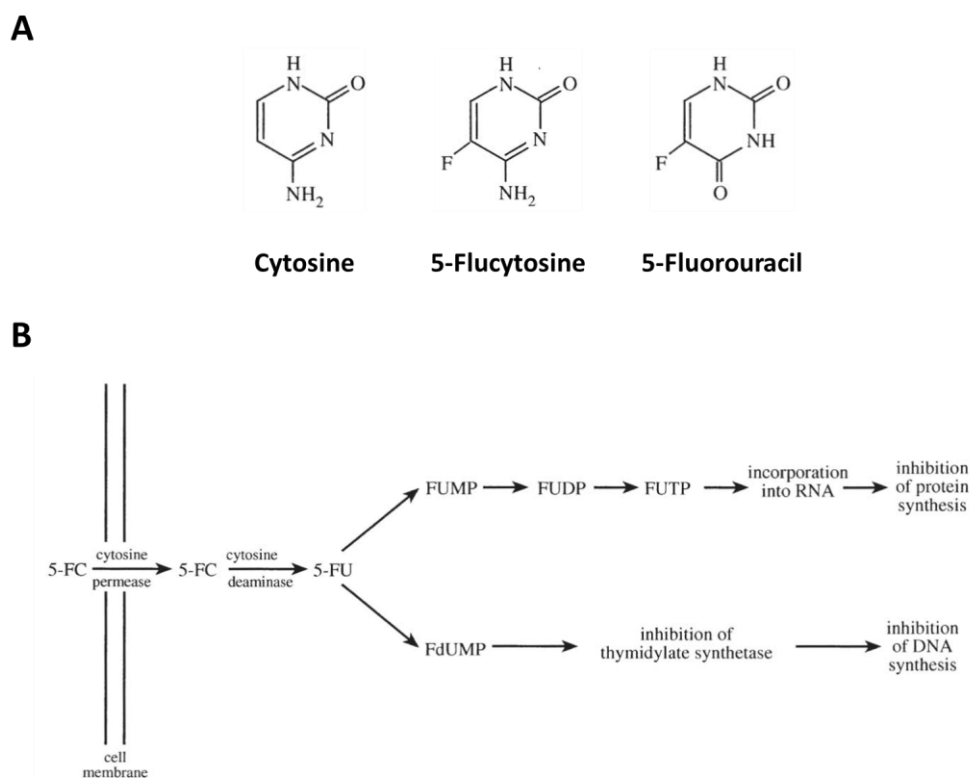


Figure 7: Pyrimidine analogs. (A) Chemical structure comparison between 5-flucytosine (5-FC), 5-fluorouracil (5-FU) and cytosine. (B) Mode of action of 5-FC in the fungal cell. Adapted from Vermes *et al.* [22].

Resistance to 5-FC is observed in 3-10 % of isolates *in vitro* and it has been observed that up to 30 % of isolates develop resistance during treatment. This resistance is linked to deficiencies in the enzymes involved in uptake (*FCY2*) and metabolism of 5-FC (*FCY1* and *FUR1*) (Table 4) [19, 21, 23]. Due to this prevalence of resistance acquisition, 5-FC is usually used as monotherapy of life-threatening candidiasis or as adjunctive to amphotericin B or azoles treatments[15, 19].

Fungal membrane disruptors

Polyenes

Polyenes were among the first antifungals available for clinical use. They are fungicidal and have a broad spectrum of activity compared to other antifungal drugs. Only three polyenes are currently available for clinical use including nystatin, natamycin and amphotericin B. These molecules are natural compounds isolated from bacteria species such as *Streptomyces noursei*, *S. natalensis* and *S. nodosum*, respectively (Figure 8A) [19]. These molecules have an amphiphilic structure and bind phospholipids in the membrane to form complexes with ergosterol, an important component of the fungal cell wall and absent in mammalian cells (Figure 8B). Two modes of action have been described. The first model consists of the formation of pores which disrupt the cell membrane and cause leakage of cytoplasmic content leading to fungal cell death (Figure 8B) [19, 23]. A more recently described model of action of polyenes consists of the formation of large extra-membranous aggregates which sequester ergosterol from fungal cell membranes (Figure 8B). By accumulating ergosterol, these sterol “sponges” disrupt membrane functions and lead to fungal cell death [23].

Besides the intrinsic high affinity for ergosterol, polyenes also have a slight affinity for host cholesterol. This may explain the high toxicity of amphotericin B to host cells and adverse effects such as chills, fever, headache, nausea, vomiting and severe nephrotoxicity [18].

Resistance to polyenes is uncommon and linked to a decreased in ergosterol content due to loss of function mutations in genes of the ergosterol biosynthetic pathway (for example *ERG3* and *ERG6*, Figure 9), resulting in the accumulation of other sterols in the membrane [15, 21].

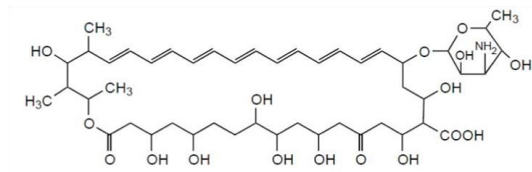
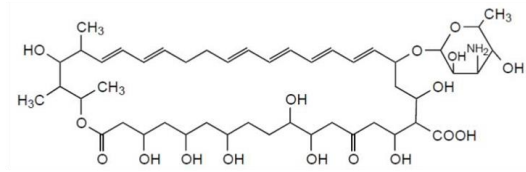
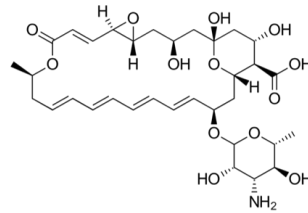
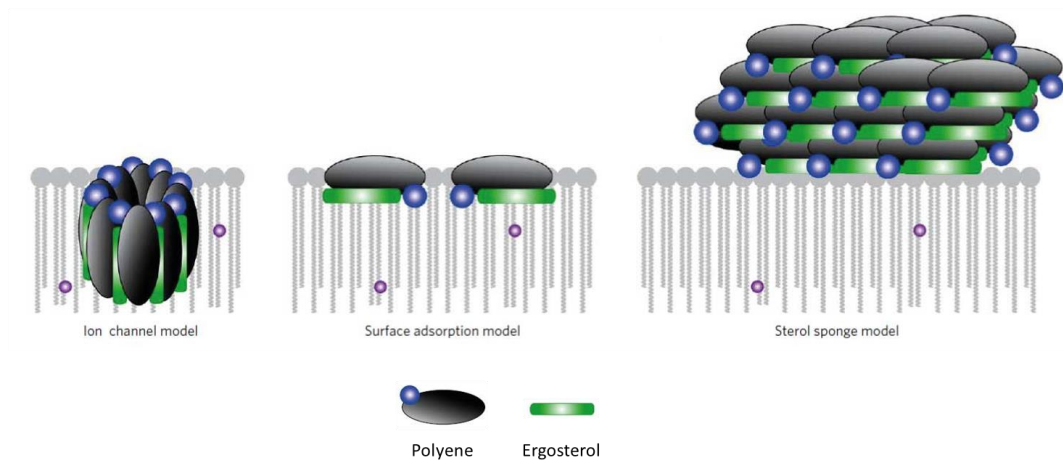
A**Amphotericin B****Nystatin****Natamycin****B**

Figure 8: Polyenes. (A) Chemical structures of the three clinically used polyenes: amphotericin B, nystatin and natamycin. (B) Mode of action of polyenes at the fungal cell's membrane. Polyenes can either form a pore by binding to ergosterol (ion channel model) or bind and adsorb ergosterol and act as a "sterol sponge". Adapted from Anderson *et al.* [23].

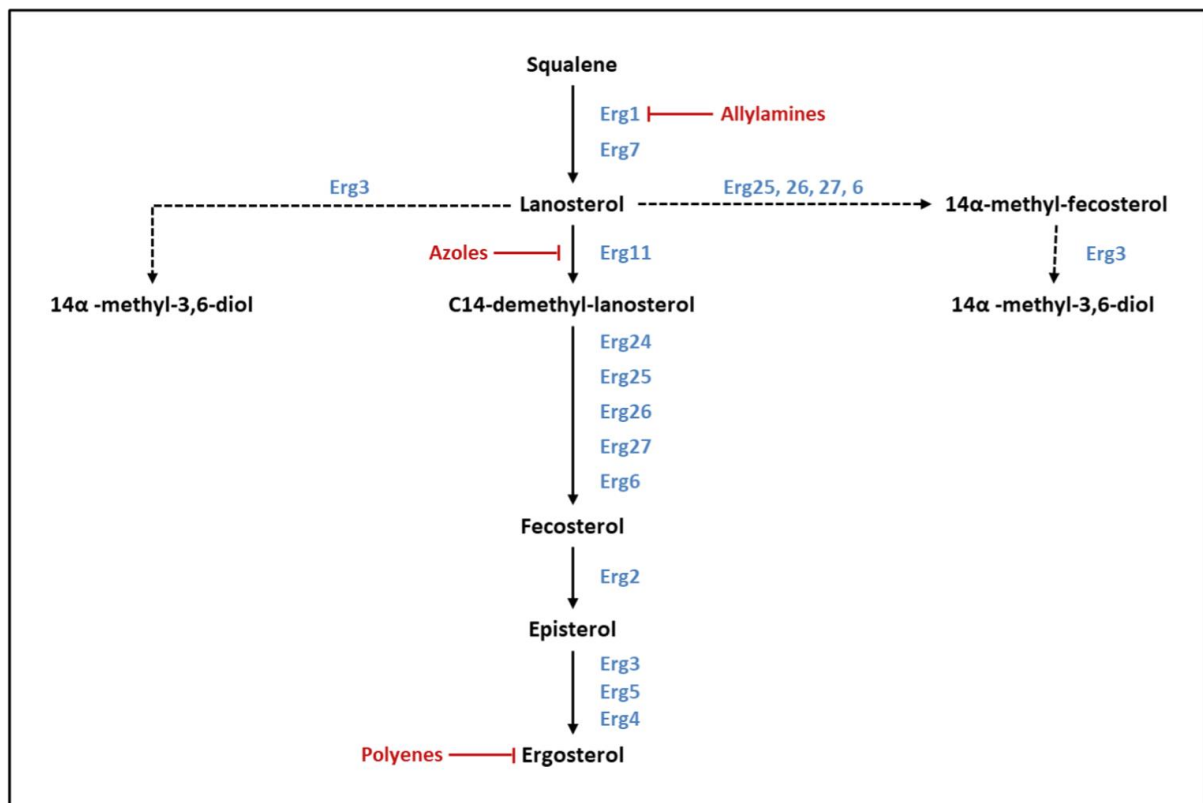


Figure 9: Ergosterol pathway in *C. albicans*. Antifungals targeting the pathway (azoles, allylamines and polyenes) are highlighted in red with their respective targets. The dashed arrows represent the alternative pathways activated under azole treatment. Adapted from Sanglard *et al.* [19] and Campoy and Adrio [24].

Inhibitors of fungal cell wall synthesis

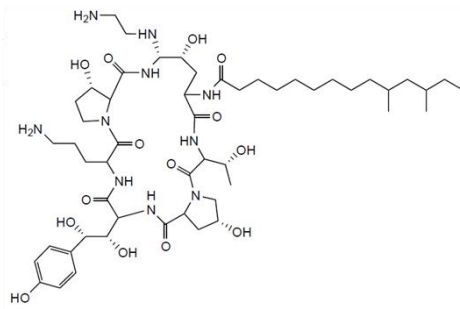
Echinocandins

Echinocandins are semisynthetic compounds derived from fungal natural products. Currently, only three echinocandins are available for clinical use: caspofungin, derived from pneumocandin B produced by *Glarea lozoyensis*, micafungin derived from echinocandin B produced by *Aspergillus nidulans* and finally anidulafungin, derived from a fermentation product of *Coleophoma empetri* (Figure 10A). These three compounds are non-competitive inhibitors of the β -(1,3)-D-glucan synthase complex and more specifically the subunits *FKS1* and *FKS2*. The β -(1,3)-D-glucan synthase is an enzyme responsible for the synthesis of β -(1,3)-D-glucan, a polysaccharide constituting more than 50 % of the fungal cell wall (Figure 10B). Blocking the synthesis of β -(1,3)-D-glucan leads to a disruption of the structure and stability of the cell wall, resulting in osmotic instability and lysis of the fungal cell [19].

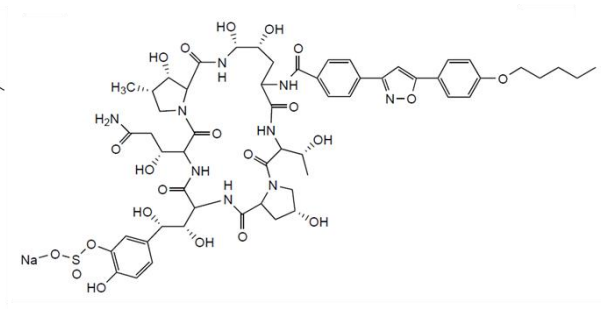
Due to their specificity for the fungal cell wall, echinocandins have low toxicity for mammalian cells. However, some adverse effects can be observed such as headache, rash, fever, liver toxicity, phlebitis, histamine release and hemolysis [18]. Echinocandins also have low interactions with other antifungals, allowing their use in combination with drugs like azoles or polyenes, which could avoid the development of antifungal resistance [25]. However, due to low absorption by the GI tract (due to their high molecular weight) and their short half-life, echinocandins must be injected once per day intravenously, limiting their clinical application [19, 25].

Resistance to echinocandins is linked to specific mutations leading to amino acid substitutions in two different regions (known as Hot-spot 1 and 2 or HS1 and HS2) of the two subunits of the 1,3- β -glucan synthase complex, *FKS1* and *FKS2*. These amino acid substitutions decrease the affinity of echinocandins to the enzyme active site (Table 4) [19, 26].

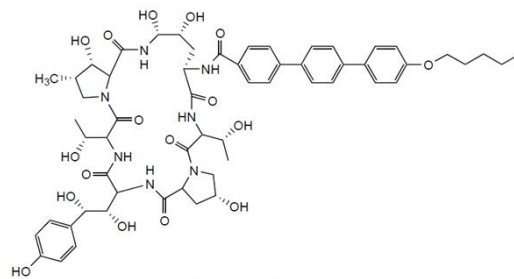
A



Caspofungin



Micafungin



Anidulafungin

B

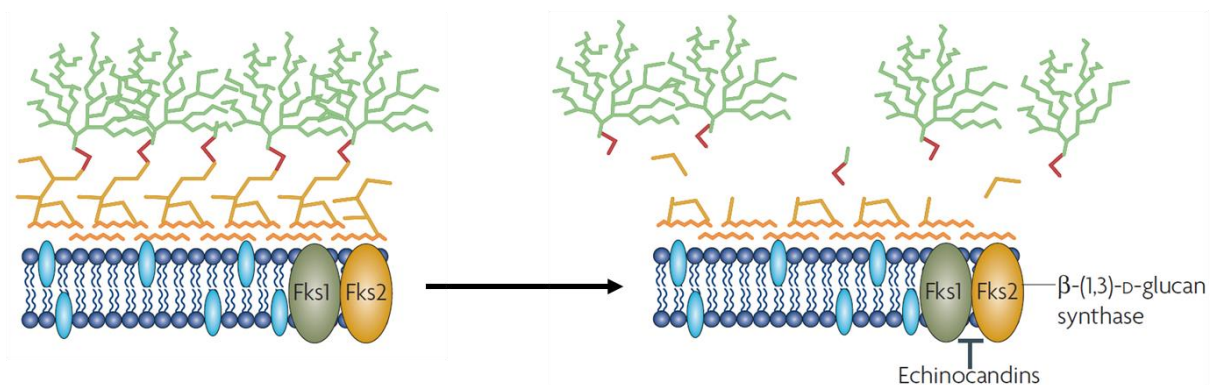


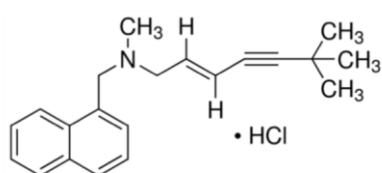
Figure 10: Echinocandins. (A) Chemical structures of the three available echinocandins; caspofungin, micafungin and anidulafungin. (B) Mode of action of echinocandins. Echinocandins block the β -(1,3)-D glucan synthase subunits (Fks1 and Fks2), thus impairing cell wall formation. Adapted from Cowen [27]

Inhibitors of ergosterol biosynthesis

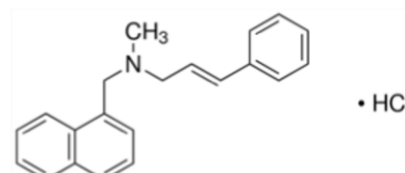
One major difference between fungal and human cells is the presence of ergosterol as the major sterol in the fungal membrane instead of cholesterol in mammalian cells. Ergosterol is required for membrane fluidity, asymmetry and integrity which are essential for fungal growth and survival. Since ergosterol is a fungal-specific molecule, its biosynthetic pathway has been targeted by several drugs (Figure 9) [28, 29].

Allylamines

Terbinafine and naftinine are the principal allylamines drugs used in the clinic, mainly for the treatment of dermatophytic infections (Figure 11). Allylamines are synthetic agents which inhibit ergosterol biosynthesis by binding to the squalene epoxidase Erg1, a key enzyme responsible for the conversion of squalene into lanosterol (Figure 9) [19, 29]. This inhibition results in the accumulation of high amounts of squalene inside the fungal cell and results in increased membrane permeability, alteration of the cellular organization and finally leads to cell death [19].



Terbinafine



Naftinine

Figure 11: Allylamines. Chemical structures of the two major allylamines used in clinic; terbinafine and naftinine.

Allylamines display synergistic activities with other antifungal drugs, particularly with triazoles, the main drug class used against *Candida* spp., demonstrating a potentially useful strategy against azole-resistant *Candida* spp. isolates. However, the effect of allylamines against *Candida* spp. appears to be relatively poor *in vivo*, limiting its clinical interest when used alone [29].

Azoles

Azoles are the first-line drugs used against *Candida* infections [30] due to their high tolerability in patients (even at high concentrations), limited side-effects, broad spectrum of activity, advantageous treatment cost as well as worldwide availability (Figure 12). Azoles possess a fungicidal activity against *Aspergillus* spp., but a fungistatic activity against *Candida* spp. and are divided in two major categories: the imidazoles (clotrimazole, miconazole and ketoconazole) (Figure 13A) and the triazoles (itraconazole, fluconazole, voriconazole, posaconazole and isavuconazole) (Figure 13B) [18]. Imidazoles were the first developed azoles. Due to their toxicity and side effects, the development and use of triazoles is now favored in the clinic. Triazoles can be separated into two groups. The first generation triazoles, represented by itraconazole and fluconazole (FLC) have a broad spectrum of activity but are not efficient against pathogens such as *Scedosporium*, *Fusarium* and *Mucorales* [19]. Due to its activity against different *Candida* spp., FLC has been established as the first-line antifungal against localized and systemic candidiasis, mainly against *C. albicans*. FLC prophylactic administration can be useful in patients at risk of infections, for example in immunocompromised patients [31]. The second generation of triazoles, represented by voriconazole, posaconazole and isavuconazole have a broader spectrum of activity than the first generation. Voriconazole is being used as a first-line drug against invasive *Aspergillus fumigatus* infections. Posaconazole generally exhibits increased activity as compared to other azoles and has a broader activity spectrum. It is used as prophylaxis against invasive candidiasis and aspergillosis [19].

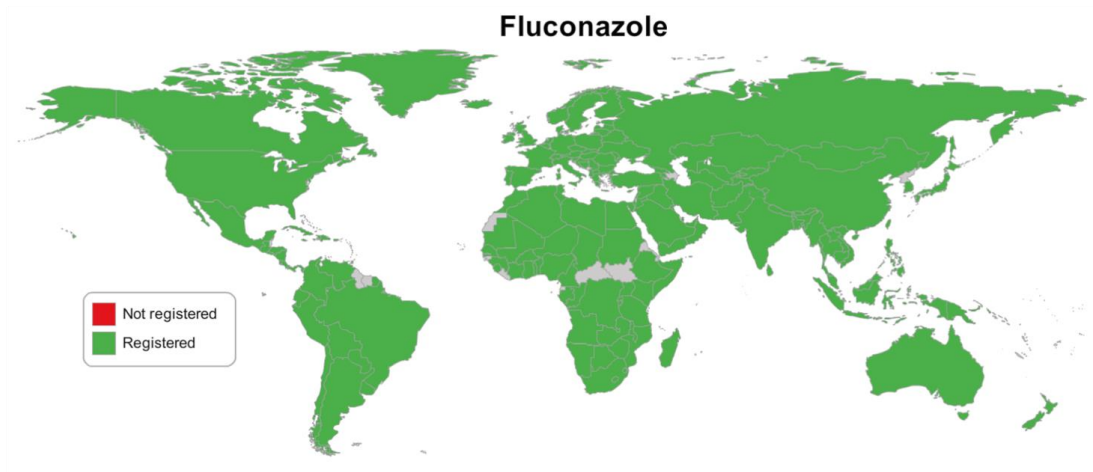
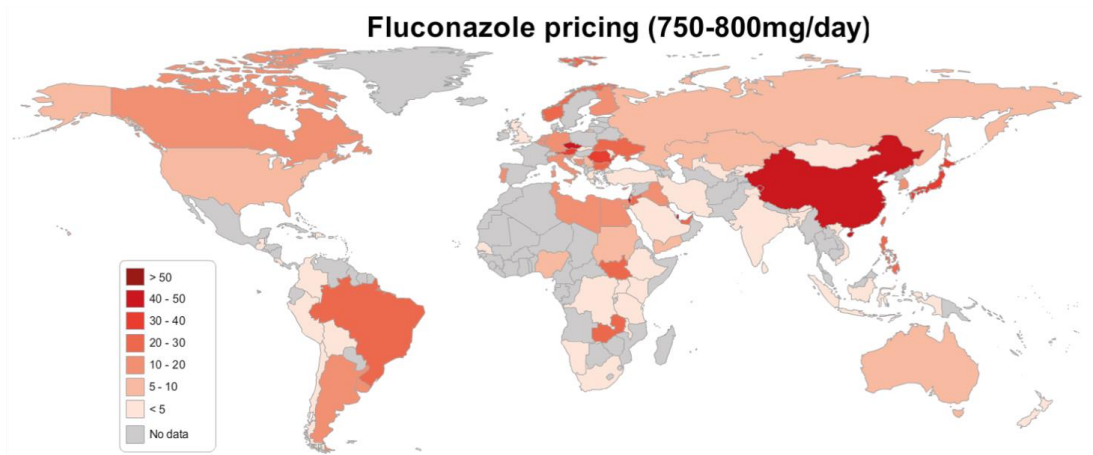
A**B**

Figure 12: Worldwide FLC availability (A) and pricing in US \$ (B). Adapted from www.antifungals-availability.org.

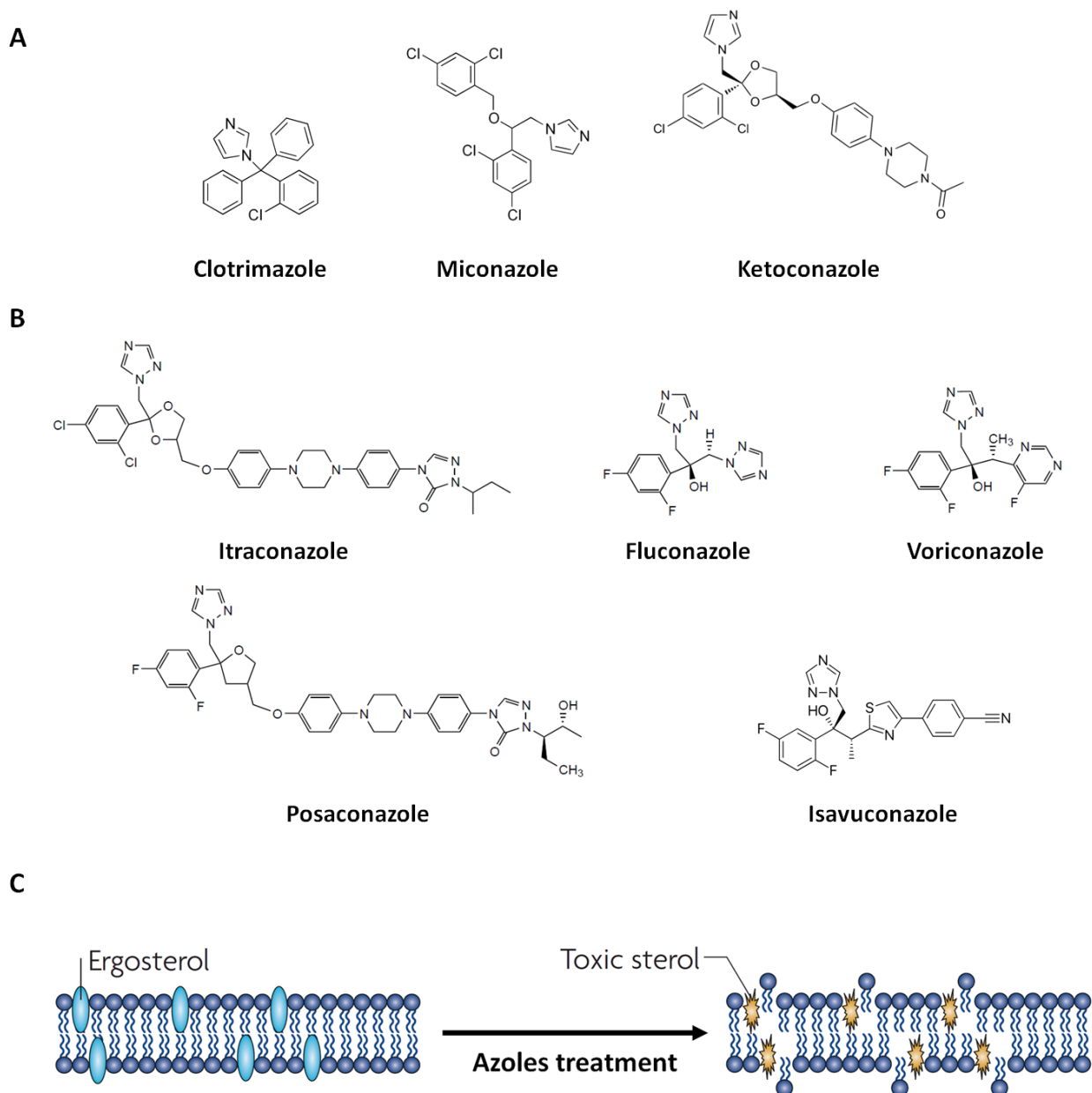


Figure 13: Azoles. Chemical structures of imidazoles (A) and triazoles (B). Azoles act by impairing ergosterol biosynthesis, leading to the accumulation of toxic sterols in the membrane (C). Adapted from Cowen [27].

Azoles inhibit the production of ergosterol by targeting the cytochrome P450-dependent lanosterol 14- α -demethylase, encoded by *ERG11*, which is responsible for the conversion of lanosterol into C14-demethyl-lanosterol, a key element in ergosterol biosynthesis (

Figure 9). Azoles bind to the iron contained in the porphyrin unit of the active site of the enzyme, blocking its activity, thus resulting in the accumulation of lanosterol in the fungal cell [19]. The accumulated lanosterol is then processed by the cell into several methylated sterols among which a

toxic methylated sterol (14-methylergosta-8,24(28)-dien-3,6-diol) that is responsible for growth inhibition (Figure 9, Figure 13C) [28]. Each type of azole antifungal binds to the active sites with different affinities, determining their antifungal effect and their affinity for the host cytochrome P450s, which may predict their side-effects [19].

However, due to the wide use of azoles (mainly FLC) and their fungistatic activity against *Candida* spp., a strong selection for azole-resistant strains has been observed [15, 32]. The rapidly growing resistance of *C. albicans* to other commonly used antifungals is an important medical concern. Emergence of resistant strains also resulted in an increased mortality rate among patients [18].

Resistance mechanisms to azoles

It has been observed that the repeated use of FLC can result in the acquisition of resistance in fungi. In fact, the fungistatic nature of FLC allows long-term fungal survival in the presence of high drug levels. This long exposure to drugs is known to increase the apparition of resistance in *C. albicans*. The mechanisms of resistance acquisition in *C. albicans* have been widely studied and are well characterized (Figure 14, Table 4 and Table 5). Drug resistance can be the result of the alteration of the drug target by mutations in order to diminish drug binding, the increase of the drug target concentration in the cell by up-regulation of specific genes, or even high levels of efflux pumps to prevent the accumulation of the drug in the cell (Figure 14) [32, 33].

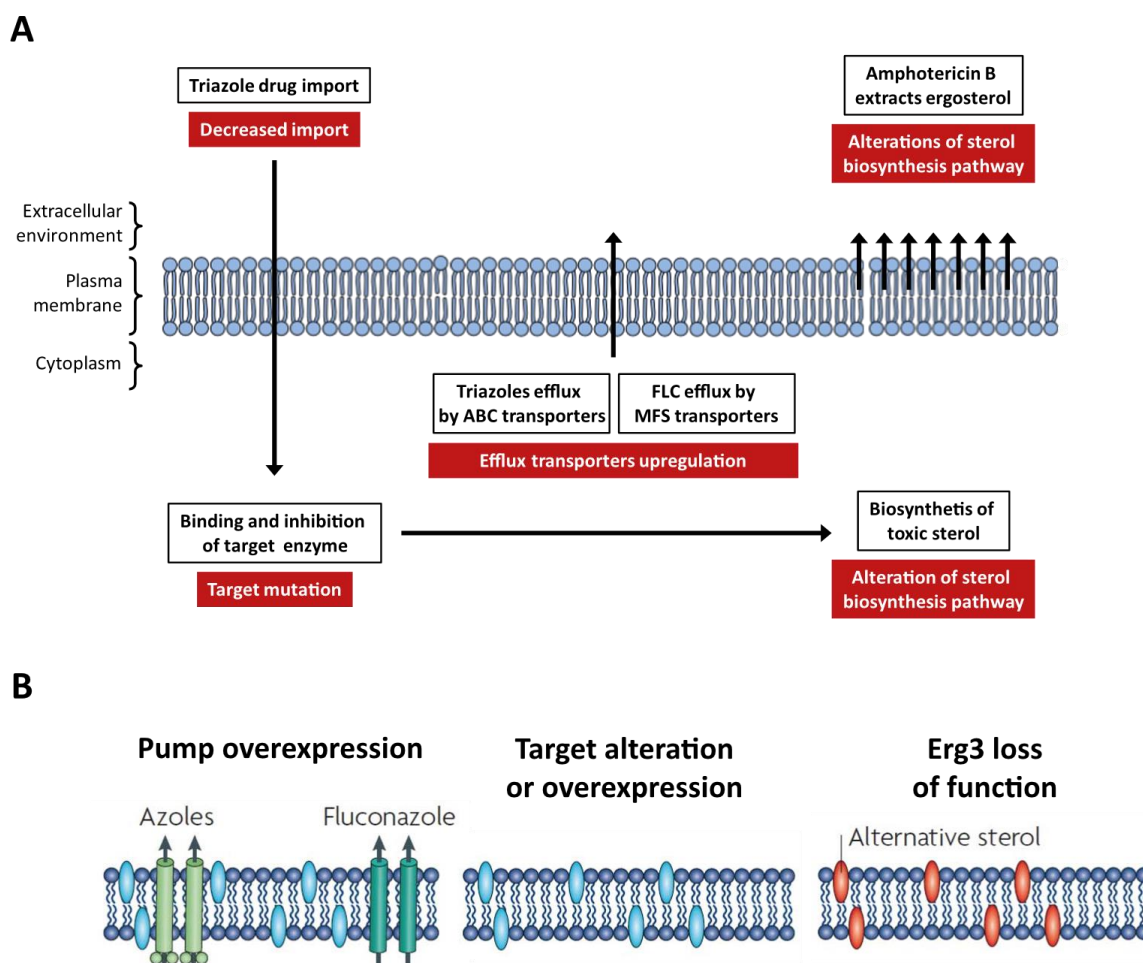


Figure 14: Resistance mechanisms of azoles and polyenes. (A) Mode of actions of azoles and polyenes (white background) and the respective mechanisms of resistance (red background) in *C. albicans*. (B) Detailed mechanisms of resistance to azoles. Adapted from Cowen [27] and Vale-Silva [34].

Alteration of Erg11 has been identified as a cause of resistance in many clinical isolates [35]. Several alterations of *ERG11* such as point mutations and overexpression have been identified to result in resistance to azoles (Figure 14, Table 5). Mutations in *ERG11* can cause structural or functional alterations of the active site that reduce the FLC ability to bind to its target (Table 5). Diminution of the drug affinity leads to an increase of resistance [30]. The increase of *ERG11* expression has also been identified in many resistant *C. albicans* isolates (Figure 14, Table 5). Upc2, a zinc-cluster transcription factor, regulates *ERG11* expression. It has been observed that gain-of-function mutations of this transcription factor can result in an increased expression of the target gene. Overexpression of *ERG11*, mediated by *UPC2* mutations, results in increase of FLC resistance (Figure 14, Table 5) [32].

ERG3 is a gene responsible for the conversion of lanosterol into the toxic methylated intermediate responsible for cell growth defect during azole treatment (Figure 9). Its inactivation results in the absence of accumulation of this toxic compound, conferring azole resistance to the fungal cell (Figure 14, Table 5). However, even if mutations repressing *ERG3* transcription could be expected in *C. albicans* clinical isolates, they have not been reported yet [36].

Another frequently encountered resistance mechanism consists of the active export of the drug out of the cell (Figure 14). In *C. albicans*, three efflux pumps, the ATP Binding Cassette (ABC) transporters Cdr1 and Cdr2, and the major facilitator transporter Mdr1 are involved in resistance (Figure 14, Table 5). In fact, many FLC-resistant strains overexpress at least one of these pumps. The transporters' up-regulated activity in resistant isolates is the result of gain-of-function mutations in zinc-cluster transcription factors Tac1 and Mrr1 that regulate *CDR1*, *CDR2* and *MDR1* expression, respectively (Table 5) [32].

Highly resistant isolates often exhibit a combination of different resistance mechanisms. Accumulation of mutations results in an additive increase of resistance. Highly resistant strains resulting from strong FLC selective pressure are frequently found in patients treated for a long period [32]. It has been observed that other mechanisms can be involved in FLC resistance. For example, the transcription factor Cap1 is involved in oxidative stress response by inducing *MDR1* expression. When Cap1 is hyperactive (C-terminally truncated), it causes a constitutive overexpression of *MDR1* and has been linked to increased FLC resistance. Alternatively, Fcr1, another transcription factor, has been linked to increase FLC resistance when deleted. However, to our knowledge, these mechanisms have not yet been detected in clinical isolates [32]. It is also thought that zinc cluster transcription factors other than Mrr1, Tac1 and Upc2 might play a role in FLC resistance. Indeed, it has already been shown that hyperactive Mrr2 can control the expression of *CDR1* and not *CDR2*, and has been linked to increased resistance both *in vitro* but not in clinical isolates so far [32]. Standardized antifungal susceptibility assays are essential to provide a clear diagnosis of fungal infections and their required treatments, especially when strains are causing severe infections or are unresponsive to routine treatments.

Table 5: Known mechanisms of resistance to azoles. Adapted from Morschhäuser *et al.* [32].

Gene	Function	Effect of mutation	Resistance mechanism
<i>ERG3</i>	Transformation of lanosterol into a toxic sterol	Loss-of-function of $\Delta^{5,6}$ -desaturase	No toxic sterol accumulation
<i>ERG11</i>	Target of azoles; First-step transformation of lanosterol into ergosterol	Structural change in target enzyme	Reduced drug binding
<i>MRR1</i>	Transcription factor (TF) regulating <i>MDR1</i> expression	Hyperactive TF	Efflux pump overexpression (<i>MDR1</i>)
<i>TAC1</i>	TF regulating <i>CDR1</i> and <i>CDR2</i> expression	Hyperactive TF	Efflux pump overexpression (<i>CDR1</i> , <i>CDR2</i>)
<i>UPC2</i>	TF regulating <i>ERG11</i> expression	Hyperactive TF	Drug target overexpression (<i>ERG11</i>)

Antifungal susceptibility assays

Several techniques are available to establish the susceptibility profile of a defined *Candida* isolate. Most of them are based on drug diffusion in either a solid agar medium or in liquid conditions, with each protocol having its specific endpoint readout [5]. Despite having the same purpose (*i.e.* identifying susceptible and resistant isolates), each method has its advantages and flaws. Indeed, depending on the *Candida* species and the tested drug, a given protocol might be more optimal than the other (Table 6) [5].

To standardize laboratory protocols and interpretation of drug susceptibility testing, two basic methods have been established. First, the Clinical and Laboratory Standard Institute (CLSI) (formerly the National Committee for Clinical Laboratory Standard) have established a reference method for broth dilution antifungal susceptibility testing of yeasts which aims to standardize antifungal susceptibility testing for yeasts that cause invasive infections. The CLSI method relies on visual observation of fungal growth in the presence of different antifungal concentrations in broth media. The growth in the tubes (or in U-shaped wells in the case of microtiter plates) containing the antifungal is visually compared to growth in control tubes without drug. The main readout of the test is the visual observation of the Minimum Inhibitory Concentration (MIC) defined by the CLSI as the lowest concentration of the drug that prevents visible growth of a microorganism in a broth dilution susceptibility test [37].

Similarly to CLSI, the European Committee on Antimicrobial Susceptibility Testing (EUCAST) developed a method relying on optical density reading by spectrophotometry of flat-bottomed micro-dilution plates to quantify fungal growth compared to a drug free control. The main readout of the test is also the determination of the MIC defined by EUCAST as the lowest antifungal concentration that inhibits growth of fungi within a defined period of time taking a cut-off of 50 % of growth as compared to the drug-free control [38].

Table 6: Reference diagnostic methods available for antifungal susceptibility profiling. Adapted from Pappas *et al.* [5].

Test (method)	End point reading	Resistance detection			Advantages	Disadvantages
		<i>Echinocandins</i>	<i>Azoles</i>	<i>Amphotericin B</i>		
EUCAST (microbroth dilution)	Automated	Easy	Easy	Easy	<ul style="list-style-type: none"> • Pattern for the most resistant organism reported if mixed cultures are tested • Growth inhibition can be quantified in percent of growth control by a spectrophotometer • Objective endpoint reading 	<ul style="list-style-type: none"> • Not all antifungal compounds are commercially available • Most laboratories are not familiar with plate production and test principle • Requires an ELISA reader • The amphotericin B MICs tend to cluster in a narrow concentration range (which may lead to difficulties in correctly separating susceptible from resistant strains)
CLSI (microbroth dilution)	Visual (50 % or 100 % growth inhibition)	Easy	Difficult for isolates displaying trailing growth, which is defined as only partial growth inhibition over a wide concentration range	Easy	<ul style="list-style-type: none"> • Pattern for the most resistant organism reported if mixed cultures are tested • Growth inhibition can be quantified in percent of growth control by a spectrophotometer 	<ul style="list-style-type: none"> • Not all antifungal compounds are commercially available • Most laboratories are not familiar with plate production and test principle • Subjectivity in endpoint reading is inevitable • The amphotericin B MICs tend to cluster in a narrow concentration range

CLSI and EUCAST protocols differ in several technical aspects and variability can be observed in MIC values between both protocols while comparing the same strain treated with the same amount of drug. The different incubation times (24 h and 48 h for CLSI and 24 h for EUCAST), the sugar content of the culture's media (0.2 % for CLSI and 2 % for EUCAST), and the different approaches to determinate the MIC in CLSI and in EUCAST might be the reason for these differences in values. In fact, the EUCAST spectrophotometry method allows a proper quantification of fungal growth and eases the comparison of results between laboratories, while the CLSI visual approach is more subjective thus more prone to misinterpretation [20].

The EUCAST and CLSI defined two different limit values for a given drug: the epidemiological cut-off (ECOFF) and the clinical breakpoints (CBP), based on the MIC distribution in the pathogen's population. There is a light variability in these values depending on the standard protocol used due to the difference between the readout in both techniques (Table 7). The ECOFF can be determined visually and corresponds to the limit above which an isolate is no more considered as WT [20]. As example, the ECOFF value for FLC in *C. albicans* is 1 µg/ml (Figure 15, Table 7). On the other hand, CBPs are specific MIC values for discrimination between resistant and susceptible strains [38] and should reflect the relationship between *in vitro* antifungal activity and therapy outcome (Figure 15) [20]. These values have been determined by EUCAST, relating different clinical parameters such as *in vivo* pharmacodynamics and pharmacokinetics, resistance mechanisms and clinical response [39]. In the case of FLC, *C. albicans* strains with a MIC ≤ 2 µg/ml are considered susceptible, while strains with MIC ≥ 4 µg/ml are considered resistant. Therefore, 4 µg/ml is considered the CBP for FLC (Figure 15, Table 7) [38]. Resistance can be observed as an increase in MIC compared to values measured in reference susceptible organisms (Figure 17B) [33].

However, the power of the CBP to predict therapy outcome in *C. albicans* infections is limited. A 92 % success rate is observed over 550 events with FLC MICs of ≤ 2 µg/ml, while it decreases to 83 % success among 52 events with FLC MICs of ≥ 4µg/ml, and down to 37 % success over 212 events with MIC of 8

µg/ml [39]. These results demonstrate that antifungal susceptibility methods have a limited capacity to predict the response of fungal pathogens to antifungals *in vivo*. Strains determined as susceptible *in vitro* can thus still lead to therapeutic failure in animal experiments and more importantly in patients [20].

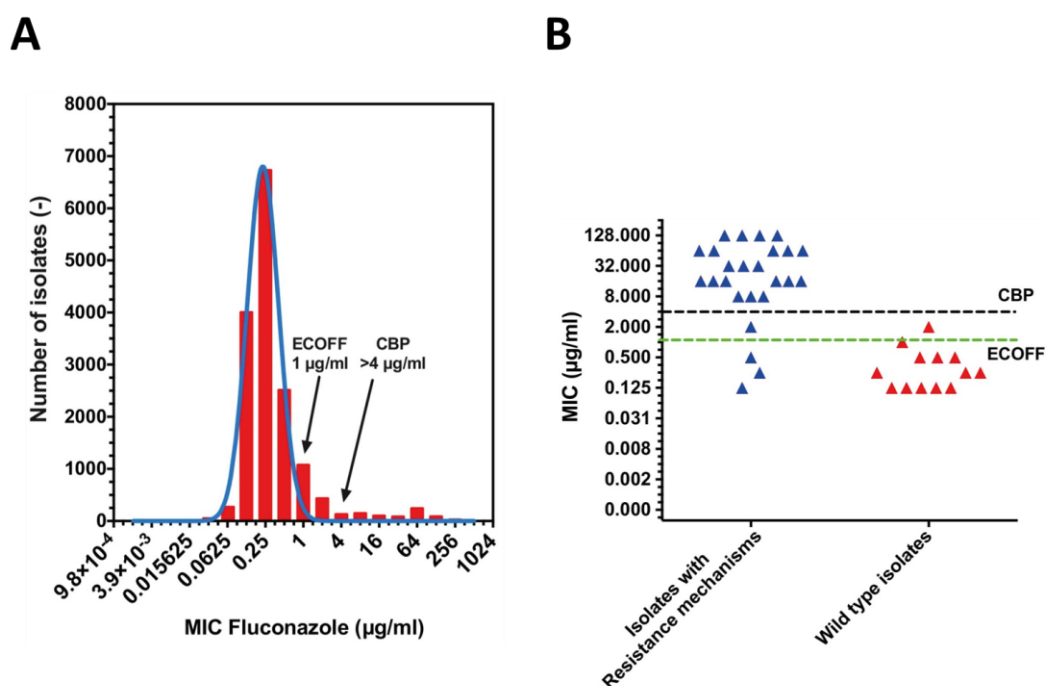


Figure 15: Distribution of FLC MIC values in *C. albicans*. (A) Gaussian curve representation of the FLC MIC distribution in the *C. albicans* population. (B) Distribution of MIC values accordingly to the occurrence of FLC resistance mechanisms. Clinical breakpoint value for resistance (CBP) and epidemiological cutoff value (ECOFF) are represented with corresponding drug concentrations. Blue and red triangles (B) represent isolates with and without known resistance mechanisms, respectively. Adapted from Delarze and Sanglard [20].

Table 7: ECOFF and CBP of different antifungal agents and *Candida* species. Both CLSI and EUCAST values are represented. Adapted from Delarze and Sanglard [20].

Species	Method	ECOFF (µg/ml)			CBP (µg/ml)					
		FLC ¹	AFG ¹	MFG ¹	FLC		AFG		MFG	
					S ²	R ²	S	R	S	R
<i>C. albicans</i>	CLSI	0.5	≤0.12	0.03	2	4	0.25	0.5	0.25	0.5
	EUCAST	1	0.03	0.015	2	4	0.03	0.03	0.016	0.016
<i>C. glabrata</i>	CLSI	32	≤0.25	≤0.03	0.002	32	0.12	0.25	0.06	0.12
	EUCAST	32	0.06	0.03	0.002	32	0.06	0.06	0.03	0.03
<i>C. parapsilosis</i>	CLSI	2	≤4	4	2	4	2	4	2	4
	EUCAST	2	4	2	2	4	0.002	4	0.002	2
<i>C. tropicalis</i>	CLSI	2	≤0.12	≤0.12	2	4	0.25	0.5	0.25	0.5
	EUCAST	2	0.06	0.06	2	4	0.06	0.06	IE ^c	IE
<i>C. krusei</i>	CLSI	64	≤0.12	≤0.12	- ³	-	0.25	0.5	0.25	0.5
	EUCAST	128	0.06	0.25	-	-	0.06	0.06	IE	IE

¹ (FLC) Fluconazole, (AFG) Anidulafungin, (MFG) Micafungin

² (S) Susceptible, (R) Resistant

³ (-) Antifungal use not recommended for this species, (IE) Insufficient Evidence of that the species is a good target for therapy with the drug.

Antifungal tolerance: definitions, relevance and known mechanisms

Definition of tolerance to antifungals

Among all the factors than can dictate the outcome of antifungal treatments, the ability of the pathogen to tolerate the presence of the drug is often neglected [20]. Drug tolerance is a well-known phenomenon in the field of antimicrobials and is globally defined as the ability of a pathogen to withstand killing at drug concentrations above the MIC [40].

Antimicrobial tolerance was first described for bacteria treated with bactericidal antibiotics [41, 42]. In bacteria, tolerance arises in the presence of drug where a subpopulation of dormant cells resists the “cidal” effect of the treatment. These cells, also known as persister-cells, have no genetic discrepancies with the rest of the population, thus highlighting a role of epigenetic modifications instead of the acquisition of mutation(s) as is the case for resistance [41]. These tolerant persister-cells have also been identified as a subpopulation of bacterial biofilms and might be linked to disease resurgence in the patient [41].

Antimicrobial tolerance has also been observed for fungal pathogens and can again be defined as the ability to survive at drug concentrations above the MIC. However, in comparison with antibacterial tolerance, it is necessary to adjust antifungal tolerance to the antifungal classes. Indeed, antifungal tolerance is mainly observed with fungistatic (*i.e.* azoles) rather than with fungicidal (*i.e.* echinocandins, polyenes) drugs. Somehow, one might say that fungal pathogens such as *C. albicans* are intrinsically tolerant to azoles as shown by their survival even at high drug concentration. However, the degree of azole tolerance can vary within the same species (Figure 16, Figure 17A) [20]. In susceptibility assays, tolerance is characterized by a phenomenon known as the trailing growth or residual growth that differentiates from an increase of MIC characterizing resistance mechanisms (Figure 16, Figure 17B-C) [20, 42].

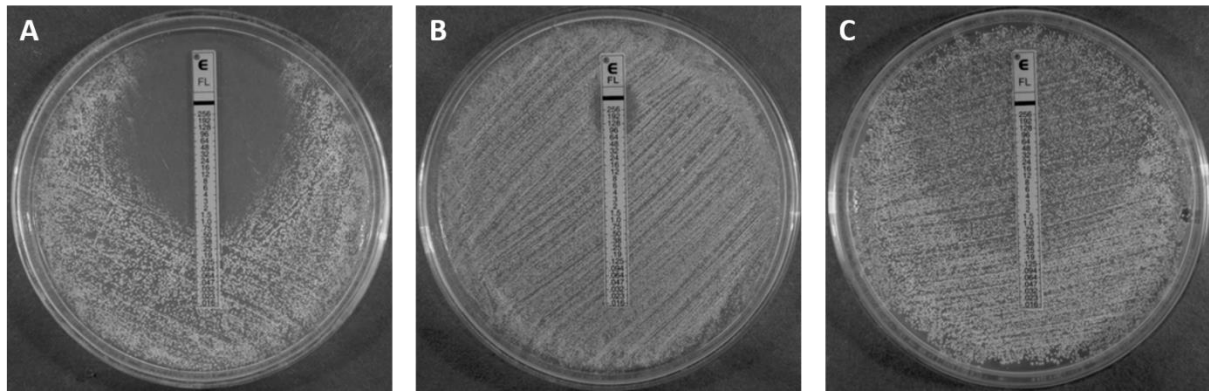


Figure 16: Susceptibility profiles to FLC on Etest. Strain susceptible to FLC (MIC < 4 µg/ml) (A), resistant to FLC (MIC > 4 µg/ml) (B) and tolerant to FLC characterized by a well-defined susceptible MIC (MIC < 4 µg/ml) and a residual growth (trailing growth) in the inhibition area (C). Adapted from Budzyńska *et al.* [43].

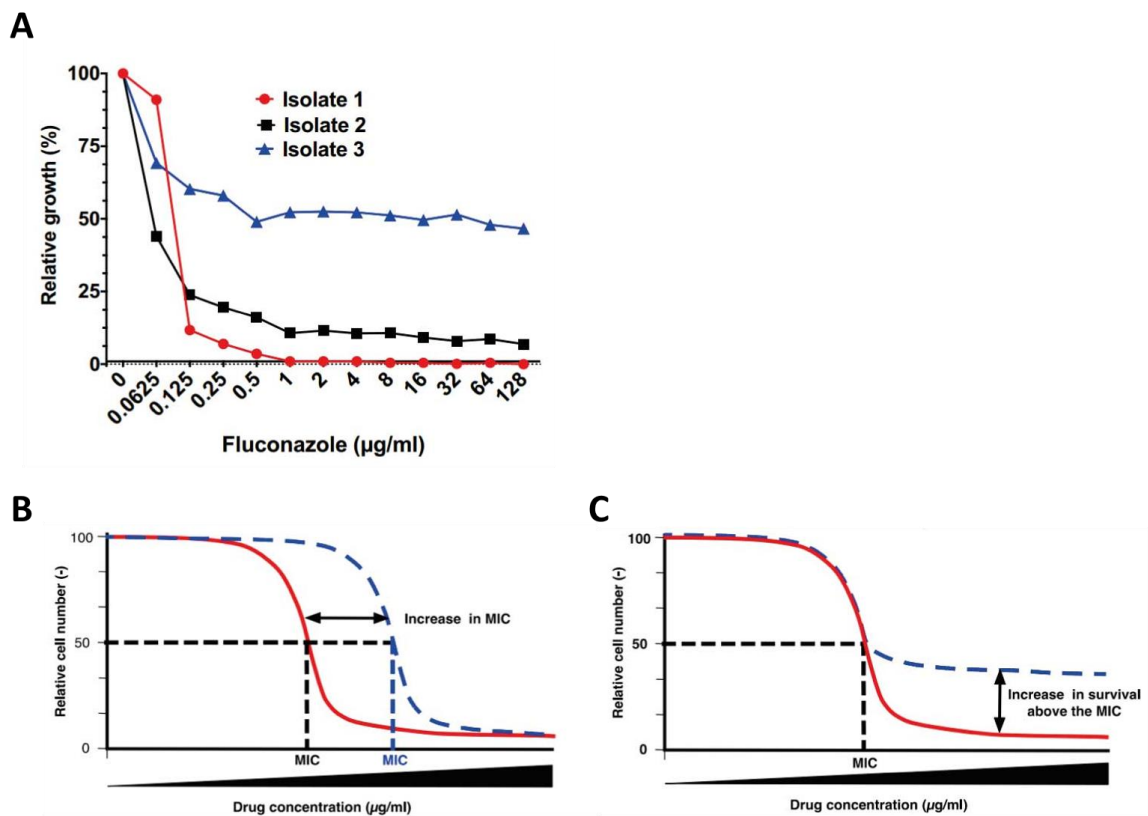


Figure 17: Susceptibility profiles to FLC in microdilutions assay. Susceptibility profiles of three clinical *C. albicans* isolates: isolate 1 is susceptible (MIC < 4 µg/ml), isolate 3 resistant (MIC > 4 µg/ml) and isolate 2 susceptible (MIC < 4 µg/ml) but with an increased residual growth, thus an increased tolerance to FLC (A). (B-C) Illustrations of the occurrence of antifungal resistance (B) and tolerance (C). The red curve corresponds to a susceptible wild type strain. An increased resistance is characterized by an increase of the MIC (panel B, blue dashed-curve) while an increase in tolerance is characterized by an increase of the residual growth without modification of the MIC (panel C, blue dashed-line). Adapted from Delarze and Sanglard [20].

Known mechanisms involved in FLC tolerance in *C. albicans*

The different levels of trailing growth reflect the different degrees of tolerance and thus might have an incidence on therapy outcome [20]. Until now, tolerance mechanisms have been poorly studied. It has been demonstrated that the immunosuppressive drug cyclosporine A can act with FLC and could convert this fungistatic drug into a strong fungicidal agent *in vitro*, thus reflecting a loss of tolerance [44]. Cyclosporine A, associated with cyclophilin A (*CYP*), targets calcineurin, which is a protein phosphatase activated by a calcium-dependent pathway [33]. Calcineurin is essential for the response of *C. albicans* to stress generating agents such as changes in temperature or antifungal treatment. It has been demonstrated that exposure of the calcineurin subunit A (*CNA/CMP1*) deletion mutant to FLC results in a strong loss of viability reflecting a loss of tolerance for the drug. In contrast, the deletion of the *CYP* gene was viable in presence of FLC and cyclosporine A. Calcineurin regulates drug tolerance only and not resistance, since the presence or absence of its activity does not affect drug susceptibility in drug susceptibility assays [44]. Calcineurin was also shown to be a client protein of the chaperone heat shock protein 90 (Hsp90) [27]. Inhibition of Hsp90 results in a loss of calcineurin activity and, therefore, in a loss of tolerance such as observed with the *CNA* deletion mutant [20, 45]. In another study, it was shown that the membrane trafficking through the late endosome/ pre-vacuolar compartment (PVC) had an impact upon *C. albicans* FLC tolerance. In fact, deletion of *VPS21*, an endosomal Rab family GTPase, was involved in PVC trafficking and enhanced *C. albicans* growth in the presence of FLC despite depletion of cellular ergosterol. This enhanced growth appeared as trailing growth in standard susceptibility assays, thus pointing to a potential role of Vps21 in azole tolerance. The *VPS21* deletion mutant presented less plasma membrane damage in presence of FLC than wild type strains. Indeed, the *VPS21* mutant released less cytoplasmic content following FLC treatment. In addition, the *VPS21* mutant contained abnormally high levels of intracellular Ca^{2+} , thus potentially increasing the basal level of calcineurin expression and/or activation. Indeed, in presence of FLC, an increase of calcineurin expression was observed in the *VPS21* mutant by using a reporter gene. A potential relationship between the endosomal trafficking and calcineurin pathway was thus

established which at least involved tolerance in *VPS21* deletion mutants. Furthermore, it was observed that the trailing growth with FLC was more present at 35°C than at 30°C, indicating that the drug caused less membrane damage at 35°C [46].

It has also been observed that *Rta3*, a putative lipid translocase, is co-upregulated with multidrug transporters by the transcription factor *TAC1* in resistant *C. albicans* strains. While deletion of *RTA3* increases the susceptibility to FLC, overexpression of *RTA3* results in an increase of tolerance characterized by a trailing growth in the susceptible *C. albicans* strain SC5314. The mechanisms by which *TAC1* and *RTA3* contribute to tolerance still remain unclear [47].

Recently, it has also been reported in *C. albicans* that the genes *FEN1* and *FEN12*, two genes involved in sphingolipid biosynthesis, might be involved in FLC tolerance. Indeed, it was observed that upon deletion of *FEN1* or *FEN12*, tolerance level increased in the presence of FLC. The increased survival of the mutants seemed to be linked to an increased intracellular FLC concentration and a decreased level in the plasma membrane of the toxic sterol 14-methylergosta-8,24(28)-dien-3,6-diol responsible for the toxic effect of FLC in *C. albicans*. These modifications in toxic sterol concentrations were reflected by a high level of sphingolipids which may improve cell membrane strength [48].

Another recently published study highlighted a tolerance mechanism involving the pH response via the Rim pathway. This pathway includes Rim9, Rim21/Dfg16, Rim8, Rim20 and Rim13. Under neutral-alkaline pH, this cascade leads to the cleavage of the C-terminal inhibitory domain of the transcription factor Rim101 leading to its activation. The culture medium's pH was already known to impact the level of tolerance *in vitro* [42] and it has been observed that tolerance decreases under acidic conditions, while it is not affected in neutral conditions (pH 6-7) [42]. A phenotypic and transcriptomic analysis of the Rim pathway showed that all Rim proteins were important for FLC tolerance as their respective deletion mutants exhibited increased FLC susceptibility [49]. The transcriptomic comparison between a *RIM101* deletion mutant and a WT strain at alkaline and acidic pH led to the identification of two Rim101 downstream targets including *HSP90* and *IPT1*. *HSP90* is already known to be involved

in antifungal tolerance on the opposite to *IPT1*, which encodes an enzyme involved in the biosynthesis of the most abundant sphingolipid in the plasma membrane (mannose-(inositol-P)₂-ceramide) [49]. Interestingly, *Ipt1* is part of the sphingolipid's biosynthesis pathway, downstream of *Fen1* and *Fen12*, both of which were reported as FLC tolerance mediators (see above). These data thus reinforce the idea that sphingolipids homeostasis is of relevance for FLC tolerance in *C. albicans*.

Even if the above-listed mechanisms may lead to azole tolerance, the exact molecular basis of tolerance is not completely understood. Moreover, these mechanisms have not been proved to mediate tolerance in clinical isolates. Tolerance may allow a better survival of *C. albicans* at high drug concentrations. The strong selective pressure induced by administered drugs and persistence resulting from residual growth may favor the acquisition of resistance mechanisms and may ultimately lead to treatment failure. Unraveling genetic and epigenetic mechanisms underlying tolerance and the discovery of tolerance mediators are essential steps for the development of potential inhibitors that, in combination with FLC, might offer new strategies to fight against *Candida* infections.

Aims of this work

In this project, our goal is to gain a better understanding of the mechanisms behind FLC tolerance in *C. albicans*. We aimed to better define FLC tolerance as well as to develop methods to rapidly and consistently identify tolerant isolates. These measures are necessary for the identification of genetic mediators of FLC tolerance.

To reach this goal, the following main objectives were defined:

- To give a clear definition of FLC tolerance to avoid misleading with resistance.
- To develop a method to identify and quantify FLC tolerance and to determine optimal test conditions.
- To identify tolerant clinical isolates for further investigations.
- To identify new mediators of FLC tolerance using forward genetic approaches.
- To characterize and confirm these candidate genes as mediators of FLC tolerance in *C. albicans* and especially clinical isolates.
- To determine the FLC response imprint in tolerant clinical isolates at the transcriptomic level.

Summary of main findings

In the first part of this thesis, a collection of known tolerant *C. albicans* clinical isolates was used to better defined FLC tolerance using the standard antifungal susceptibility assay protocol proposed by EUCAST. Basing ourselves on this protocol, a tolerance index (TI), reflecting the residual growth at FLC concentration above the FLC clinical breakpoint (4 µg/ml) was defined by conversion of the residual growth at 8 µg/ml FLC in an index ranging from 0 to 1 ($TI = \% \text{ of growth} / 100$). Selecting a single concentration to quantify tolerance allows an easy and quick way to assess tolerance of large strain collections. Establishment of the TI allowed the establishment of tolerance-thresholds at $TI = 0.2$ and $TI = 0.8$ or further discrimination between tolerant and resistant isolates. This definition and thresholds of tolerance as well as the effect of environmental pH on FLC tolerance were further confirmed using a collection of 172 clinical isolates which could be clustered depending of their TI and their response to pH.

In the second part of this thesis, we used the definition of tolerance proposed in the first part to identify new genetic mediators of FLC tolerance. For this purpose, a collection of 579 strains was used, each overexpressing a specific gene on a doxycycline dependent manner and bearing specific barcodes for their identification by sequencing. By pooling all strains in a single population and maintaining a selective pressure of FLC and doxycycline, we were able to enrich the pool in FLC-tolerant strains. The best candidates were tested in classical susceptibility assays to confirm their role in tolerance and three genes, *CRZ1*, *GZF3* and *YCK2* were related to an increased TI in when overexpressed. However, only *CRZ1* and *GZF3* overexpression reached the lower tolerance threshold and were further confirmed by overexpression in *CRZ1* and *GZF3* deletion mutant strains and by deletion in tolerant clinical isolates. Unfortunately, no negative regulators of tolerance could be identified.

In the third and final part of this thesis, a transcriptomic approach was used to assess the footprint response to FLC in the wild type strain SC5314 and related tolerant clinical isolates. These clinical

isolates were obtained over 8 years of persistence in an endocarditis patient treated with FLC and showed increased FLC tolerance over time. This approach confirmed that SC5314 activates several pathways related to the presence of FLC, particularly the calcineurin pathway and its downstream effector *CRZ1*. This response to FLC was also observed in the related clinical isolates and, interestingly, the calcineurin pathway and *CRZ1* were more overexpressed than in the susceptible SC5314. This overexpression pattern was also observed in the tolerant clinical isolates, thus suggesting the relevance of the calcineurin pathway for FLC tolerance in clinical isolates

Part one: Implementation of a tolerance index for the study and quantification of tolerance to fluconazole in *Candida albicans*.

Abstract

Candida spp. are major human pathogens and a major issue in intensive care units around the world. *Candida* spp. possess a high mortality rate despite the presence of antifungal treatments. One cause of these therapeutic failures is the acquisition of antifungal resistance by mutations in fungal genomes. In the case of the fungistatic azole fluconazole, the most widely used antifungal, the mechanisms of resistance have been extensively studied. However, some clinical isolates are known to be able to survive at high fluconazole concentrations without acquiring resistance mutations, a phenotype known as tolerance. Mechanisms behind fluconazole tolerance are not well studied, mainly due to the lack of a proper way to identify and quantify tolerance of clinical isolates. In this study, we proposed optimal culture conditions to study tolerance and presented a new easy and efficient method to identify and quantify tolerance to fluconazole. The method is based on the EUCAST microdilution susceptibility assay and is used to determine a tolerance index reflecting the level of tolerance in tested isolates. Tolerance indexes were used to delimit thresholds which can separate susceptible wild type isolates from tolerant and resistant ones.

Introduction

Candida species are major fungal pathogens which can cause life-threatening systemic infection known as invasive candidiasis. *Candida* infection are linked to a high mortality rate despite the presence of treatment with antifungals. This high degree of therapeutic failures might be partially explained by acquisition of resistance upon treatment [15, 19]. In the case of the widely used fungistatic drug fluconazole, resistance mechanisms have been extensively studied [32]. However, despite an extensive knowledge of these mechanisms, the acquisition of resistance does not explain all therapeutic failures. Indeed, it has been observed that some isolates identified as susceptible to fluconazole *in vitro* cannot be treated efficiently in the patient. It is known that some clinical isolates of *C. albicans* tolerate the presence of fluconazole more than others. These are characterized by an increased growth, known as residual growth, at drug concentrations above their minimum inhibitory concentration (MIC). This residual growth, which is a characteristic of drug tolerance, is in general not coupled to an increased MIC (unlike resistance) and is thought to favor the acquisition of resistance mechanisms due to extended survival of some *C. albicans* isolates upon treatment. Tolerant isolates may also to be a source of reinfection upon arrest of antifungal treatment [20].

A few mechanisms have been linked to FLC tolerance in *C. albicans* in the past and involve stress response mediators such as the heat shock protein Hsp90 or calcineurin [21, 44, 45], membrane composition through membrane trafficking (*VPS21*) [46], lipid translocation (*RTA3*) [47] and sphingolipid homeostasis (*FEN1*, *FEN12*, *IPT1*) [50, 51], and also the pH response (*RIM101*) [49]. However, while it remains unclear how these mechanisms exactly play a role in tolerance, these might be used as potential drug targets to increase FLC efficacy. It is thus important to identify new mediators of tolerance. To be able to identify tolerant strains as well as genes involved in tolerance, one needs a reliable method to quantify tolerance to FLC. A method based on disk diffusion assay on an agar medium has already been proposed in agar diffusion tests by the group of J. Berman. This assay quantifies the density of growth in the inhibition area and compares this density with the diameters of inhibition [50, 51]. This technique needs images captured in constant conditions (lighting, exposition,

etc.) as well as software manipulations. Here we propose an alternative approach to quantify tolerance based on the EUCAST microdilution assay and the use of spectrophotometry to determine a so-called tolerance index (TI) that allows the comparison of tolerant isolates and the future identification of mediators of tolerance to FLC. This method can easily be implemented in other laboratories and for other *Candida* species. We also discuss the selection of optimal growth conditions for tolerance assays as well as the definition of tolerance thresholds for the assignment of clinical strains to different phenotypic categories.

Material and methods

Strains used in this study

The wild type (WT) strain SC5314 and the *C. albicans* clinical isolates used in this study were selected for their known susceptibility to FLC and belong to D. Sanglard's lab collection (Table 8). SSI strains were kindly provided by M.C. Arendrup (Staten Serum Institute, Copenhagen, Denmark) and C. d'Enfert provided the CEC strain collection (Pasteur Institute, Paris, France) (Table 8 and Supplementary File 1 respectively).

Table 8: Strains and clinical isolates used in this study.

Lab ID	Alternative ID	FLC MIC (µg/ml)	Comments	Reference
DSY486	SC5314	NA ¹	wild type laboratory strain	[52]
DSY2102	572-10	2	Low-High phenotype ²	[42]
DSY2103	578-8	2	Low-High phenotype	[42]
DSY2104	623-11	2	Low-High phenotype	[42]
DSY2105	630-20	2	Low-High phenotype	[42]
DSY2106	630-11	2	Low-High phenotype	[42]
DSY2107	707-15	0.5	Low-High phenotype	[42]
DSY2108	34-023-096	1	Low-High phenotype	[42]
DSY2109	34-504-040	2	Low-High phenotype	[42]
DSY2110	34-028-117	1	Low-High phenotype	[42]
DSY4452	<u>11</u> 01-334 ³	NA	Isolated from an endocarditis patient	This study
DSY4453	<u>10</u> 52-920 ³	NA	Isolated from an endocarditis patient	This study
DSY4454	<u>05</u> 26-6020 ³	NA	Isolated from an endocarditis patient	This study
DSY4585	<u>12</u> 1206 1565 ³	NA	Isolated from an endocarditis patient	This study
DSY4586	<u>12</u> 1211 2250 ³	NA	Isolated from an endocarditis patient	This study
DSY4587	<u>13</u> 0411 1219 ³	NA	Isolated from an endocarditis patient	This study
DSY4588	<u>13</u> 0420 0673 ³	NA	Isolated from an endocarditis patient	This study
DSY4751	SSI 1489	0.25	"WT" ⁴	This study
DSY4752	SSI 2503	> 128	Resistant ⁴	This study
DSY4754	SSI 4622	0.125	Weak Trailing ⁴	[53]
DSY4758	SSI 5579	> 128	Heavy trailing ⁴	[54]
DSY4759	SSI 6028	0.25	Medium trailing ⁴	This study
DSY4806	SSI 3407	> 128	NA	This study
DSY4807	SSI 3408	0.25	NA	This study
DSY4808	SSI 5053	0.25	NA	This study
DSY4810	SSI 6037	0.25	NA	This study

¹Not Applicable/Not Available

²As described by Marr *et al.* [42]

³Boldfaced-underlined number indicate the year of sampling as 20xx

⁴Information from M.C. Arendrup

Media and growth conditions

All strains were stored in 20 % glycerol at -80°C and routinely grown at 30°C under constant shaking (220 rpm) in complete Yeast Extract Peptone Dextrose (YEPD) medium (1 % Bacto peptone, Difco Laboratories, Basel, Switzerland), 0.5 % Yeast extract (Difco) and 2 % glucose (Fluka, Buchs, Switzerland). When grown on solid YEPD plates (YEPDA), 2 % agar (Difco) was added and plates were incubated at 35°C.

For FLC susceptibility assays, strains were grown according to the EUCAST or CLSI recommendations [39, 40] in RPMI1640 medium with phenol-red (Sigma-Aldrich) complemented with 0.2 or 2 % glucose (Fluka, Buchs, Switzerland) and buffered with 0.33 M morpholinepropanesulfonic acid (MOPS). The pH was adjusted to pH 7.5, pH 7, pH 6 and pH 4.5, respectively, using NaOH or HCl. Stock solutions were prepared as 2x concentrated RPMI as recommended by EUCAST [38].

FLC susceptibility and tolerance assays

All FLC susceptibility assays were performed according to the *Reference Method for Broth Dilution Antifungal Susceptibility Testing of Yeasts* (M27-A3) [37] and the *Method for the determination of broth dilution minimum Inhibitory concentrations of antifungal agents for yeasts* (E.DEF 7.3.1) [38] with slight modifications when necessary. Susceptibility assays were performed in flat-bottom 96-well plates (Costar) and the fungal growth was measured spectrophotometrically for both methods. The minimal inhibitory concentration (MIC) was defined as the first concentration of drug inhibiting at least 50 % of fungal growth as compared to a drug free control. Strains with a MIC below 4 µg/ml FLC were defined as susceptible as described by EUCAST [38]. Susceptibility assays were performed in RPMI at pH 7.5, pH 7, pH 6 or pH 4. Tolerance assays were performed in the same conditions but using one fixed only at FLC concentration as specified in the corresponding experiment.

Briefly, individual colonies of each tested strain were grown overnight in YEPD medium at 30°C under constant shaking (220 rpm). Cultures were centrifuged (5 min, 4600 rpm, 4°C) and washed twice with PBS (137 mM NaCl, 10 mM Phosphate, 2.7 mM KCl, and pH 7.4). Cell concentration was estimated by

spectrophotometry ($OD_{540\text{ nm}}$) and cells resuspended at 5×10^5 cells/ml in distilled water. Then, 100 μ l of this suspension were transferred into the wells of flat-bottom 96-well plates (Costar) containing 100 μ l of 2x RPMI (0.2 or 2 % glucose for CLSI and EUCAST condition, respectively) complemented with 256-0 μ g/ml FLC in two-fold dilutions or fixed FLC concentrations (16 μ g/ml), to obtain a final cell concentration of 2.5×10^5 cells/ml and FLC concentrations ranging from 128 to 0 μ g/ml (8 μ g/ml for tolerance assays) per well. Plates were incubated at 35°C without shaking for 24 h. Cell growth in each well was measured by spectrophotometry ($OD_{570\text{ nm}}$) using a microplate reader (Multiskan Ascent) and compared to the drug free control after correction with a blank control. From these susceptibility curves, both the MIC and the tolerance index (TI), corresponding to the relative growth (% GC) at 8 μ g/ml FLC divided by a factor 100 ($TI = \% GC/100$) were extracted for strain comparisons. The TI is used to determine the level of tolerance of the tested strains.

Growth curve

To determine the growth rate of selected *C. albicans* isolates, growth curves were performed in EUCAST culture conditions. Briefly, individual colonies of *C. albicans* clinical isolates were grown overnight at 30°C in YEPD medium under constant shaking (220 rpm). Cultures were centrifuged (5 min, 4600 rpm, 4°C) and washed twice with PBS. Cell concentration was estimated by spectrophotometry ($OD_{540\text{ nm}}$) and cells resuspended at 5×10^5 cells/ml in distilled water. and 100 μ l of this suspension were transferred in the wells of a flat-bottom 96-well plates containing 100 μ l of 2x RPMI (2 % glucose) adjusted to pH 7.5, pH 7, pH 6 and pH 4.5 to obtain a final cell concentration of 2.5×10^5 cells/ml. Plates were incubated at 30°C without lids and the $OD_{540\text{ nm}}$ of each well automatically measured every 15 min for 24 h using a microplate reader (FLUOstar Omega, BMG Labtech). Plates were not incubated at 35°C as recommended for drug susceptibility assay due to evaporation issues. Growth rates were estimated in the exponential phase of the growth curves by calculating the exponential growth equation (non-linear regression) using GraphPad Prism.

Software and statistical analysis

Graphics and statistical analysis were performed in GraphPad Prism 7.03 (GraphPad Software, Inc., La Jolla, CA, USA). The online software Morpheus (<https://software.broadinstitute.org/morpheus>) was used to create heatmaps for the tolerance profile screening.

Results

Determination of optimal culture condition for FLC tolerance identification

Several techniques are available to establish the antifungal susceptibility profiles of defined *Candida* isolates. Most of them are based on drug diffusion assays in either a solid agar medium or in liquid conditions, with each protocol having its specific endpoint readout [5]. Despite having the same purpose (*i.e.* identifying susceptible and resistant isolates), each method has its advantages and flaws. Indeed, depending on the *Candida* species and the tested drug, a given protocol might be more optimal than another [5]. Since a method for the identification and quantification of tolerance to FLC on agar medium has already been proposed by the group of J. Berman [51, 52], we focused here on the identification of tolerance using standardized susceptibility assays in microtiter plates (proposed by the EUCAST and the CLSI) as it could be implemented in most laboratories.

First of all, to determine which method was the best to identify azole-tolerant strains, we performed drug susceptibility assays for known tolerant isolates (kindly provided by M.C. Arendrup, Table 8, Figure 18) using both EUCAST and CLSI protocols. In order to compare both methods, we decided to slightly modify the CLSI protocol by performing the assay in flat-bottom microtiter plates and using endpoint spectrophotometry as recommended by EUCAST. As stated by *Marr et al.* [42], the pH of the culture medium might influence the level of tolerance. Thus, we decided to perform FLC susceptibility assays at pH values of 7.5, 6 and 4.5. As shown in Figure 18, the tested strains clearly exhibited different growth profiles in the tested conditions, with a global increase of the residual growth at acidic pH.

The clinical isolates DSY4751, DSY4754 and DSY4759 could be categorized as susceptible in all the tested conditions, as represented by their MIC below the breakpoint (CBP) of 4 µg/ml for FLC in *C. albicans*. However, each strain clearly exhibited a different level of residual growth above the MIC, ranging from low values (1-2 %) to around 50 % depending of the strain and the condition (Figure 18, blue, green and purple curves, respectively). On the other hand, strain DSY4752 was considered as resistant, with a relative growth remaining at around 100 % independently of the FLC concentration,

pH and the protocol tested (Figure 18, red curves). Finally, isolate DSY4758 was more ambiguous. Indeed, using the EUCAST definitions, DSY4758 should be considered as resistant as its relative growth almost never lied under the 50 % threshold, except at pH 7.5 for both protocols where it was equal to 50 % (Figure 18, orange curves). However, when we compared the susceptibility profiles of DSY4758

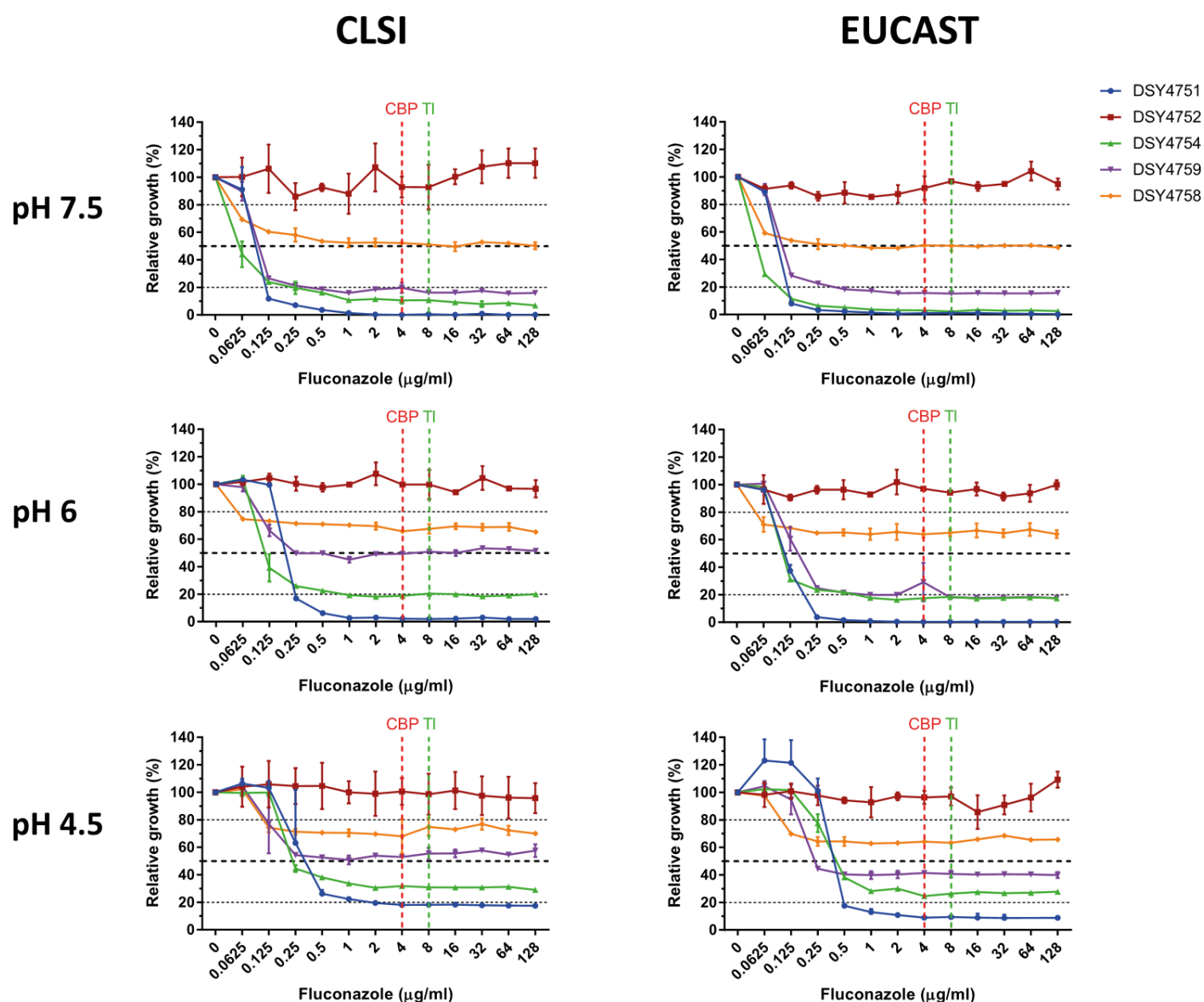


Figure 18: Comparison of EUCAST and CLSI conditions for the identification of tolerant *C. albicans* isolates using FLC susceptibility assays. Curves are representative of the mean relative growth of at least biological duplicates with their standard deviation. Vertical dotted lines correspond to the CBP (red line, 4 µg/ml FLC) and the concentration at which the tolerance index is established (TI, green line, 8 µg/ml).

with those of the resistant strain DSY4752, a growth reduction could still be observed at low FLC concentrations (0-0.125 µg/ml FLC), even if growth stayed below 50 % (Figure 18). This growth

reduction suggests that FLC still possessed a fungistatic effect on DSY4758 and thus indicates that this strain might not be considered as resistant, but rather as highly tolerant to FLC. A more detailed analysis on the occurrence of resistance mechanism(s) in this strain may confirm this hypothesis.

Establishment of a tolerance index and tolerance thresholds

To determine which strains could be considered as tolerant, we decided to set thresholds which will help to assign strains as susceptible or resistant. We decided to consider all strains that show a decreased growth in the presence of FLC as tolerant, even if some strains would be considered resistant depending on EUCAST recommendation (*i.e.* strains remaining above the 50 % cut-off value). For such strains, additional controls should be undertaken to ascertain the absence of resistance mechanisms to FLC. On the other hand, susceptible isolates with low residual growth above the MIC (1-10 % relative to growth control) may be considered to exhibit wild type characteristics. Taken the isolates of Figure 18 as guides, it is proposed here to assign strains as tolerant to FLC when the residual growth ranges between 20 % and 80 % as compared to a drug-free control after 24 h incubation and at drug concentrations above the FLC CBP (4 µg/ml) (Figure 19A). Even though these thresholds are not based on the occurrence of molecular markers of tolerance, they still allow a discrimination that will be useful in this study. These threshold ranges were further validated with additional strain collections (see below). To facilitate strain comparisons, a tolerance index (TI) was established. This index (ranging from 0 to 1) reflects the relative growth at 8 µg/ml FLC ($TI = \% \text{ of growth} / 100$) and was chosen since it is above the CBP for FLC (4 µg/ml) (Figure 19A). Strains with a TI between 0.2 and 0.8 are thus considered as tolerant (Figure 19B). The choice of using only the residual growth at a concentration of 8 µg/ml FLC instead of measuring the mean residual growth at all concentrations above the CBP (which might be more precise) was made to facilitate the screening of large strain collections.

For further discrimination between tolerant strains, a level of tolerance was established which was adapted from the work of Rueda *et al.* [55]. Indeed, Rueda *et al.*, defined tolerance as an inhibition of

the growth by the drug in at least four consecutive wells which maintained a residual growth with increasing concentrations of the drug [55]. From this definition, they proposed the following categories which are based on the relative growth as compared to the drug free growth control (% GC): (i) no tolerance (≤ 5 % GC), moderate tolerance (6-24 % GC) and strong tolerance (25-49 % GC). Strains with a relative growth above 50 % GC were considered as resistant according to EUCAST recommendations [55]. In our case, as we decided to consider all strains showing growth reduction in presence of FLC as tolerant, we propose the following thresholds and categories of tolerance: strains with TIs between 0.2 and 0.25 were defined as low trailers, between 0.25 and 0.5 as medium trailers and between 0.5 and 0.8 as heavy trailers. Strains with TIs above the 0.8 threshold ($TI > 0.8$) were indicative of resistance, since such strains do not respond to growth inhibition by FLC at a concentration of 8 $\mu\text{g/ml}$. Strains with a TI under the 0.2 threshold ($TI < 0.2$) indicate that they are fully FLC-susceptible and, since they differ from tolerant strains by their residual growth, were categorized as “wild type” as suggested above.

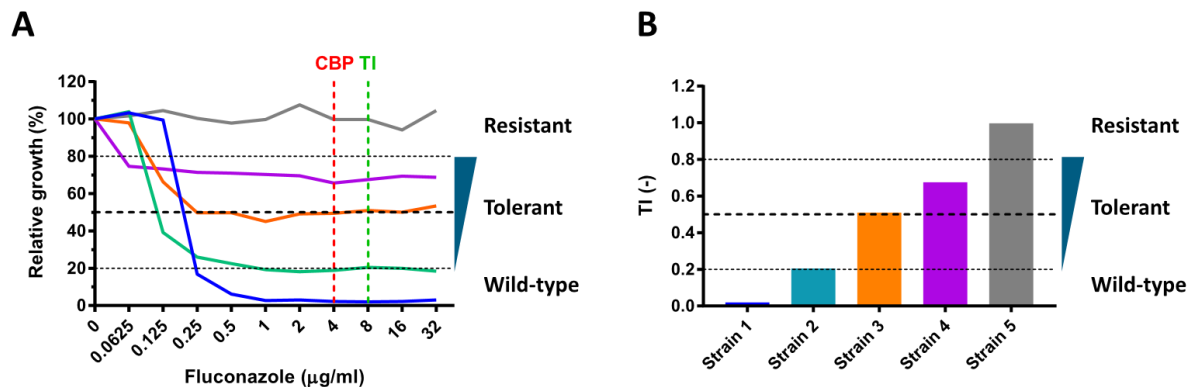


Figure 19: Identification of tolerant strains and definition of tolerance index (TI). Panel A represents 5 clinical isolates with different susceptibility profiles to FLC. The level of tolerance is characterized by the tolerance index (TI, green dashed-line) which corresponds to the residual growth above the FLC clinical breakpoint (CBP, red dashed-line) at 8 $\mu\text{g/ml}$ FLC (green dashed-line). Panel B represents the TI as bar-plot after transformation into an index ranging from 0 to 1 ($TI = Y/100$, Y being the relative growth in % from panel A). This TI allows the discrimination between wild type susceptible isolates (blue strain, $TI < 0.2$), susceptible but tolerant isolates (indigo, orange and purple strains, $0.2 \leq TI \leq 0.8$) and true resistant isolates (grey isolate, $TI > 0.8$).

Selection of culture conditions for the identification of tolerance

Using these definitions of tolerance and these thresholds, we analyzed which of the CLSI and EUCAST protocols was optimal for the assessment of tolerance in *C. albicans*. For this, we determine the TIs of the five previously used clinical isolates (Table 8) and compared them using both the CLSI and the

EUCAST methods (Figure 20). Fundamentally, no differences between the two protocols could be observed except for DSY4759 at pH 6 (Figure 20B). The absence of differences between both protocols was confirmed by the high correlation between the TIs in both approaches at every tested pH ($R^2 > 0.88$, Figure 20D). Despite the absence of differences, the CLSI method seemed to slightly increase the tolerance of most strains tested even if this observation was not significant (Figure 20A-C). Due to the similarities between both CLSI and EUCAST conditions to assess tolerance, we decided to use the EUCAST protocol as our standard protocol to assess and identify tolerance in *C. albicans* as it does not require any modification of the approach, unlike the CLSI method where the readout and culture conditions were slightly modified.

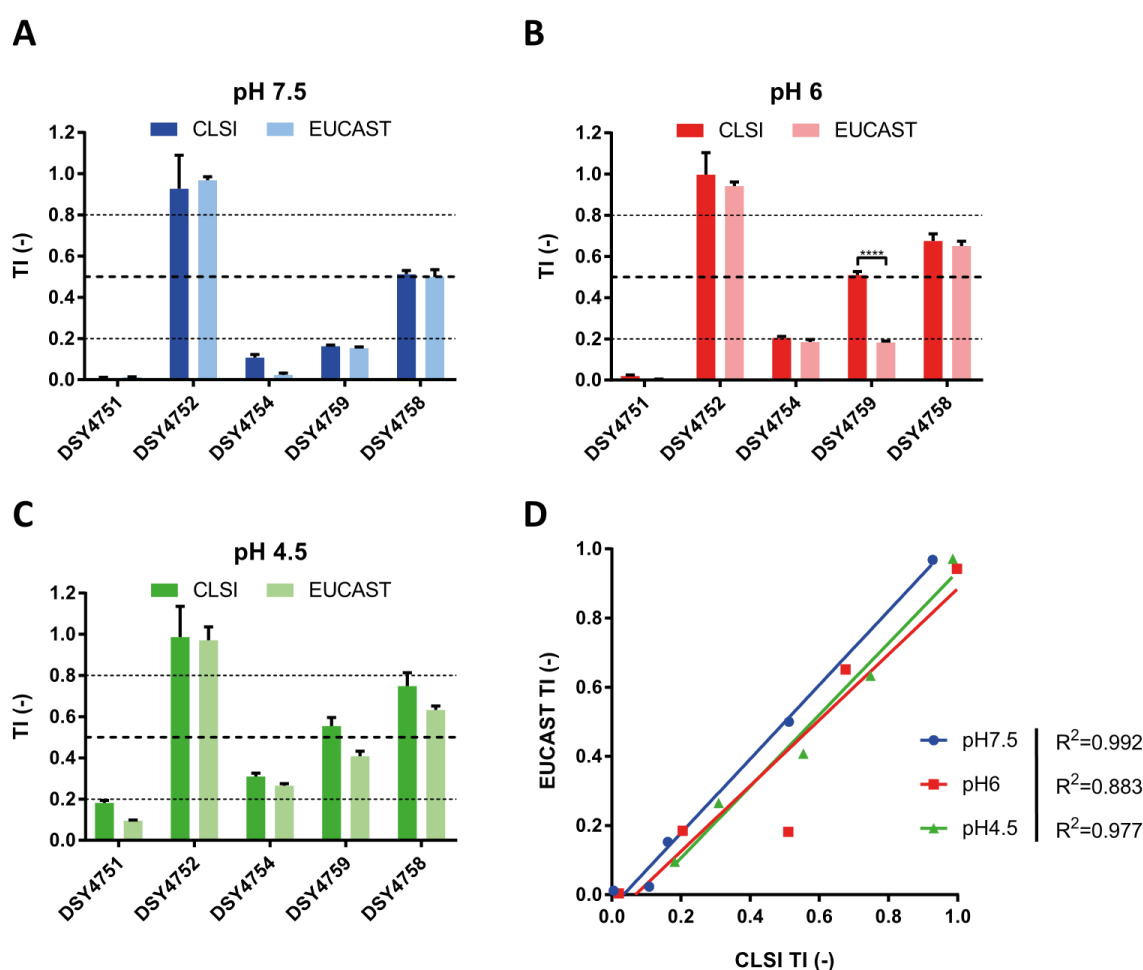


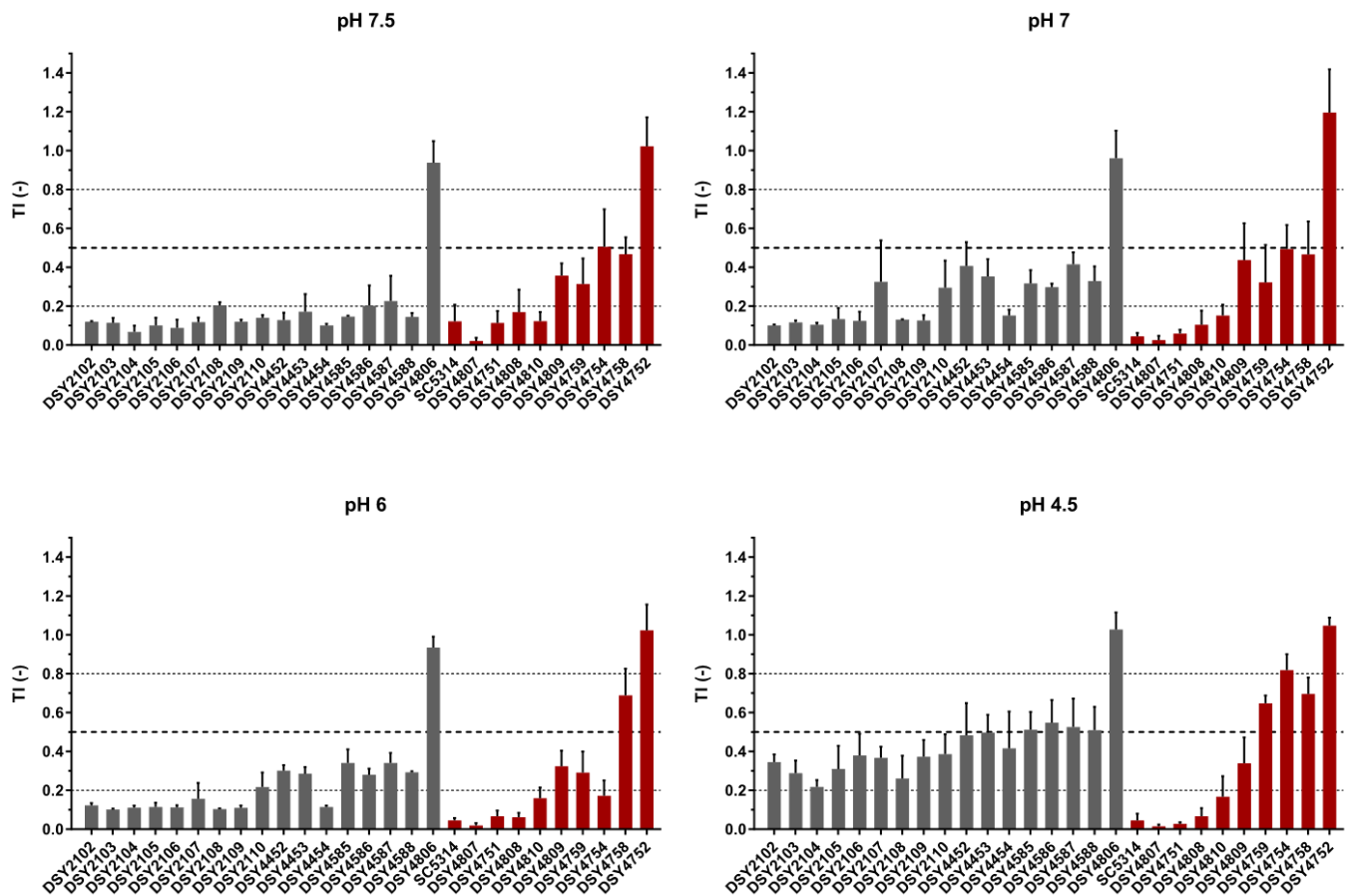
Figure 20: Comparison of CLSI and EUCAST protocols for the identification of tolerant isolates. Comparison was performed at pH 7.5, 6 and 4.5 (panel A, B and C respectively) to assess the pH effect upon tolerance as stated by Marr *et al.* [42]. Panel D represents the correlation between both approaches with the respective R^2 corresponding to each tested pH (Two-tailed Pearson correlation, confidence interval = 95 %). Each bar corresponds to the mean of biological duplicates. Statistical significance was calculated using Sidak's multiple comparison tests (two-way ANOVA, 95 % confidence interval). P-values: 0.1234 (ns), 0.0332 (*), 0.0021 (**), 0.0002 (***), < 0.0001 (****).

Application of the tolerance assay for the identification of tolerant strains

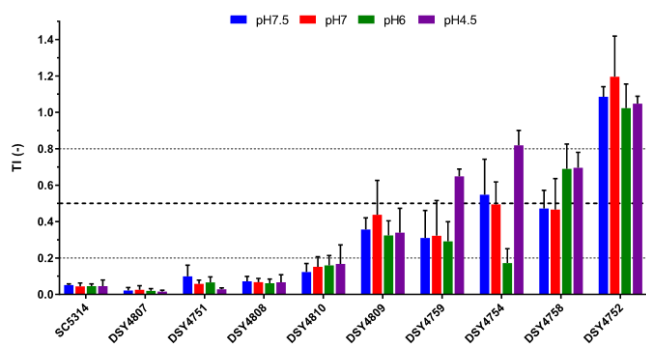
To confirm the efficiency of the TI to identify tolerant strains, we next performed a small-scale screening of 28 strains (also including the strains DSY4751 to DSY4759 discussed above) (Figure 21, Table 8, including the WT strain SC5314 as a susceptibility control. To extend our view of the pH effect on tolerance and to be exactly in the EUCAST standard conditions, a fourth condition at pH 7 was added. Using our definition of tolerance, we obtained 7 strains out of 28 with a TI between 0.2 and 0.8, whatever the tested pH condition (DSY2110, DSY4586, DSY4587, DSY4809, DSY4759, DSY4754, and DSY4758) (Figure 21A). All these strains originate from patients with either candidemia or endocarditis (Table 8). Out of these tolerant isolates, three strains could be defined as heavy trailers ($0.5 \leq TI \leq 0.8$), but in a pH-dependent manner. Indeed, strains DSY4759 and DSY4754 had a $TI > 0.5$ at pH 4.5 only, while DSY4758 exhibited a $TI > 0.5$ at pH 6 and 4.5. However, these strains exhibited $TIs < 0.5$ at more alkaline pH (Figure 21A).

Interestingly, and according to the work of Marr *et al.* [42], we were also able to observe an effect of the culture pH upon tolerance (Figure 21A). However, unlike their observations, the tolerance level of the tested strains seemed to increase at acidic pH. Indeed, most of the tested strains exhibited TIs between 0.2 and 0.5 at pH 4.5. Fifteen strains defined as wild type at pHs 7.5, 7 and 6 became tolerant ($0.2 \leq TI < 0.5$) at pH 4.5 (Figure 21A and B). The pH-dependent effect of the pH on tolerance is consistent with previous publications [42], but is strain-dependent. Additional strains must be screened to confirm a more general effect of the pH on tolerance.

A



B



C

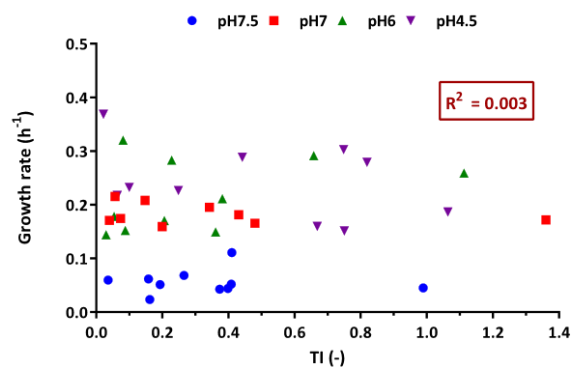


Figure 21: Screening of clinical isolates and TI determination. TI level at different pH conditions of 28 *C. albicans* strains (Panel A). Red columns correspond to selected isolates (Panel B) used to calculate their growth rates and to correlate them with their respective TIs (Panel C). Horizontal dashed lines represent the TI = 0.2, 0.5 and 0.8 thresholds used to determine the tolerance profile to FLC. Each bar corresponds to the mean of at least 3 biological replicates. Correlation analysis was done using a two-tailed Pearson correlation (confidence interval =95 %).

To exclude that these differences in tolerance levels are not simply due to differential growth between strains and growth conditions, the growth rates of 10 selected isolates (Figure 21A, red columns and Figure 21B) were calculated for the exponential phase after 24 h in conditions similar to tolerance assays. The growth rate (h^{-1}) of each strain was then compared to its respective TI in the same conditions (Figure 21C, right panel). No correlation could be observed between growth rates and TIs ($R^2 = 0.003$; Figure 21C), indicating that a growth rate difference does not explain an increased tolerance to FLC. Thus, other yet unknown mechanisms must be involved in FLC tolerance.

Now that the protocol for identification of tolerant strains was optimized, a larger isolate collection was tested. In collaboration with the group of C. d'Enfert (Pasteur Institute, Paris), a screen of 154 clinical isolates (Supplementary File 1) was undertaken to determine TIs at pH 7.5, 7, 6 and 4.5 (Figure 22). Data from our previous screen (strains SC5314, DSY4752, DSY4758, DSY4808 and DSY4809) were also included as controls for a total of 159 tested strains.

From the available data we were able to identify 6 main categories of phenotypes, according to the level of tolerance of the tested strains (Figure 22). A first category contained susceptible strains with TIs between 0 and 0.2 at all tested pH levels (Figure 22, category 1). As defined earlier, the wild type isolates belong to this category of strains. A second category contained a few strains which were clearly resistant ($\text{TI} > 0.8$) in all conditions (Figure 22, category 6). Between these two categories, several profiles corresponding to tolerant strains were observed. Indeed, strains from category 2 (Figure 22) were clearly tolerant ($0.2 < \text{TI} < 0.5$), but only at acidic pH (pH 4.5). On the other side, strains from category 3 (Figure 22) were tolerant, but only at alkaline and neutral (for some) pH (pHs 7.5 and 7, respectively). Some strains were also tolerant, but at both alkaline and acidic pHs (Figure 22, category 4). We were also able to identify strains which were tolerant at all (or almost all) tested pH levels. These strains also showed the highest tolerance of all tested strains ($0.5 \leq \text{TI} \leq 0.8$) and, some of them at a TI limit that could assign them as resistant ($\text{TI} > 0.8$) at some pH levels (Figure 22, category 5).

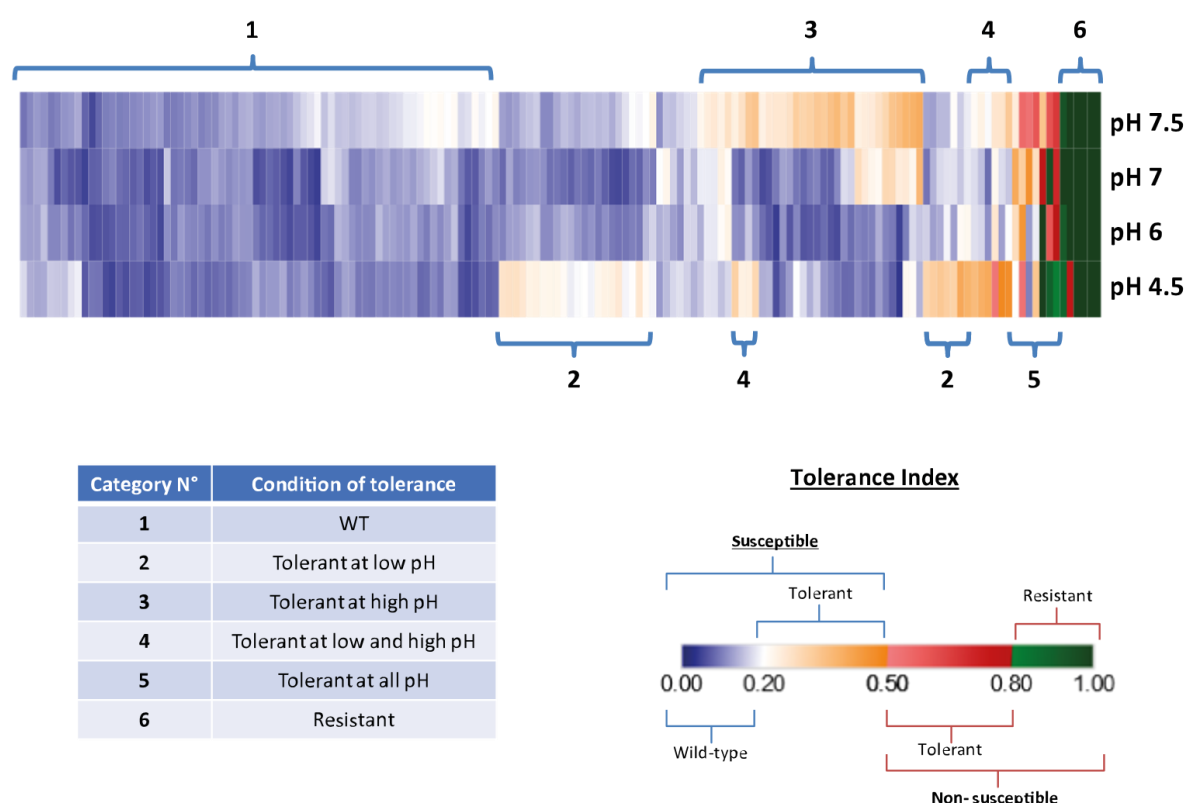


Figure 22: Tolerance screen of 159 *C. albicans* strain. The heatmap represents the mean TI values of at least biological duplicates. The “Susceptible” and “Non-susceptible” categories of the legend are based on the EUCAST definitions. Detailed results can be found in Supplementary File 1.

Conclusions

Up to now, most of *C. albicans* treatment failures with FLC were imputed to the development of resistance, however, in some cases, strains defined as susceptible were also observed to cause treatment failures. Tolerance, by its increased survival in the presence of drug, may also be involved in such failures. Up to now, tolerance mechanisms have been poorly studied and characterized and remain unclear. In this project, we aimed to better define tolerance to FLC and to identify tolerance mediators in *C. albicans*. Indeed, nowadays, tolerance is too often confounded with the description of drug resistance in published studies. In this study, we aimed first to establish a clearer definition of tolerance and, second, to propose a simple method for its quantification in order to compare the FLC tolerance between different strains. Microdilution susceptibility assays are widely used to assess antifungal susceptibility of fungi. The two standardized protocols (*i.e.* CLSI and EUCAST) slightly differ from each other, the main differences being the initial inoculum, the glucose concentration and the

endpoint readout in different types of microtiter plates. By adjusting the CLSI protocol to use the same readouts as the EUCAST protocol, we were able to compare the susceptibility of different *C. albicans* clinical isolates. However, to be able to quantify and compare the tolerance of the different isolates, we first proposed an adequate definition of tolerance for microdilution assays. Using the optical readout of the EUCAST protocol, we decided to consider as tolerant all strains that show a decreased growth in the presence of FLC, but with their residual growth ranging between 20 and 80 % of growth as compared to drug-free control after 24 h incubation and at drug concentrations above the FLC CBP (4 µg/ml). This measure distinguishes these isolates from those that are true susceptible (*i.e.* wild type isolates) and true resistant ones. Isolates exhibiting residual growth above 50 % should be further analyzed for the occurrence of known FLC resistance mechanisms. To be able to quantify FLC tolerance and compare strains, we established a tolerance index (TI) which reflects the relative growth of isolates at 8 µg/ml FLC ($TI = \% \text{ of growth}/100$). Among strains considered as tolerant ($0.2 \leq TI \leq 0.8$), further discrimination was made based on the work of Rueda *et al.* [55], who proposed categories of tolerance according to EUCAST and thus avoiding all strains with a $TI \geq 0.5$ which were considered as resistant. Here we proposed extended thresholds, considering all strains affected by FLC as tolerant, and different levels of tolerance that included low trailers ($0.2 \leq TI < 0.25$), medium trailers ($0.25 \leq TI < 0.5$) and heavy trailers ($0.5 \leq TI \leq 0.8$).

Using this new TI to determine which of the CLSI or the EUCAST conditions were optimal to assess tolerance in clinical isolates, we showed that no major differences between these methods could be observed after 24 h incubation. The CLSI culture conditions seemed however to slightly increase tolerance, but not significantly. Thus, to be as close as possible to the standardized protocols (*i.e.* without modifications), the EUCAST protocol was chosen as the standard condition for further tolerance assays. The selection of a single dilution to assess the level of tolerance (8 µg/ml) allowed us to develop a rapid and convenient method to perform a large screening of tolerance by performing assays at this single concentration ("Tolerance assay"). This versatile method can easily be adapted to

other *Candida* spp. as well as other antifungal agents. It can also be used for the screening of synergy between different drugs.

Using this newly established protocol, we first performed a screening of 28 clinical *C. albicans* isolates (already characterized as susceptible or resistant) to identify tolerant strains and to characterize the effect of culture pH on residual growth. This screening allowed the identification of 7 strains out of 28 that were tolerant at every pH conditions tested. The tolerance level of the other strains was influenced by the tested pH. Indeed, 15 strains defined as WT ($TI < 0.2$) at pH 7.5, 7 and 6 became tolerant at pH 4.5 ($TI \geq 0.2$). We rejected the role of altered growth patterns in this increase of tolerance by estimating the correlation between the TI and the growth rate of the corresponding isolates. This pH effect upon tolerance was also observed in a second and larger screen of 159 *C. albicans* strains where different tolerance categories could be established. Indeed, of the 159 tested strains, 73 were considered as WT ($TI < 0.2$) at all tested pHs. Twenty-four isolates showed a tolerance between $TI = 0.2$ and 0.5 at pH 7.5, against 22 isolates tolerant at pH 4.5 only. A few strains (10) were tolerant at both pH 7.5 and 4.5. Only 2 strains were tolerant at all tested pHs, but with a high tolerance level ($0.5 \leq TI \leq 0.8$). Isolate DSY4758 was also tolerant at all pHs except at pH 4.5 where it was borderline with the upper threshold of tolerance ($TI = 0.81$). Interestingly, out of the 9 isolates which were considered as resistant to FLC ($TI > 0.8$) at one or more pH, 6 were known to harbor amino acid substitutions linked to resistance in *ERG11*, *TAC1* and *UPC2* (Table 9), and 5 were resistant at all pH values. The TI threshold that was chosen here for assigning strains as resistant appeared therefore validated since tested resistant strains harbored known genetic alterations associated with resistance mechanisms. So far, our observations highlighted a strain-dependent effect of pH upon FLC tolerance. The tendency of decreasing tolerance with decreasing pH was reported earlier by Marr *et al.* [42] and more recently by Rosenberg *et al.* [51]. It is not clear as to why our results differ from these published results. The methods used in these studies referred to minimal culture medium and to agar diffusion assays, respectively. Thus, one might argue that these assay conditions could have impacted on the obtained results. Since different isolates were used in these different studies including ours, it is difficult to

identity the cause of such disagreements. Another study published by Luna-Tapia *et al.* in which a *VSP21* mutant exhibited high tolerance to FLC assayed the mutant at both pH 7 and pH 3 [46]. In this work, a CLSI protocol was used which therefore was more closely related to the conditions tested here. Luna-Tapia *et al.* demonstrated that tolerance of the *VSP21* mutant was decreased at pH 3 compared to neutral conditions [46]. While these data support pH dependency on FLC tolerance, the results used a specific mutant which might trigger pH-specific response and might differ from clinical wild type isolates. Thus, pH dependency of FLC tolerance remains controversial.

To conclude, the different screens performed in this study showed the effectiveness of our tolerance assay protocol which, in addition with the establishment of the TI, offers an easy and rapid way to identify tolerant isolates for further study and which can be implemented as a routine protocol in most laboratories. This tolerance assay can also be easily modified and adapted to other antifungals and fungal pathogens.

Table 9: Amino acid substitutions leading to azole-resistance in CEC strains resistant to FLC.

Lab ID	CEC ID	FLC MIC (µg/ml)	Amino acid substitutions		
			Erg11	Tac1	Upc2
DSY5096	CEC718	>256	Y132H ¹ , P236S ² , S405F	A736T	G657D
NA ³	CEC4509	>256	R157K	H263Y, H838Y, C858Y	NA
NA	CEC4503	>256	R157K	H263Y, H838Y, C858Y	NA
NA	CEC4520	>256	Y132H, G45OE	H263Y, P971S	NA
NA	CEC4525	>256	Y64H , T123I, Y132H, R467I	H263Y, P971S	D654N ^h
NA	CEC4528	8	G448E	A737T, N823K, C858Y	NA

¹Amino acid substitutions previously involved in azole resistance or described as a gain-of-function mutation

²New mutations

³Not Applicable

^hHeterozygous mutation

Part two: Identification and characterization of the transcription factors *CRZ1* and *GZF3* as mediators of tolerance to fluconazole in *C. albicans*.

Abstract

Candida albicans remains a challenging human fungal pathogen, mainly due to the limited treatment options available and the acquisition of resistance leading to treatment failures. Resistance mechanisms to azoles, mainly fluconazole (FLC), the most widely used antifungal have been extensively studied in the past decades. However, another phenomenon, called antifungal tolerance, characterized by the ability to withstand growth in the presence of high drug concentrations without acquiring resistance mutations may also be involved.

Little is known about mechanisms behind FLC tolerance but identifying mediators of tolerance might lead to the development of new treatment strategies by increasing fluconazole efficiency. In this study we proposed an approach based on the use of a collection of 579 strains, each overexpressing a specific gene and possessing a distinct barcode allowing its identification by sequencing. By pooling the whole collection and by maintaining the isolates under strong FLC pressure for several days, we were able to identify 79 strains which were enriched and 39 which were depleted in the pool in the presence of the drug. Out of these, two transcription factors *CRZ1* and *GZF3* were further confirmed to be positive mediators of FLC tolerance and their role was confirmed by overexpression of each gene in deletion mutants. We show here that *GZF3* acts probably downstream of *CRZ1*. Each of these factors were deleted in a set of clinical strains exhibiting FLC tolerance. Our results show that *CRZ1* plays a critical role in FLC tolerance in these strains while *GZF3* seems to be less important.

Introduction

Candida albicans is one of the most commonly isolated pathogens in intensive care unit worldwide and remains a challenging organism despite the different treatment strategies available [1, 3]. The high degree of treatment failure can partially be explained by the limited number of antifungal classes available and the acquisition of resistance upon treatment [19, 21]. In the past decades, the resistance mechanisms to fluconazole (FLC), the most widely used antifungal drug, have been extensively studied and are well understood [32]. Unfortunately, resistance is not the only factor leading to treatment failure and it has been proposed that strains with an increased tolerance to the drug might also contribute to this effect. These strains, known as tolerant strains, are characterized by an increased residual growth at drug concentrations above their minimum inhibitory concentration (MIC) but without acquiring any known antifungal resistance mechanisms. Tolerance to FLC is thought to be an appropriate condition for the acquisition of resistance mutations and/or to be a source of reinfection upon arrest of the treatment [20]. Unlike resistance, mechanisms behind tolerance to FLC are still understudied and only a few potential mechanisms have been reported, involving major stress response pathways (through *HSP90* and calcineurin) [21, 45, 46], response to pH (through *RIM101*) [49] and membrane composition modifications (*VSP21*, *FEN1/FEN12*, *IPT1*) [46]. Even if it remains unclear how these mechanisms result in tolerance, their mediators may be used as potential drug targets to increase FLC efficacy [20]. It is thus important to identify new mediators of tolerance.

In order to better understand tolerance and to identify additional mechanisms, we used here a novel approach based on a systematic gene overexpression (OE) strategy. Gene OE may lead to the identification of genes potentially involved in tolerance to FLC. Using a collection of 579 strains under doxycycline (Dox)- dependent OE, with each strain tagged with a specific DNA barcode (BC), we were able to identify and characterize two putative positive mediators of tolerance consisting of the transcription factors *CRZ1* and *GZF3*. In addition to this positive selection of tolerance the OE strategy helped to identify regulators that were decreasing tolerance, so-called negative tolerance regulators.

Material and methods

Strains used in this study

The collection of 579 Tet-inducible overexpression barcoded *C. albicans* strains used in this study was kindly provided by Pr. Christophe D'Enfert (Pasteur Institute, Paris, France) (Table 11, Supplementary file 2). Each strain of the collection overexpresses a specific gene (or gene of interest, GOI) encoding transcription factors, protein kinases, protein phosphatases, proteins related to DNA replication, recombination and repair, predicted cell surface proteins, or others, under the control of tetracycline. The collection was constructed as described by Chauvel *et al.* [56].

To test optimal overexpression culture condition, the strain CEC3083, overexpressing the *Gaussia princeps* luciferase (*gLUC*) was used. This strain was built in parallel to the OE collection and also provided by Pr. C. D'Enfert (Table 11) [56].

The clinical *C. albicans* isolates (Table 10) used for the overexpression of the candidate negative regulators of tolerance (Table 12, Supplementary Table 1) and for the deletion of the candidate positive mediators (Table 14) were selected from their tolerance profile and were part of D. Sanglard laboratory collection.

The *CRZ1* and *GZF3* deletion mutants used for the identification of the role of both gene upon tolerance and to build the double *crz1Δ/Δ*, *gzf3Δ/Δ* mutant originated from the Homann's transcription factor deletion library and are listed in Table 13 [57].

The wild type (WT) strain used in the different experiments was the strain SC5314. In other experiments, the control strains were the parental clinical isolates used to construct the OE and deletion strains or the WT strain of the Homman's collection (Table 10, Table 13) [53, 54].

Table 10: Reference strains and clinical isolates used in this study.

Lab ID	Alternative ID	Type of isolate	Comment	Genotype	Reference
DSY386	SC5314	NA ¹	Wild type laboratory strain	Reference strain	[52]
DSY2904	BWP17	NA	SC5314-derived strain	<i>ura3Δ::λimm434/ura3Δ::λimm434,iro1Δ::λimm434/iro1Δ::λimm434, his1Δ::hisG/his1Δ::hisG, arg4Δ::hisG/arg4Δ::hisG</i>	[58]
DSY3291	SN152	NA	SC5314-derived strain	<i>URA3/ura3Δ::λimm434, IRO1/iro1Δ::λimm434, his1Δ::hisG/his1Δ::hisG, arg4Δ::dpl200/arg4Δ::dpl200, leu2Δ::dpl200/leu2Δ::dpl200</i>	[59]
DSY2110	34-028-117	Blood	Low-High phenotype ²	Unknown	[42]
DSY4454	0526-6020	Blood	Isolated from endocarditis patient (2005) ³	Unknown	This study
DSY4588	13 0420 0673	Blood	Isolated from endocarditis patient (2013) ³	Unknown	This study
DSY4754	SSI 4622	NA	Weak Trailing ⁴	Unknown	[53]

¹Not available²As described by Marr *et al.* [42]³Isolates were isolated from the same patient⁴Information provided by M.C. Arendrup

Table 11: Parental strains of the OE collection and derivative. The collection was built by transforming the CEC2907 strain with a collection of Clp10-P_{TET}-GOI plasmids and have a genotype derived from CEC3083 [56]. The detailed collection can be found in Supplementary File 2.

Lab ID	Alternative ID	Parental strain	Transformed plasmid	Genotype	Reference
NA ¹	CEC161	BWP17	NA	<i>ura3Δ::λimm434/ura3Δ::λimm434, iro1Δ::λimm434/iro1Δ::λimm434, his1Δ::hisG/HIS1, arg4Δ::hisG/ARG4</i>	[60]
DSY4993	CEC2907	CEC161	pNIMX	<i>ura3Δ::λimm434/ura3Δ::λimm434, iro1Δ::λimm434/iro1Δ::λimm434, his1Δ::hisG/HIS1, arg4Δ::hisG/ARG4, ADH1/adh1::P_{TDH3}-cartTA::SAT1</i>	[56]
DSY4737	CEC3083	CEC2907	Clp10-P _{TET} -gLUC59	<i>ura3Δ::λimm434/ura3Δ::λimm434, iro1Δ::λimm434/iro1Δ::λimm434, his1Δ::hisG/HIS1, arg4Δ::hisG/ARG4, ADH1/adh1::P_{TDH3}-cartTA::SAT1, RPS1/RPS1::Clp10-P_{TET}-gLUC59</i>	[56]
NA	CPY2	CEC2907	pDS1945	<i>ura3Δ::λimm434/ura3Δ::λimm434, iro1Δ::λimm434/iro1Δ::λimm434, his1Δ::hisG/HIS1, arg4Δ::hisG/ARG4, ADH1/adh1::P_{TDH3}-cartTA::SAT1, RPS1/RPS1::Clp10-P_{TET}-GTW</i>	This study

¹Not Available

Table 12: Clinical isolates and derivatives used for the OE of putative negative regulators of tolerance.

Alternative ID	Parental strain	Transformed plasmid	Genotype	Reference
CPY21	DSY4588	pSFSUI	<i>ura3Δ::FRT/ura3Δ::FRT</i>	This study
CPY23	DSY4454	pSFSUI	<i>ura3Δ::FRT/ura3Δ::FRT</i>	This study
CPY25	SC5314	pSFSUI	<i>ura3Δ::FRT/ura3Δ::FRT</i>	This study
CPY27	DSY4754	pSFSUI	<i>ura3Δ::FRT/ura3Δ::FRT</i>	This study
CPY29	DSY2110	pSFSUI	<i>ura3Δ::FRT/ura3Δ::FRT</i>	This study
CPY42 ¹	CPY29	pNIMX	<i>ura3Δ::FRT/ura3Δ::FRT, ADH1/adh1::P_{TDH3}-cartTA::SAT1</i>	This study
CPY43 ¹	CPY23	pNIMX	<i>ura3Δ::FRT/ura3Δ::FRT, ADH1/adh1::P_{TDH3}-cartTA::SAT1</i>	This study
CPY44 ¹	CPY21	pNIMX	<i>ura3Δ::FRT/ura3Δ::FRT, ADH1/adh1::P_{TDH3}-cartTA::SAT1</i>	This study
CPY45 ¹	CPY27	pNIMX	<i>ura3Δ::FRT/ura3Δ::FRT, ADH1/adh1::P_{TDH3}-cartTA::SAT1</i>	This study

¹The derivative strains transformed with the Clp10-P_{TET}-GOI plasmids are detailed in Supplementary Table 1

Table 13: *CRZ1* and *GZF3* mutant strains used for the OE of either *CRZ1* or *GZF3*.

Lab ID	Alternative ID	Parental strain	Transformed plasmid	Genotype ¹	Reference
NA ²	"Wild type" ³	SN152	NA	<i>URA3/ura3Δ, IRO1/iro1Δ, his1Δ/his1Δ::HIS1, arg4Δ/Δ, leu2Δ/leu2Δ::LEU2</i>	[57]
NA	TF068	SN152	NA	<i>URA3/ura3Δ, IRO1/iro1Δ, his1Δ/Δ, arg4Δ/Δ, leu2Δ/Δ, crz1Δ::CdLEU2/crz1Δ::CmHIS1⁴</i>	[57]
NA	TF101	SN152	NA	<i>URA3/ura3Δ, IRO1/iro1Δ, his1Δ/Δ, arg4Δ/Δ, leu2Δ/Δ, gzf3Δ::CdLEU2/gzf3Δ::CmHIS1</i>	[57]
DSY5253	EDY16-3	TF068	pSFSU1	<i>ura3Δ/Δ, IRO1/iro1Δ, his1Δ/Δ, arg4Δ/Δ, leu2Δ/Δ, crz1Δ::CdLEU2/crz1Δ::CmHIS1</i>	This study
DSY5254	EDY17-3	TF101	pSFSU1	<i>ura3Δ/Δ, IRO1/iro1Δ, his1Δ/Δ, arg4Δ/Δ, leu2Δ/Δ, gzf3Δ::CdLEU2/gzf3Δ::CmHIS1</i>	This study
DSY5270	EDY35	"Wild type" ³	pSFSU1	<i>ura3Δ/Δ, IRO1/iro1Δ, his1Δ/his1Δ::HIS1, arg4Δ/Δ, leu2Δ/leu2Δ::LEU2</i>	This study
DSY5255	EDY20-3	EDY16-3	pNIMX	<i>ura3Δ/Δ, IRO1/iro1Δ, his1Δ/Δ, arg4Δ/Δ, leu2Δ/Δ, crz1Δ::CdLEU2/crz1Δ::CmHIS1, ADH1/adh1Δ::P_{TDH3}-cartTA::SAT1</i>	This study
DSY5256	EDY21-1	EDY17-3	pNIMX	<i>ura3Δ/Δ, IRO1/iro1Δ, his1Δ/Δ, arg4Δ/Δ, leu2Δ/Δ, gzf3Δ::CdLEU2/gzf3Δ::CmHIS1, ADH1/adh1Δ::P_{TDH3}-cartTA::SAT1</i>	This study
DSY5273	EDY38	EDY35	pNIMX	<i>ura3Δ/Δ, IRO1/iro1Δ, his1Δ/his1Δ::HIS1, arg4Δ/Δ, leu2Δ/leu2Δ::LEU2, ADH1/adh1Δ::P_{TDH3}-cartTA::SAT1</i>	This study
DSY5274	EDY39	EDY38	pDS1945	<i>ura3Δ/Δ, IRO1/iro1Δ, his1Δ/his1Δ::HIS1, arg4Δ/Δ, leu2Δ/leu2Δ::LEU2, ADH1/adh1Δ::P_{TDH3}-cartTA::SAT1, RPS1/RPS1::Clp10-P_{TET}-GTW</i>	This study
DSY5275	EDY40	EDY38	pDS1997	<i>ura3Δ/Δ, IRO1/iro1Δ, his1Δ/his1Δ::HIS1, arg4Δ/Δ, leu2Δ/leu2Δ::LEU2, ADH1/adh1Δ::P_{TDH3}-cartTA::SAT1, RPS1/RPS1::Clp10-P_{TET}-GZF3</i>	This study
DSY5276	EDY41	EDY38	pDS1998	<i>ura3Δ/Δ, IRO1/iro1Δ, his1Δ/his1Δ::HIS1, arg4Δ/Δ, leu2Δ/leu2Δ::LEU2, ADH1/adh1Δ::P_{TDH3}-cartTA::SAT1, RPS1/RPS1::Clp10-P_{TET}-CRZ1</i>	This study
DSY5271	EDY36	EDY20-3	pDS1945	<i>ura3Δ/Δ, IRO1/iro1Δ, his1Δ/Δ, arg4Δ/Δ, leu2Δ/Δ, crz1Δ::CdLEU2/crz1Δ::CmHIS1, ADH1/adh1Δ::P_{TDH3}-cartTA::SAT1, RPS1/RPS1::Clp10-P_{TET}-GTW</i>	This study
DSY5257	EDY22	EDY20-3	pDS1997	<i>ura3Δ/Δ, IRO1/iro1Δ, his1Δ/Δ, arg4Δ/Δ, leu2Δ/Δ, crz1Δ::CdLEU2/crz1Δ::CmHIS1, ADH1/adh1Δ::P_{TDH3}-cartTA::SAT1, RPS1/RPS1::Clp10-P_{TET}-GZF3</i>	This study
DSY5259	EDY24	EDY20-3	pDS1998	<i>ura3Δ/Δ, IRO1/iro1Δ, his1Δ/Δ, arg4Δ/Δ, leu2Δ/Δ, crz1Δ::CdLEU2/crz1Δ::CmHIS1, ADH1/adh1Δ::P_{TDH3}-cartTA::SAT1, RPS1/RPS1::Clp10-P_{TET}-CRZ1</i>	This study

DSY5272	EDY37	EDY21-1	pDS1945	<i>ura3Δ/Δ, IRO1/iro1Δ, his1Δ/Δ, arg4Δ/Δ, leu2Δ/Δ, gzf3Δ::CdLEU2/gzf3Δ::CmHIS1, ADH1/adh1Δ::P_{TDH3}-cartTA::SAT1, RPS1/RPS1::Clp10-P_{TET}-GTW</i>	This study
DSY5260	EDY25	EDY21-1	pDS1997	<i>ura3Δ/Δ, IRO1/iro1Δ, his1Δ/Δ, arg4Δ/Δ, leu2Δ/Δ, gzf3Δ::CdLEU2/gzf3Δ::CmHIS1, ADH1/adh1Δ::P_{TDH3}-cartTA::SAT1, RPS1/RPS1::Clp10-P_{TET}-GZF3</i>	This study
DSY5258	EDY23	EDY21-1	pDS1998	<i>ura3Δ/Δ, IRO1/iro1Δ, his1Δ/Δ, arg4Δ/Δ, leu2Δ/Δ, gzf3Δ::CdLEU2/gzf3Δ::CmHIS1, ADH1/adh1Δ::P_{TDH3}-cartTA::SAT1, RPS1/RPS1::Clp10-P_{TET}-CRZ1</i>	This study
DSY5263	EDY28	EDY16-3	pED20-7	<i>ura3Δ/Δ, IRO1/iro1Δ, his1Δ/Δ, arg4Δ/Δ, leu2Δ/Δ, crz1Δ::CdLEU2/crz1Δ::CmHIS1, gzf3Δ/Δ</i>	This study
DSY5265	EDY30	EDY28	pNIMX	<i>ura3Δ/Δ, IRO1/iro1Δ, his1Δ/Δ, arg4Δ/Δ, leu2Δ/Δ, crz1Δ::CdLEU2/crz1Δ::CmHIS1, gzf3Δ/Δ, ADH1/adh1Δ::P_{TDH3}-cartTA::SAT1</i>	This study
DSY5269	EDY34	EDY30	pDS1945	<i>ura3Δ/Δ, IRO1/iro1Δ, his1Δ/Δ, arg4Δ/Δ, leu2Δ/Δ, crz1Δ::CdLEU2/crz1Δ::CmHIS1, gzf3Δ/Δ, ADH1/adh1Δ::P_{TDH3}-cartTA::SAT1, RPS1/RPS1::Clp10-P_{TET}-GTW</i>	This study
DSY5267	EDY32	EDY30	pDS1997	<i>ura3Δ/Δ, IRO1/iro1Δ, his1Δ/Δ, arg4Δ/Δ, leu2Δ/Δ, crz1Δ::CdLEU2/crz1Δ::CmHIS1, gzf3Δ/Δ, ADH1/adh1Δ::P_{TDH3}-cartTA::SAT1, RPS1/RPS1::Clp10-P_{TET}-GZF3</i>	This study
DSY5266	EDY31	EDY30	pDS1998	<i>ura3Δ/Δ, IRO1/iro1Δ, his1Δ/Δ, arg4Δ/Δ, leu2Δ/Δ, crz1Δ::CdLEU2/crz1Δ::CmHIS1, gzf3Δ/Δ, ADH1/adh1Δ::P_{TDH3}-cartTA::SAT1, RPS1/RPS1::Clp10-P_{TET}-CRZ1</i>	This study

¹The complete genotype can be found in Supplementary Table 2

²Not Available

³Refers to Homann's "Wild type" strain [57]

⁴*Cd* = *C. dubliniensis*, *Cm* = *C. maltosa*

Table 14: *CRZ1* and *GZF3* deletion mutants in tolerant clinical isolates.

Lab ID	Alternative ID	Parental strain	Transformed plasmid	Genotype	Reference
DSY5208	NA ¹	DSY2110	pED19-2	<i>CRZ1/crz1Δ::FRT</i>	This study
DSY5227	NA	DSY5208	pED19-2	<i>crz1Δ::FRT/crz1Δ::FRT</i>	This study
NA	LBY6 ²	DSY5227	pLB1	<i>crz1Δ/crz1Δ::FRT::CRZ1</i>	This study
DSY5210	NA	DSY2110	pED20-7	<i>GZF3/gzf3Δ::FRT</i>	This study
DSY5230	NA	DSY5210	pED20-7	<i>gzf3Δ::FRT/gzf3Δ::FRT</i>	This study
DSY5279 ¹	NA	DSY5230	pET3	<i>gzf3Δ::FRT/gzf3Δ::GZF3</i>	This study
DSY5235	NA	DSY4454	pED19-2	<i>CRZ1/crz1Δ::FRT</i>	This study
DSY5236	NA	DSY5235	pED19-2	<i>crz1Δ::FRT/crz1Δ::FRT</i>	This study
NA	LBY8 ²	DSY5236	pLB1	<i>crz1Δ/crz1Δ::FRT::CRZ1</i>	This study
DSY5225	NA	DSY4457	pED20-7	<i>GZF3/gzf3Δ::FRT</i>	This study
DSY5231	NA	DSY5225	pED20-7	<i>gzf3Δ::FRT/gzf3Δ::FRT</i>	This study
DSY5280 ¹	NA	DSY5231	pET3	<i>gzf3Δ::FRT/gzf3Δ::GZF3</i>	This study
DSY5209	NA	DSY4588	pED19-2	<i>CRZ1/crz1Δ::FRT</i>	This study
DSY5229	NA	DSY5209	pED19-2	<i>crz1Δ::FRT/crz1Δ::FRT</i>	This study
NA	LBY7 ²	DSY5229	pLB1	<i>crz1Δ/crz1Δ::FRT::CRZ1</i>	This study
DSY5217	NA	DSY4588	pED20-7	<i>GZF3/gzf3Δ::FRT</i>	This study
DSY5252	NA	DSY5217	pET2-1	<i>gzf3Δ::FRT/gzf3Δ::FRT</i>	This study
DSY5277 ¹	NA	DSY5252	pET3	<i>gzf3Δ::FRT/gzf3Δ::GZF3</i>	This study
DSY5224	NA	DSY4754	pED19-2	<i>CRZ1/crz1Δ::FRT</i>	This study
DSY5237	NA	DSY5224	pED19-2	<i>crz1Δ::FRT/crz1Δ::FRT</i>	This study
NA	LBY9 ²	DSY5237	pLB1	<i>crz1Δ/crz1Δ::FRT::CRZ1</i>	This study
DSY5218	NA	DSY4754	pED20-7	<i>GZF3/gzf3Δ::FRT</i>	This study
DSY5239	NA	DSY5218	pED20-7	<i>gzf3Δ::FRT/gzf3Δ::FRT</i>	This study
DSY5278 ¹	NA	DSY5239	pET3	<i>gzf3Δ::FRT/gzf3Δ::GZF3</i>	This study

¹Not Available²Revertant were built by reinsertion of the SC5314 allele at the deleted locus

Media and growth conditions

All strains were stored in 20 % glycerol at -80°C and routinely grown at 30°C under constant shaking (220 rpm) in complete Yeast Extract Peptone Dextrose (YEPD) medium (1 % Bacto peptone, Difco Laboratories, Basel, Switzerland), 0.5 % Yeast extract (Difco Laboratories, Basel, Switzerland) and 2 % glucose (Fluka, Buchs, Switzerland). When grown on solid YEPD plates (YEPDA), 2 % agar (Difco Laboratories, Basel, Switzerland) was added and plates were incubated at 35°C.

For FLC susceptibility and tolerance assays, strains were grown in RPMI1640 medium (Sigma-Aldrich) complemented with 2 % glucose (Fluka, Buchs, Switzerland) and buffered with 0.33 M morpholinepropanesulfonic acid (MOPS) according to the European Committee on Antimicrobial Susceptibility Testing (EUCAST) recommendations [38]. The pH was adjusted to pH 7.5, pH 7, pH 6 and pH 4.5 respectively, using NaOH or HCl. Double strength stock solutions were prepared as recommended by EUCAST. RPMI was supplemented or not with FLC (Toronto Research Chemicals), Doxycycline (Dox) (Sigma-Aldrich) and iron (FeCl_3) to compensate iron chelation by the Dox when necessary [61]. For luciferase assays, water-soluble coelenterazine (CTZ, Nanolight Technologies, USA) was added prior to measurement.

Primers and plasmids

All primers used in this study are listed in Supplementary Table 4 and were synthesized and delivered by Kaneka Eurogentec S.A.. Plasmids used in this study are listed in Supplementary Table 3. The maps of each plasmid can be found in Supplementary Figure 1. The insertion of each plasmid and gene deletion were verified by PCR as stated in Supplementary Table 4. All reactions were amplified as follows: a first cycle with 4 min of denaturation at 94°C, 1 min of annealing (temperatures are indicated in Supplementary Table 4) and an elongation step at 72°C (elongation times are indicated in Supplementary Table 4). This first cycle was followed by 30 cycles in the same conditions. Finally, a final elongation step at 72°C for 10 min was performed.

Escherichia coli DH5 α was used as a host for plasmid construction and propagation. Bacteria were grown in Luria-Bertani (LB) broth or LB 2 % agar plates, supplemented with 100 μ g/ml ampicillin (AppliChem) or 34 μ g/ml chloramphenicol (Fluka, Buchs, Switzerland) when required and incubated at 37°C.

Yeast transformation

Yeasts were transformed by a lithium-acetate procedure with slight modifications as previously described [62]. Nourseothricin resistant (Nour^R) transformants were selected on YEPD agar plates complemented with 200 μ g/ml nourseothricin (Werner Bioagents, Germany). For selection of Ura⁺ transformants, the cells were resuspended in 100 μ l Tris-EDTA (TE) buffer (0.1 M Tris, pH 7.5, 10 mM EDTA, pH 8) and plated on Yeast Nitrogen Base (YNB, Difco Laboratories, Basel, Switzerland) minimal medium complemented with Complete Supplemented Medium without uracil (CSM-URA, MP Biomedicals, LLC, CA, USA) (0.67 % YNB, 2 % glucose, 0.79 g/L CSM-URA, 2 % agar).

Construction of Deletion Mutants and Revertant Strains

The clinical isolates DSY2110, DSY4454, DSY4754 and DSY4588 as well as the “WT”, the *crz1* Δ/Δ and the *gzf3* Δ/Δ strains from the Homann’s collection [57] were used to delete: (i) *URA3*, in order to transform the strains with the OE system [56] and (ii) either *CRZ1*, *GZF3* or both to assess their role in FLC tolerance. All gene deletions were performed by insertion of the PCR amplified 5’ and 3’ untranslated regions (UTR, 500bp) into the *SAT1*-flipper plasmid pSFS2A [63]. Details for the resulting plasmids could be found in Supplementary Table 3. pSFS2A contains the *SAT1*-flipping cassette which replace the target gene by the nourseothricin resistance gene *SAT1* under the control of the *ACT1* promoter. It also introduces a flippase (*FLP*) under the control of a maltose-inducible promoter (*MAL2*). The whole deletion cassette is flanked by two flippase recognition target (FRT) sequences, allowing the flipping of the deletion cassette and the recovery of the *SAT1* marker which can then be reused in the deleted strain. To obtain homozygous mutants, the deletion plasmids were thus inserted twice.

URA3 was deleted using the plasmid pSFSU1 (Supplementary Table 3, Supplementary Figure 1). Due to technical issues with some clones, the second allele was deleted by plating the heterozygous mutants on 5-fluoro-orotic acid (5-FOA) to force deletion of the second allele as already described [64]. For deletion of *CRZ1* and *GZF3*, the plasmids pED19-2, pED20-7 and pET2-1 were used, respectively (Supplementary Table 3, Supplementary figure 1). The plasmid pET2-1 was only used to delete the second *GZF3* allele of DSY5217 (which failed with pED20-7), resulting in strain DSY5252 (Table 13). All plasmids were transformed into their target strains after digestion by *KpnI* and *SacI* to isolate the *SAT1* flipper-cassette. The transformants were plated and selected on YEPD plates containing 200 µg/ml nourseothricin. The cassette was flipped-out by picking singles colonies and incubating them overnight (o/n) in YEP maltose (2 % maltose instead of glucose) and nourseothricin-sensitive colonies were recovered by plating on YEPD plates complemented with 15 µg/ml nourseothricin. At this concentration, susceptible colonies are still able to grow but more slowly than resistant ones, thus yielding smaller colonies which can be picked up, resuspended in TE buffer and plated on both YEPD or YEPD-nourseothricin (100 µg/ml) to confirm their susceptible phenotype and thus confirming the flipping-out of the cassette and deletion of the allele. The same procedure was used for deletion of the second allele.

To verify the gene deletions of the selected isolates, the presence of the wild type allele was verified by PCR using specific primers for each allele (Supplementary Table 4) after each recovery of the *SAT1* flipping cassette.

To construct revertant strains in which *CRZ1* and *GZF3* were reintroduced in the background of deletion mutants (Table 14), the wild type alleles from SC5314 and corresponding 5'- and 3'- UTR (± 500 bp) were reinserted by replacing the 5'-UTR of the deletion plasmid by the *CRZ1* and *GZF3* amplified genes (Supplementary Figure 1), resulting in plasmids pLB1 and pET3, respectively (Supplementary Table 3). The wild type alleles were then reintroduced in addition to the *SAT1*-flipper cassette into the homozygous mutants by *KpnI* and *SacI* digestion of the plasmids (Supplementary Figure 1).

Determination of optimal Dox concentration for OE

To optimize the culture conditions for overexpression with the OE collection, the ability of Dox to induce OE was evaluated using the *gLUC*-OE strain CEC3083 (Table 11). Briefly, individual colonies were grown o/n in liquid YEPD medium at 30°C under constant shaking. The culture was then centrifuged (5 min, 4600 rpm, 4°C) and the cell pellet washed twice with phosphate buffered saline (PBS). Cells were then resuspended at 7.5×10^6 cells/ml in RPMI medium at pHs 7.5, 7, 6 and 4.5. Each inoculum was split in five subcultures and complemented with 100, 50, 10 and 2 and 0 µg/ml Dox, respectively. Cultures were then incubated for 24 h at 30°C under constant shaking. The next day, 50 µl of each culture were transferred into the wells of a flat-bottom, half-area, black microtiter plate (COSTAR). The plates were placed in a luminometer (FLUOstar Omega, BMG Labtech) and 50 µl of 2.5 µM water soluble CTZ (Nanolight Technologies, USA) injected prior to the measurement of luciferase activity of each well. The settings of the luminometer were the following: Top optic; Emission filter: Lens; Gain: 3600; Injection volume: 50 µl, Injection speed: 400 µl/s; Shaking: 200 rpm, double orbital, 3 s before reading; Measurement start time: 4.4 s, Measurement interval time: 1.0 s; Incubation: 30°C. In addition to the biological replicate, each inoculum was tested as technical duplicate on the same plate.

Iron compensation of the FLC-Dox synergistic effect

Due to the known synergistic effect of Dox with FLC [64], cell viability in the presence of both FLC and Dox in the presence and absence of FeCl_3 was assessed using serial dilution spotting assay on YEPD agar plates. Briefly, individual colonies of the strain SC5314 were grown o/n at 30°C under constant shaking in YEPD medium. The culture was then centrifuged (5 min, 4600 rpm, 4°C) and the cell pellet washed twice with PBS. Cells were then resuspended at 2.5×10^5 cells/ml in RPMI medium at pH 6 and split into six subcultures complemented with: (i) growth control, (ii) 32 µg/ml FLC, (iii) 10 or 100 µg/ml Dox only, (iv) 1mM FeCl_3 only, (v) 32 µg/ml FLC and 10 or 100 µg/ml Dox, (vi) 32 µg/ml FLC and 10 or 100 µg/ml Dox and 1mM FeCl_3 . Two hundred microliters of each condition were transferred in the first column of a 96-well plate (COSTAR), adding a blank control with only RPMI medium, and the plate was

incubated at 35°C for 24 h. The next day, four 10-fold serial dilutions were performed for each subculture and 5 µl of each well were spotted onto YEPD plates and incubated for 24 h at 35°C.

FLC susceptibility and tolerance assays

All FLC susceptibility assays were performed according to the *Method for the determination of broth dilution minimum Inhibitory concentrations of antifungal agents for yeasts* [38] as recommended by the EUCAST, with slight modifications when necessary. The minimal inhibitory concentration (MIC) was defined as the concentration of drug inhibiting at least 50 % of fungal growth as compared to a drug free control. Strains with a MIC below 4 µg/ml FLC were defined as susceptible as described by EUCAST [38]. Susceptibility assays were performed in RPMI at pHs 7.5, 7, 6 or 4.5 with additions of Dox and FeCl₃ when necessary, as stated in the corresponding experiments. Tolerance assays were performed in the same conditions but using only a fixed FLC concentration as specified in the corresponding experiment.

Briefly, individual colonies of each tested strain were grown overnight in YEPD medium at 30°C under constant shaking. Cultures were centrifuged (5 min, 4600 rpm, 4°C) and washed twice with PBS. Cell concentration was estimated by spectrophotometry (OD_{540 nm}) and cells were resuspended at 5 x 10⁵ cells/ml in distilled water. Then, 100 µl of this suspension were transferred into the wells of 96-well plates (Costar) containing 100 µl of 2x RPMI complemented with 64-0 µg/ml FLC in two-fold dilutions or fixed FLC concentrations (16 µg/ml), to obtain a final cell concentration of 2.5 x 10⁵ cells/ml and FLC concentration ranging from 32 to 0 µg/ml (8 µg/ml for tolerance assays) per well. Plates were incubated at 35°C without shaking for 24 h. Cell growth in each well was measured by spectrophotometry (OD_{570 nm}) using a microplate reader (Multiskan Ascent) and compared to the drug free control after correction with a blank control. From these susceptibility curves, both the MIC and the tolerance index (TI), corresponding to the relative growth (% GC) at 8 µg/ml FLC divided by a factor 100 (TI = % GC/100) were determined for strain comparisons. The TI is used to determine the level of tolerance and was already described earlier (Delarze *et al.*, unpublished, Thesis part 1).

To assess the tolerance level of every single strain of the OE collection and to remain in the same conditions compared to the enrichment assay, tolerance assays of the collection were performed at a final concentration of 32 µg/ml FLC instead of 8 µg/ml.

Susceptible strains (*i.e.* MIC < 4 µg/ml FLC) with a TI between 0.2 and 0.8 were considered as tolerant while strains with TI < 0.2 were considered as susceptible (*i.e.* exhibiting a WT tolerance profile) and the ones with TI > 0.8 were considered as resistant, as described earlier (Delarze *et al.*, unpublished, Thesis part 1).

Calcium induction of tolerance

In order to rise the basal tolerance level and test our negative regulators candidate genes, calcium (CaCl₂) was added in the RPMI medium of the tolerance assays. First, serial 2-fold dilutions of CaCl₂ (from 100 to 0 µg/ml) were tested to determine the best CaCl₂ concentration for our assay. A fixed concentration of 50 µg/ml CaCl₂ was chosen to determine the tolerance profile of our candidate genes in the presence of FLC (8 µg/ml), Dox (5 µg/ml) and FeCl₃ (0.05 mM).

Pool enrichment in tolerant/resistant strains

In order to enrich the pooled OE collection in FLC tolerant/resistant isolates, strains were grown in RPMI 2 % glucose at pH 6 in the presence of 1mM FeCl₃ and with or without 100 µg/ml Dox and 32 µg/ml FLC. To be as close as possible to our drug susceptibility assay conditions (EUCAST recommendations), cells were cultured in 96-well plates with each well containing 200 µl of cell suspension in RPMI. Each condition represents 20 ml of culture.

Briefly, a pool of the 579-strain collection was incubated o/n in YEPD at 35°C under constant shaking. The next day, the cells were centrifuged (5 min, 4600 rpm, 4°C) and washed twice with PBS. The cell pellet was resuspended at 10⁷ cells/ml in RPMI pH 6 and this inoculum was split in four 20 ml subcultures. The remainders of the overnight culture were centrifuged and the pellet frozen (-20°C) prior to DNA extraction after the enrichment to estimate the initial population of our pool (Day 0). The four subcultures were respectively complemented with: (i) 32 µg/ml FLC, (ii) 100 µg/ml Dox, (iii) 32

µg/ml FLC and 100 µg/ml Dox. The last subculture was the growth control in which nor FLC or Dox were added. Each subculture was also complemented with 1 mM FeCl₃ to avoid the synergistic FLC-Dox effect. Two hundred microliter of these subcultures were then transferred in each well of 96-well plates, leaving two wells as contamination control. The plates were then incubated 24 h at 35°C. Every day for the next 5 days, cells from the overnight culture in 96-well plates were recovered using a multi-channel pipette and recovered into a 50 ml tube. The cultures were then processed as at Day 0. First, the cells were centrifuged (5 min, 4600 rpm, 4°C) and washed twice with PBS and resuspended at 10⁷ cells/ml in 20 ml fresh RPMI in four new 50 ml tubes prior to addition of FLC, Dox and FeCl₃. The rest of the overnight cultures are then centrifuged again and frozen (-20°C) until DNA extraction.

Genomic DNA extraction

Genomic DNA was prepared by spheroplasting from frozen cell pellets. Briefly, thawed cells were washed twice in TE buffer and resuspended in 5 ml PRO Buffer solution (EDTA 25 mM, Tris pH 7.5, 1 M and Sorbitol 1 M), 50 µl of 100T Zymolyase (10 mg/ml, Seikagaku, Tokyo, Japan) and 5 µl β-mercaptoethanol (Applichem). After 15 min incubation at 37°C, cells were centrifuged (4600 rpm, 5 min, room temperature (RT)) and pellets resuspended in 2 ml Lysis buffer (EDTA 0.1 M, Tris 0.1 M pH 7.5, and SDS 0.5 %) and 50 µg/ml Proteinase K (Roche Diagnostics). Cells were incubated for 30 min at 65°C. Then 500 µl K-acetate (4 M) were added and cells were incubated for 10 min on ice. Cells were then centrifuged (15 min, 4600 rpm, 4°C), the supernatant was transferred in 14 ml tubes and nucleic acids were precipitated with 5 ml 100 % EtOH. Samples were centrifuged (10 min, 4600 rpm, 4°C), the supernatant discarded, and the pellet resuspended in 500 µl TE buffer complemented with 100 µg/ml RNase A. Samples were incubated 15 min at 37°C and DNA was precipitated by adding 500 µl isopropanol. Samples were transferred into 1.5 ml tubes and centrifuged (15000 rpm, 1 min, RT). Supernatants were discarded and pellets washed once with ethanol 70 %. Samples were air-dried and the pellets resuspended in 300 µl TE buffer. DNA concentration at 260 nm was measured using a NanoDropTM 1000 Spectrophotometer (Thermo Fisher Scientific) and volumes adjusted with TE buffer to obtain a final DNA concentration of 5 ng/µl.

Amplification of the barcodes

In order to estimate the strain presence in the different populations, the BC of each cell was amplified by PCR to be sequenced following the *16S Metagenomic Sequencing Library Preparation protocol* (Illumina) recommendations to add so-called Illumina overhang sequences to the amplicons (Supplementary Table 4). However, to avoid mistakes during the sequencing due to the similar flanking regions of the BC amplicons, spacer bases (0, 4, 8 and 12 N) were added to the forward primers to shift the signal during sequencing (Supplementary Table 4). Briefly, approximatively 12.5 ng of DNA extraction was used for BC amplification using the Phusion High-Fidelity DNA Polymerase (NEB) following manufacturer recommendations. The only modification to the preparation of the samples was to use four forward primers instead of one (Supplementary Table 4), each diluted to a 1:4 ratio. The PCRs were performed in a pEqSTAR 2x thermal cycler (PEQLAB-VWR) with the following program: 3 min at 95°C followed by 30 cycles at 95°C, 57.9°C and 72°C for 30 s each. A final elongation was performed for 5 min at 72°C. To increase the quality of our samples, the whole PCR products were loaded on a 1 % agarose gel for electrophoresis and bands of interest purified using the NucleoSpin® Gel and PCR Clean-up kit (MACHEREY-NAGEL) following manufacturer recommendations.

Library preparation and sequencing

Library construction was performed at the Lausanne Genome Technologies Facility (LGTF, University of Lausanne – Centre for Integrative Genomics). Libraries were prepared adapting the *16S Metagenomic Sequencing Library Preparation protocol* (Illumina) according to manufacturer recommendations. MiSEQ Illumina 300 bp single-end sequencing was performed on the libraries by the LGTF.

Barcode quantification

The barcode quantification of the populations from the pool enrichment assay was performed using a script developed by Marion Patxot (Supplementary File 3). Each sequenced library was outputted as a FASTQ file. To process the sequencing data, a bioinformatics pipeline was set up using Perl

programming language (v. 5.24.0) and bash Shell (v. 3.2.57 for Mac OS X 10.11.16). Briefly, the pipeline counts the occurrence of known barcode sequences in a FASTQ file by running a MegaBLAST. There are two inputs to the pipeline: the FASTQ file and a text file containing the name and sequence of each barcode. Both files are first converted into FASTA format. Each barcode sequence is then aligned to each read in the FASTQ file. The alignment allowed 8 mismatches. The pipeline outputs the occurrence of each barcode as a text file. The sequence data was processed using the developed pipeline. Counts for each time point and condition were merged into a single text file with bash Shell (v. 3.2.57 – Mac OS X 10.11.6). The proportion of each strain in the population was subsequently calculated and plotted using Open Source R Software (v. 3.2.4, <http://www.R-project.org/>). In a second step, counts were analyzed using the WT statistical guideline for DMS studies described by Matuszewski *et al.* [54]. This approach calculates a selection of coefficient estimators using the log ratios of the number of counts for strains over the number of counts for the reference.

Software and statistical analysis

Graphics and statistical analysis were performed in GraphPad Prism 7.03 (GraphPad Software, Inc., La Jolla, CA, USA). The online software Morpheus (<https://software.broadinstitute.org/morpheus>) was used to create the heatmaps of the enrichment assay. Plasmid maps were realized on Adobe Illustrator CC 2018 (Adobe Inc., San Jose, CA, USA)

Results

Identification of optimal OE culture conditions

Gene OE was chosen to identify mediators of FLC tolerance. To achieve this purpose, a 579-strains collection reported in Chauvel *et al.* [56] was used, with each strain overexpressing a specific gene on a Dox-dependent manner (Figure 23C). Briefly, the OE system consists of two distinct plasmids. First, a vector (pNIMX) expressing the Tetracycline (TET)-binding transactivator (TA) under the control of the *TDH3* promoter (P_{TDH3}) is introduced in the parental strain CEC161, which is derived from BWP17,

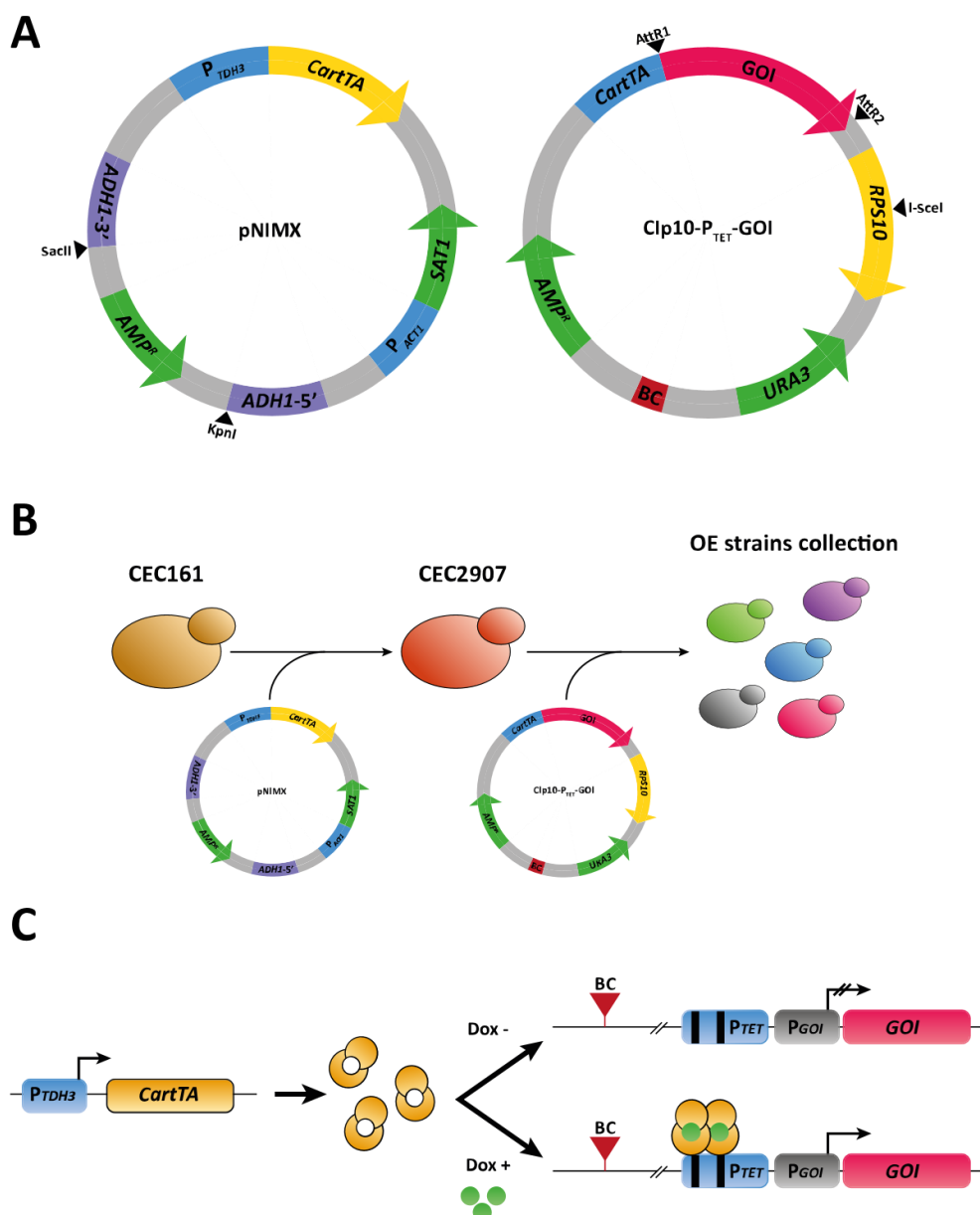


Figure 23: Doxycycline-dependent overexpression system. (A) Maps of the plasmids pNIMX and Clp10-P_{TET}-GOI used for the construction of the library. (B) Construction of the OE collection. First pNIMX was transformed in CEC161 after digestion by

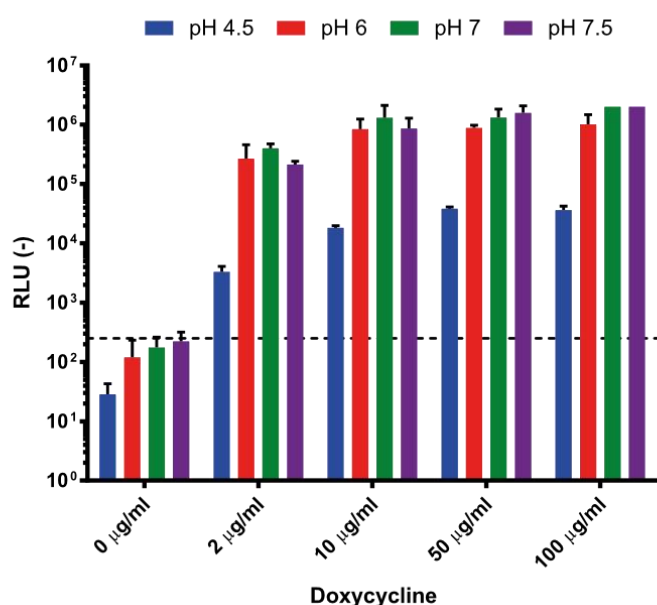
SacI/SacII leading to the strain CEC2097 used as receptacle for the Clp10-P_{TET}-GOI plasmid collection, after linearization by I-SceI, leading to the final 579 Dox-dependent OE strain collection. (C) Schematic representation of the Dox-dependent OE system.

yielding strain CEC2097 [56] (Figure 23A and B). Next, the Clp10-P_{TET} plasmid collection (579 plasmids), with each plasmid expressing a gene of interest (GOI, listed in Supplementary File 2) under the control of a TET-inducible promoter (P_{TET}) (Supplementary Figure 1) was introduced in CEC2097 (Figure 23B). These second plasmids also bear specific 20 bp tags (or barcodes, BC) allowing their identification by sequencing (Figure 23), thus enabling the design of pool experiments. In this work, the pooled strains were subjected to FLC selection in the presence of doxycycline. Under these conditions, strains expressing genes mediating tolerance may be favored over those with wild type characteristics.

However, prior to selection experiments with this collection of pooled strains, optimal OE conditions had to be determined. We chose to grow the *C. albicans* OE collection in RPMI medium to be consistent with EUCAST culture conditions. It was necessary to determine at which Dox concentration a significant OE could be detected. To address this question, a Dox-dependent *Gaussia princeps* luciferase (*gLUC*) reporter strain (CEC3083, Table 11) was used. This strain emits luminescence after addition of the *gLUC* substrate (coelenterazine). The emitted light is expected to be proportional to the level of *gLUC* expression and thus to the level of supplemented Dox. This strain was used to determine the optimal pH and Dox concentration for the pool enrichment assay (Figure 24A). First of all, it appeared that the Tet-inducible OE system was leaky: even in absence of Dox, luminescence could be detected ($3 \times 10^1 < \text{RLU} < 3 \times 10^2$), thus reflecting a basal *gLUC* expression level (Figure 24A). This basal luminescence was measured independently of the Dox concentration and the tested pH and might be a source of variability for further experiments. A second observation was that, as expected, *gLUC* expression was correlated with Dox concentration present in the growing medium (Figure 24A). However, the luminescence signal became saturated at 100 µg/ml Dox and at both pH 7 and 7.5 ($\text{RLU} > 2 \times 10^6$, Figure 24A). The medium pH also influenced the level of detected luminescence. Indeed, at pH 4.5, the signal was at least 10-fold lower compared to the other pH conditions and independently of the Dox concentration with RLU between 3×10^3 and 4×10^4 at pH 4.5 versus RLU between 3×10^5 and 2×10^6 at

higher pH (Figure 24A). The luminescence signals resulting from Dox addition appeared similar between pHs 6, 7 and 7.5 ($3 \times 10^5 < \text{RLU} < 2 \times 10^6$, Figure 24A). Thus, with these observations, pH 6 and 7 seemed to be the optimal conditions for gene OE. However, another point had to be assessed before our experiment. Indeed, it is known that Dox acts synergistically with FLC, converting this drug into a fungicidal rather than fungistatic drug. This synergistic effect is due to the ability of Dox to chelate iron but can be reversed by addition of iron (FeCl_3) in the medium [61]. To verify whether iron was able to avoid this synergistic effect in our conditions, the *C. albicans* strain SC5314 was grown in presence or absence of FLC, Dox and FeCl_3 , and cell viability was measured after 24 h by serial dilution spotting on YEPD plate (Figure 24B). As expected, a clear reduction of growth in the presence of FLC was observed, while in the presence of Dox only (10 $\mu\text{g/ml}$ and 100 $\mu\text{g/ml}$), fungal growth was not affected (Figure 24B). On the other hand, the growth in presence of both FLC and Dox was drastically reduced, with almost no growth at 100 $\mu\text{g/ml}$ Dox, confirming the synergistic effect between both drugs (Figure 24B). The addition of 1 mM FeCl_3 allowed a partial growth recovery at 100 $\mu\text{g/ml}$ Dox while growth at 10 $\mu\text{g/ml}$ Dox was similar to FLC only (Figure 24B). Thus, it seemed that experimental conditions using 10 $\mu\text{g/ml}$ Dox could be optimal. However, as we aimed here to select resistant/tolerant strains in the following experiments, a strong OE with 100 $\mu\text{g/ml}$ Dox was favored to select extreme phenotypes. Due to iron precipitation and luminescent signal saturation at 100 $\mu\text{g/ml}$ Dox in RPMI at pH 7, pH 6 was selected to perform our OE experiments.

A



B

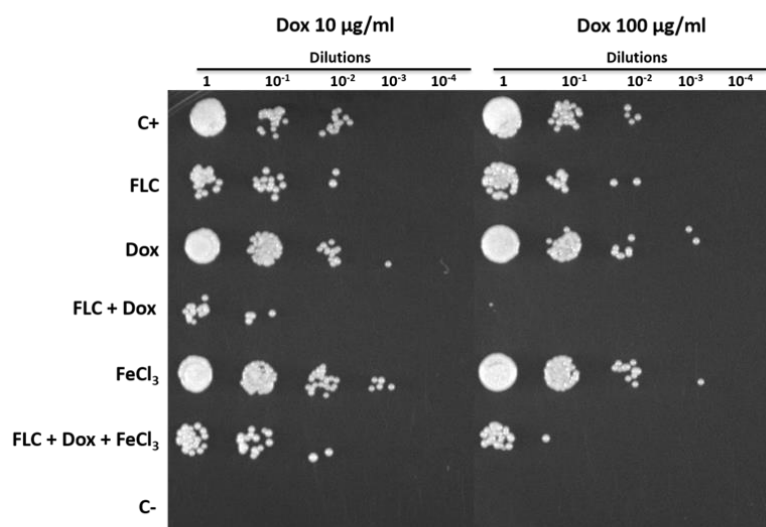


Figure 24: Dox efficiency and cell viability. (A) Light emission (in relative luminescence units, RLU) of the strain DSY4737, overexpressing *gLUC59*, after 24 h, at different pH and Dox concentrations. Each bar corresponds to the mean RLU of biological triplicates (B) SC5314 (WT) cell viability assessed by 10-fold dilutions spotting of culture at the defined conditions ([FLC] = 32 $\mu\text{g/ml}$, [FeCl₃] = 1 mM, C+ = SC5314 cells only, C- = cell-free control). Pictures are representative of a biological duplicate.

Enrichment in resistant/tolerant OE strains in pool assay

In order to identify new mediators of tolerance using the OE collection, an enrichment in tolerant strains from a pool was performed (Figure 25). Briefly, the 579 strains were pooled and grown under strong FLC pressure (32 $\mu\text{g/ml}$) and in the presence or absence of Dox (100 $\mu\text{g/ml}$). To select tolerant strains, the culture was maintained for 5 days with daily re-inoculation into fresh media to maintain FLC and Dox concentrations. After 5 days of subculture, the fraction of each strain in the population was estimated for each tested condition by sequencing of the BC (Figure 25).

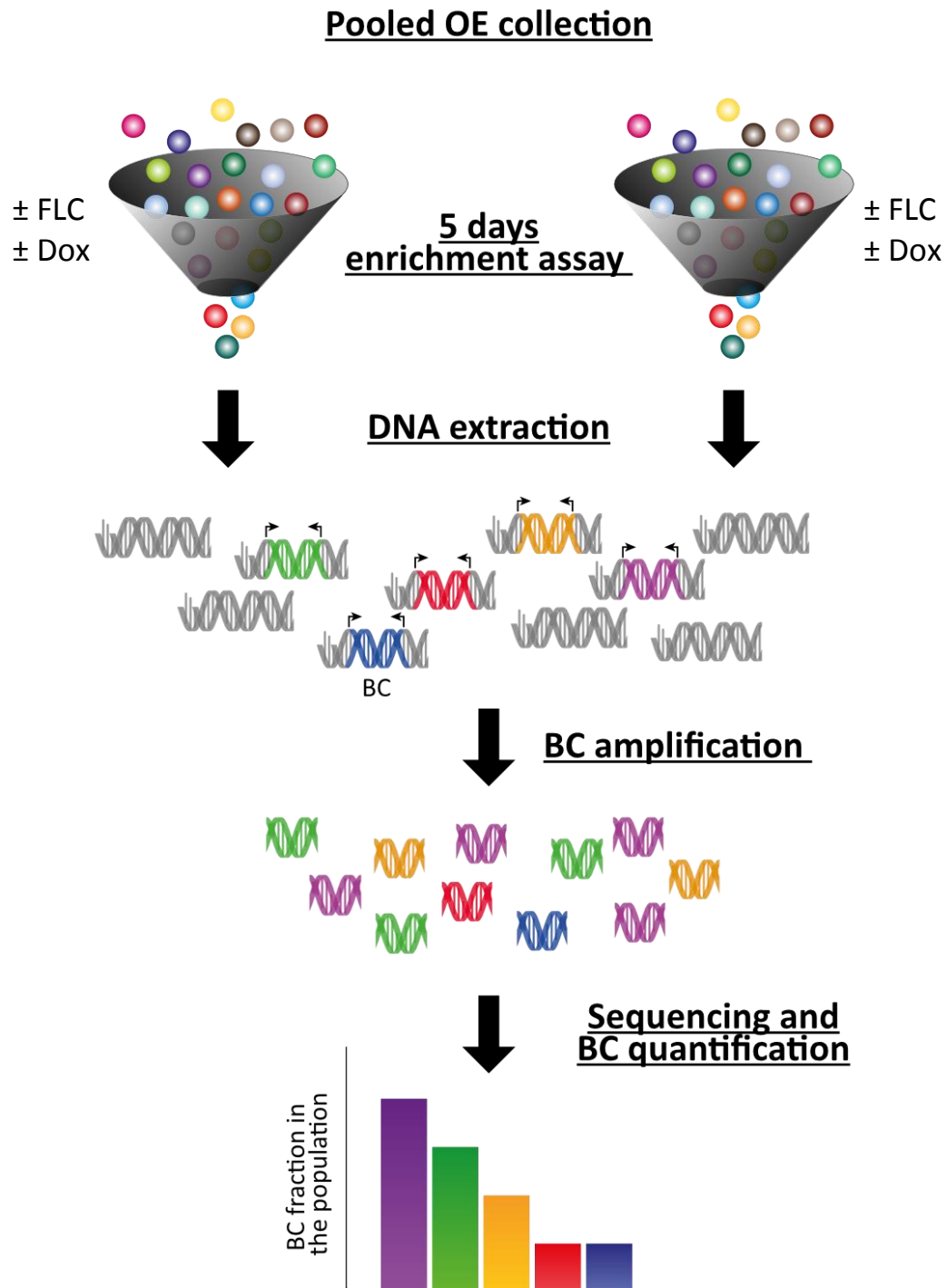


Figure 25: Summarized pool enrichment principle. See Material and Methods section for details

To evaluate the effect of this prolonged culture on the evolution of population, the population of the fifth day (D_5) in the absence of Dox and FLC (D_5 (D-F-)) was compared to the initial population (D_0). The mean ratio D_5 (F-D-)/ D_0 measured for all strains was 0.99 (Figure 26), suggesting that strains were

represented in the same proportion at D_5 and D_0 and confirming that fluctuations in populations at D_5 are due to the different growth conditions (Figure 26, top line). To evaluate the effect of FLC and Dox, the proportion of each strain in the presence of both compounds (D_5 (D+F+)) was compared to the reference condition (D_5 (D-F-)) (Figure 26, second line). Strains were up to 600-fold enriched and 25-fold depleted in the presence of FLC and Dox as compared to the reference (Supplementary File 2). Comparison of the population in the presence of FLC only (D_5 (D-F+)) to the reference allowed the identification of intrinsically resistant/tolerant strains with strains up to 900-fold enriched in presence of FLC and highly sensitive strains which were up to 15-fold depleted (Figure 26, third line, Supplementary File 2). To determine the effect of Dox in the absence of FLC on the population, the population in presence of Dox only (D_5 (D+F-)) was compared to the reference condition. Here, strains were up to 15-fold enriched and up to 500-fold depleted at D_5 (D+F-), indicating a slight effect of Dox on the population which is probably linked to the non-tightly regulated OE system (Figure 26, fourth line, Supplementary File 2). Finally, the effect of Dox in presence of FLC was estimated by comparing the population D_5 (D+F+) to the population D_5 (D-F+) (Figure 26, bottom line). This last comparison is expected to give valuable insight into the genes that mediate a selective growth advantage in the population when overexpressed in presence of FLC. In this comparison 78 strains were at least 2-fold enriched and 39 strains 2-fold depleted when their respective genes were overexpressed under strong FLC pressure (Figure 26, Supplementary File 2). Among them, the three top strains were those overexpressing *GZF3*, *orf19.399*, and *CRZ1* (60-fold, 38-fold and 25-fold enriched, respectively) (Table 15). On the other hand, the three strains which were the least represented in the pool were the strains overexpressing the *orf19.2097*, *SFL2* and *CPH1* (18-fold, 11-fold and 9-fold depleted, respectively (Table 15).

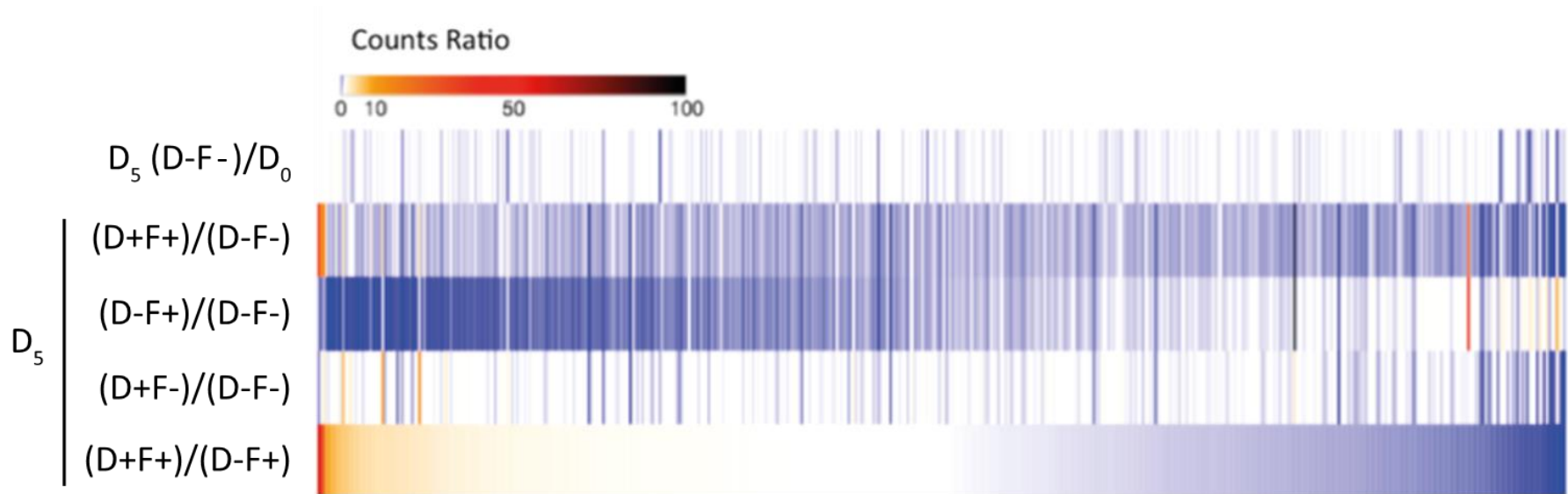


Figure 26: Comparisons of the population of the 579-Tet-inducible OE strains collection pool after 5 days of enrichment. The Heatmap represents the comparison between the cultures at day 5 (D_5) and the initial population (D_0), in presence (F+) or absence (F-) of FLC (32 $\mu\text{g}/\text{ml}$), and in the presence (D+) or absence (D-) of 100 $\mu\text{g}/\text{ml}$ Dox. Each line represents the mean relative count ratio of biological duplicates. The heatmap is filtered based on the (D_5 (D+F+) / D_5 (D-F+)) comparison. Detailed-data can be found in Supplementary File 2.

Table 15: Top 10 enriched and depleted strains after 5 days of subculture. The effect of 5 days of subculture (D_5 (D-/F-)/ D_0) and the effect of the gene OE in presence of FLC (comparison with the initial pool population (D_5 (D+/F+)/(D_5 (D-/F+)) on the pooled population is represented as the fold change of the presence of a strain in the population.

	orf n°	Gene name	(D-F-) ¹ / D_0 ²	D_5 ² (D+F+)/(D_5 (D-/F+))	Category
Top 10 enriched strains	orf19.2842	<i>GZF3</i>	1.07	60.60	Transcription factor
	orf19.399	NA ³	1.08	38.63	Protein kinase
	orf19.7359	<i>CRZ1</i>	1.07	25.87	Transcription factor
	orf19.5157	NA	1.18	9.43	Protein phosphatase
	orf19.5335	<i>SGS1</i>	1.36	9.36	DNA replication/recombination/repair
	orf19.3715	<i>ASF1</i>	0.96	8.07	DNA replication/recombination/repair
	orf19.2324	<i>UBA4</i>	1.25	7.73	Protein phosphatase
	orf19.4166	<i>ZCF21</i>	1.14	6.93	Transcription factor
	orf19.2320	NA	1.41	6.86	Protein kinase
	orf19.2907	<i>PGA42</i>	1.14	6.21	Cell wall genes
Top 10 depleted strains	orf19.217	NA	0.81	0.30	Transcription factor
	orf19.4979	<i>KNS1</i>	1.38	0.25	Protein kinase
	orf19.3300	<i>ZPR1</i>	0.43	0.21	Transcription factor
	orf19.1189	NA	0.99	0.20	DNA replication/recombination/repair
	orf19.6936	<i>RAD53</i>	0.99	0.15	Protein kinase
	orf19.7208	<i>CSK1</i>	0.97	0.14	Protein kinase
	orf19.5032	<i>SIM1</i>	0.26	0.13	Various
	orf19.4433	<i>CPH1</i>	0.86	0.11	Transcription factor
	orf19.3969	<i>SFL2</i>	0.87	0.09	Transcription factor
	orf19.2097	NA	0.83	0.05	Transcription factor

¹ D = Doxycycline, F = Fluconazole, +/- = presence/absence of the drug

² D_0 = initial population (Day 0), D_5 = population after 5 days on enrichment

³ Not Available

Fold change (-)



Single strain FLC tolerance profiling

To avoid a bias caused by growth in pools and to confirm the candidate genes identified in the pool enrichment procedure, the tolerance profile of each strain in the collection was tested individually (Figure 27). Growth in the presence of FLC and Dox (D+F+) and in the presence of FLC only (D-F+) were compared to growth in the F-D- control condition. Relative growths in the presence of Dox and FLC (D+F+) ranged from 14 % to 67 % as compared to the F-D- control condition, while relative growths under FLC pressure only (D-F+) was comprised between 8 % and 65 % (Figure 27A, Supplementary File 4).

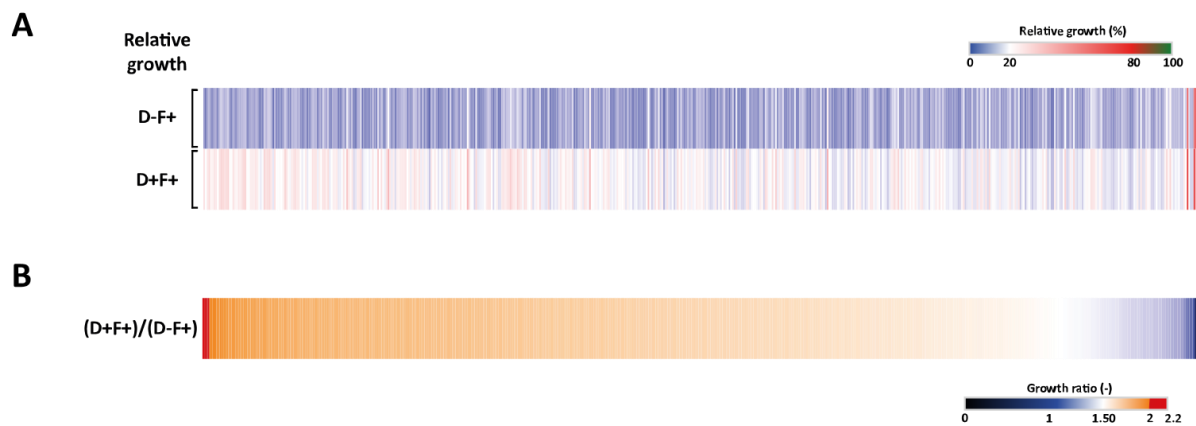


Figure 27: Single strain tolerance profiling. (A) Heatmap representing the relative growth of the 579 Tet-inducible OE BC strains collection at pH 6, in presence of 32 $\mu\text{g/ml}$ FLC pressure (F+) and in presence (D+) or absence (D-) of 100 $\mu\text{g/ml}$ Dox. Each line represents the mean relative growth of biological triplicates. (B) Heatmap highlighting the effect of Dox induction upon FLC tolerance represented as the growth ratio between the condition with and without Dox ((D+F+)/((D-F+))).

Table 16: Highlight of the 10 top-hit strains showing the highest and lowest growth ratio of the single strain assay.

	orf n°	Gene name	Relative growth (% GC) ¹		Fold change (-)	Category
			D-F+ ²	D+F+	(D+F+)/(D-/F+)	
Top 10 strains with increased tolerance	orf19.2842	<i>GZF3</i>	12.44	26.35	2.14	Transcription factor
	orf19.4401	<i>YVH1</i>	9.67	19.82	2.05	Protein phosphatase
	orf19.2538	<i>PTC2</i>	12.75	25.43	2.02	Protein phosphatase
	orf19.7001	<i>YCK2</i>	14.03	28.24	2.01	Protein kinase
	orf19.3356	<i>ESP1</i>	11.32	22.34	1.97	DNA replication/recombination/repair
	orf19.5144	<i>PGA28</i>	11.61	22.87	1.97	Cell wall genes
	orf19.6792	<i>RRD1</i>	13.17	25.83	1.96	Protein phosphatase
	orf19.799	<i>STE4</i>	13.06	25.42	1.95	Other signaling comp
	orf19.5636	<i>RBT5</i>	10.36	20.09	1.94	Cell wall genes
	orf19.5257	<i>LCB4</i>	14.57	27.58	1.94	Various
10 strains ranking last in the TI screen	orf19.3199	<i>PIKA</i>	13.76	17.56	1.32	Various
	orf19.3294	<i>MBF1</i>	13.47	17.61	1.31	Transcription factor
	orf19.1759	<i>PHO23</i>	18.91	24.34	1.31	Transcription factor
	orf19.4377	<i>KRE1</i>	16.48	20.01	1.28	Cell wall genes
	orf19.4473	NA ³	55.66	67.60	1.24	Uncharacterized
	orf19.7652	<i>CKA1</i>	17.28	19.70	1.23	Protein kinase
	orf19.6926	<i>CSC25</i>	13.31	15.76	1.20	Protein kinase
	orf19.3589	<i>SPO11</i>	14.05	16.82	1.20	DNA replication/recombination/repair
	orf19.7473	NA	53.59	63.65	1.18	DNA replication/recombination/repair
	orf19.7208	<i>CSK1</i>	65.37	34.08	0.52	Protein kinase

¹ % of the drug free growth control

² D = Doxycycline, F = Fluconazole, +/- = presence/absence of the drug

³ NA = Not Available

Fold change (-)



In order to select tolerant/resistant strains, isolates with a relative growth at least 2-fold higher in the presence of Dox and FLC (D+F+) than in presence of FLC only (D-F+) were selected (Figure 27B). Interestingly, unlike results obtained from the pool enrichment assay (78 strains at least 2-fold enriched), only four strains exhibited a 2-fold increase of growth in presence of FLC and Dox in the single strain assay. This suggests a strong pool effect in the pool enrichment assay. These four strains included those overexpressing *GZF3* (2.14-fold growth increase), *YVH1* (2.05-fold increase), *PTC2* (2.02-fold increase), and *YCK2* (2.01-fold increase) (Figure 27B, Table 16). On the other hand, no strains had a growth at least 2-fold reduced when Dox was added. Indeed, only the strain overexpressing *CSK1* showed a decreased growth in presence of Dox (0.52-fold decrease), but this growth depletion was due to an abnormal high growth (65 % of the growth control) when grown in presence of FLC only (Figure 27B). The difficulty to observe growth reduction upon Dox induction in presence of FLC might be due to the already low tolerance level of the parental CEC161 strain used to build the collection. Interestingly, the *GZF3* OE strain was the best hit in both approaches, making it an engaging potential mediator of FLC tolerance. Using results from both the enrichment and the single strains assays, a total of twelve strains were selected for further characterization of their FLC susceptibility and tolerance profile including the strains overexpressing *GZF3*, *CRZ1*, *PTC2*, *YVH1*, *YCK2*, orf19.399, orf19.5157, orf19.2320, *SGS1*, *ASF1*, *UBA4* and *ZCF21*.

Putative negative regulators of tolerance

Calcium induced tolerance

While the gene OE was useful to identify positive regulators of FLC tolerance, the same forward genetic approach may be used to identify genes that, when overexpressed, could decrease the growth of strains at supra-MIC drug concentrations. With regards to the performed enrichment assay in the presence of FLC and Dox, the potential negative regulators of tolerance were more difficult to validate due to the already low basal tolerance level of the *C. albicans* parental strain (CEC161) used to construct the OE collection (Figure 24B) [56]. Therefore, we attempted to increase the basal tolerance

level of the depleted strains in the above-mentioned pool enrichment assay. Indeed, calcium (CaCl_2) is a known modulator of tolerance necessary for the activation of the calcineurin pathway known to increase FLC tolerance [44]. As a pilot experiment, the strain overexpressing *ZPR1* (4.8-fold depleted in the enrichment assay), was selected to determine its tolerance level in presence of FLC, Dox and serial dilutions of CaCl_2 (Figure 28). At pH 4.5, there was no clear effect of calcium at all tested CaCl_2 concentrations. However, tolerance levels started to increase significantly at 1.56, 3.125 and 12.5 mM CaCl_2 at pH 7.5, pH 7 and pH 6, respectively (Figure 28A-C). Due to a strong tolerance induction above the lower tolerance threshold (TI = 0.2) at all pH conditions tested except pH 4.5 (Figure 28, Figure 29), the concentration of 50 mM CaCl_2 was selected to test whether negative regulators could be validated using the other 7 most-depleted genes of the enrichment assay.

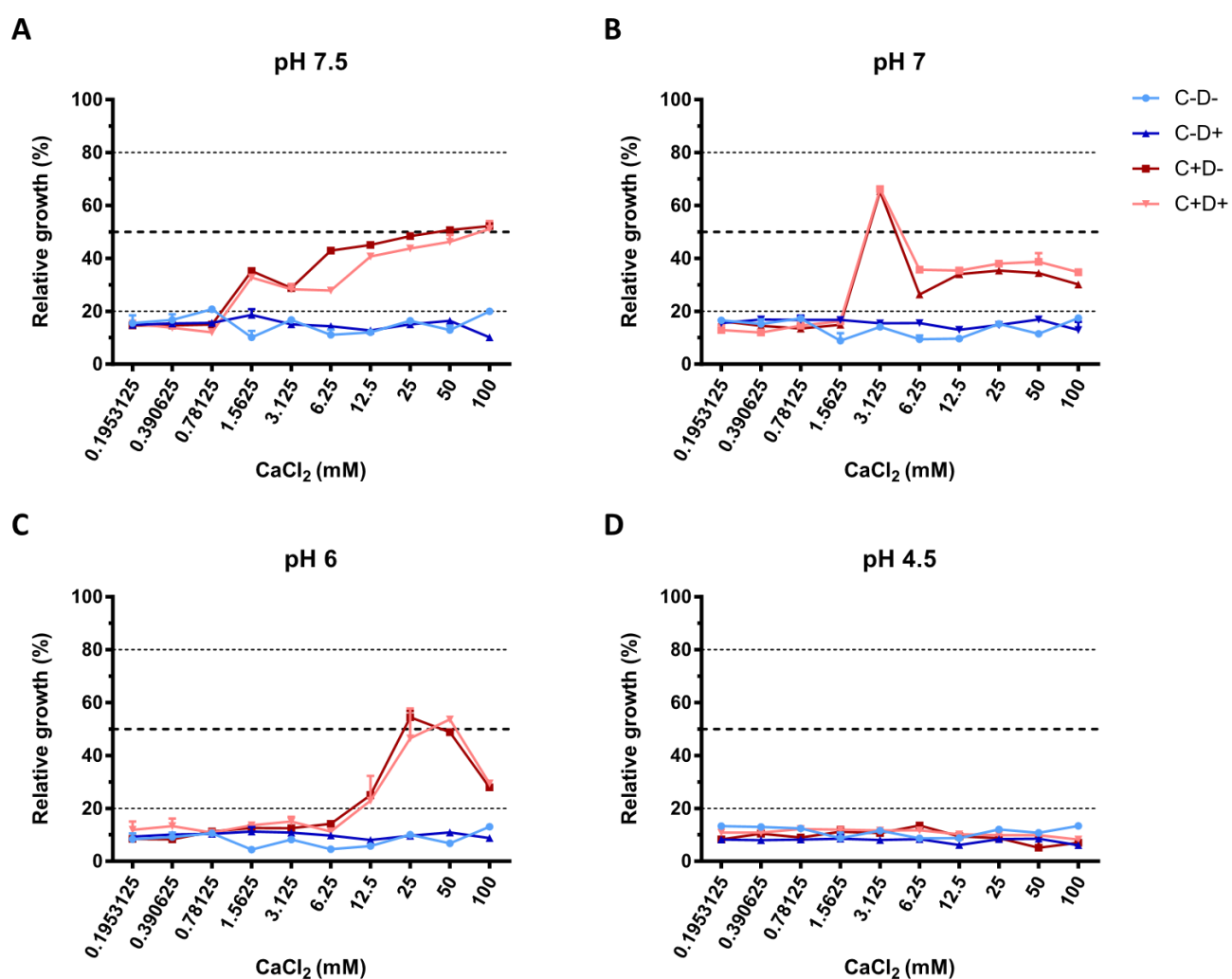


Figure 28: Calcium induction of the *ZPR1*-OE strain FLC tolerance. Tolerance assays were performed at pHs 7.5, 7, 6 and 4.5 in presence of FLC (8 $\mu\text{g}/\text{ml}$), in presence (+) or absence (-) of Dox (5 $\mu\text{g}/\text{ml}$), in the presence (+) or absence (-) of CaCl_2 (from

100 mM, two-fold dilutions) and complemented with FeCl₃ (0.5 mM). Horizontal dashed lines represent the 20, 50 and 80 % of growth (respectively, TI = 0.2, 0.5 and 0.8) thresholds used to determine the tolerance profile. Each data set represents the mean of technical duplicates.

The fluctuations in tolerance of the strains overexpressing *orf19.2097*, *SFL2*, *CPH1*, *SIM1*, *RAD53*, *orf19.1189*, *ZPR1*, *orf19.217*, *PIF1*, *RAD51*, *MDM34*, *GLC7* and *UGA32* were thus tested in presence of FLC and CaCl₂ with or without Dox induction (Figure 30). Globally, significant changes in TI under Dox induction could be observed mainly at pH 7 and pH 6 for the *orf19.1189*-OE strain in the absence of CaCl₂ (Figure 30).

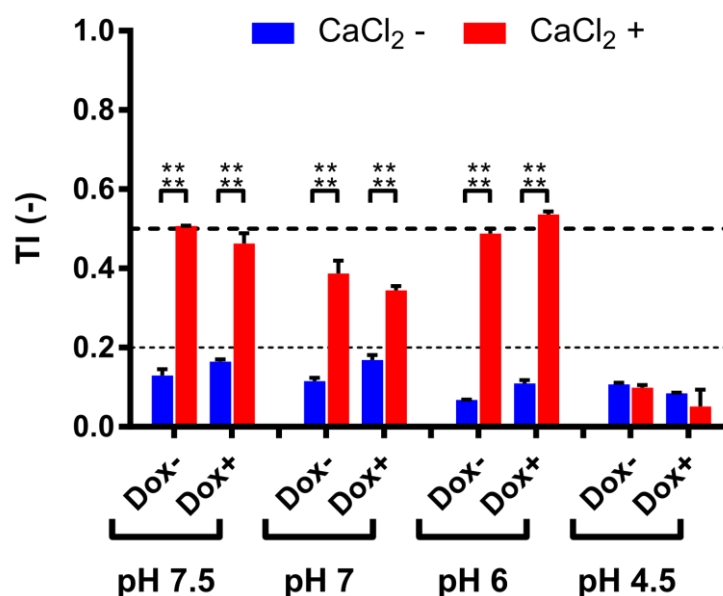


Figure 29: Susceptibility profiles of the *ZPR1*-OE strain. Tolerance assays were performed at pHs 7.5, 7, 6 and 4.5 in presence of FLC (8 µg/ml), in the presence (Dox+) or absence (Dox-) of Dox (5 µg/ml), in the presence (CaCl₂ +) or absence (CaCl₂ -) of calcium (50 mM) and complemented with FeCl₃ (0.5 mM). The horizontal dashed line represents the lower threshold of tolerance (TI = 0.2) and the limit of susceptibility (TI = 0.5) as described by EUCAST. Statistical significance was calculated by Sidak's multiple comparison tests (two-way ANOVA, 95 % confidence interval) comparing the Dox- and Dox+ conditions of each strain. Each bar is representative of biological duplicates. P-values: (ns) ≤ 0.1235, (*) ≤ 0.0332, (**) ≤ 0.0021, (***) ≤ 0.0002, (****) ≤ 0.0001.

The addition of CaCl₂ efficiently increased basal tolerance levels at pH 6, pH 7 and pH 7.5 regardless of the strain allowing to reach higher tolerance levels (0.2 < TI > 0.8). However, the presence of Dox was not significantly altering tolerance. It is likely that FLC tolerance activated by the calcineurin pathway masked the potential negative regulation of the tested strains. Based on these observations, another approach was selected to test these putative negative regulators of tolerance using known FLC-tolerant clinical isolates.

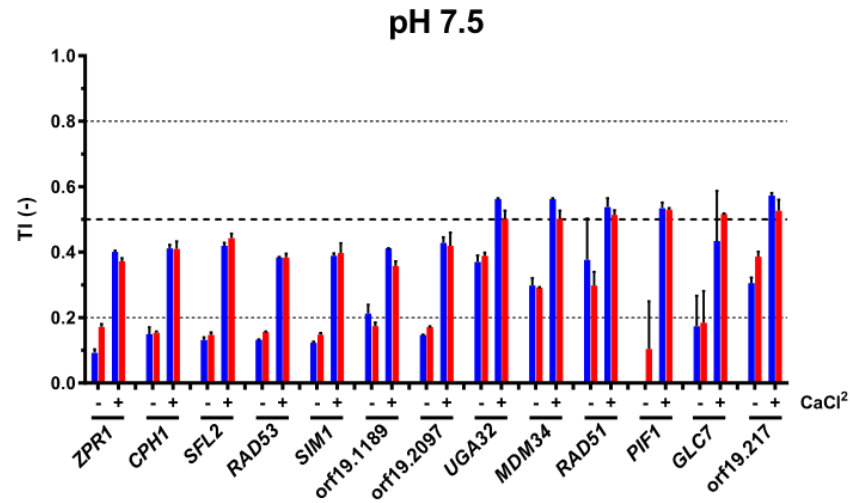
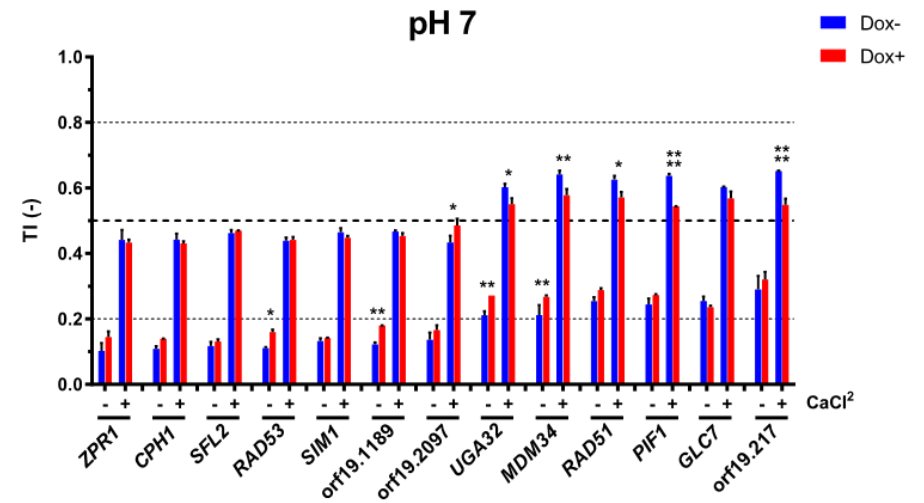
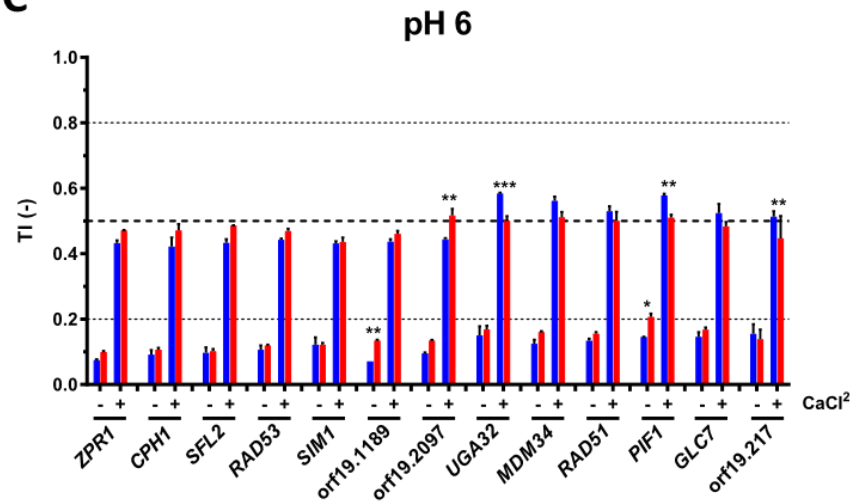
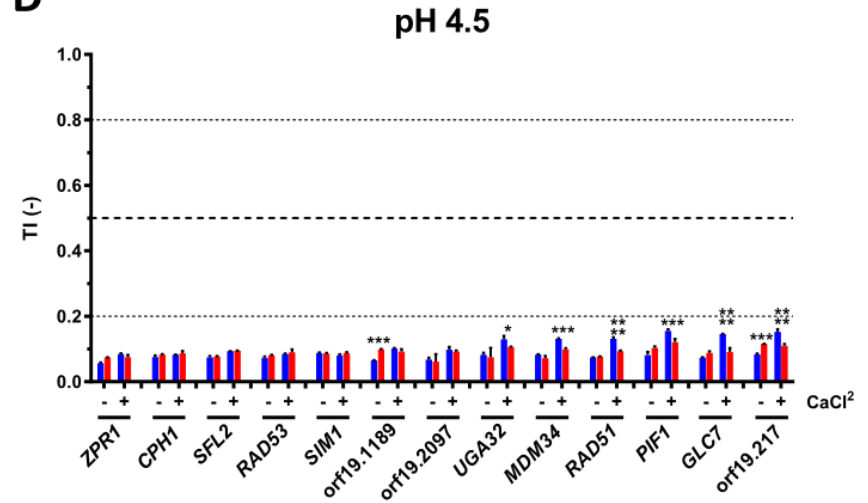
A**B****C****D**

Figure 30: Tolerance profiles of putative negative regulators of FLC tolerance. Tolerance was assessed in presence (Dox+) or absence (Dox-) of 5 µg/ml Dox and in presence (+) or absence (-) of 50 mM CaCl₂ and 0.5 mM FeCl₃. Horizontal dashed lines represent the lower and upper thresholds of tolerance (TI = 0.2 and 0.8 respectively) as well as the limit of susceptibility (TI = 0.5) as described by EUCAST. Statistical significance was calculated by Sidak's multiple comparison tests (two-way ANOVA, 95 % confidence interval) comparing the Dox- and Dox+ conditions of each strain. Each bar is representative of the mean of biological duplicates. P-values: (ns) ≤ 0.1235, (*) ≤ 0.0332, (**) ≤ 0.0021, (***) ≤ 0.0002, (****) ≤ 0.0001.

Negative regulators OE in tolerant clinical isolates

To test the putative negative regulators of tolerance identified previously without using calcium induction, each gene was overexpressed into clinical isolates already known to display high levels of tolerance. The clinical isolates DSY2110, DSY4454, DSY4588 and DSY4754 (Table 12, Figure 31) were selected based on their tolerance profiles. These isolates were either tolerant or susceptible to FLC at pH 7.5, 7, 6 and 4.5 (Figure 31).

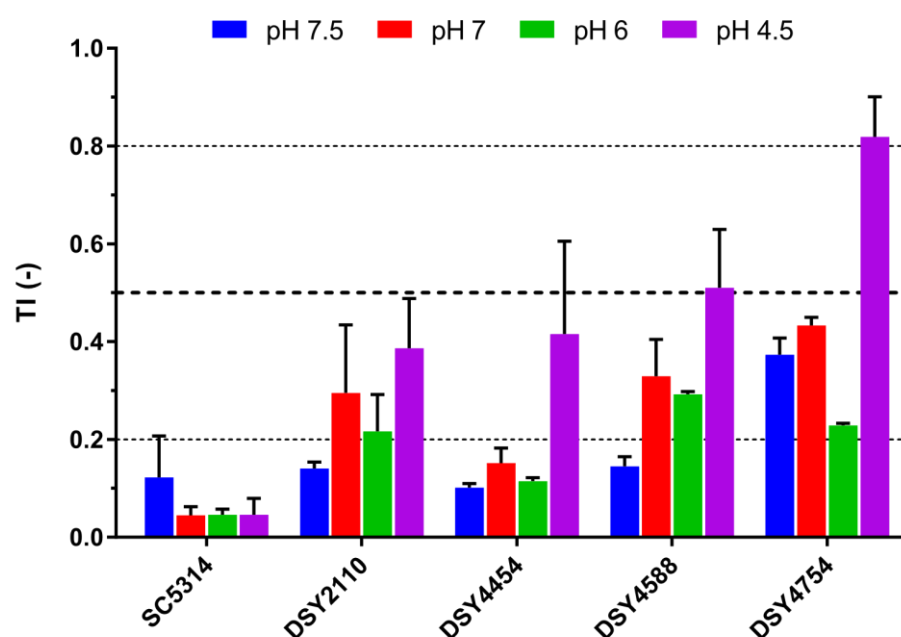
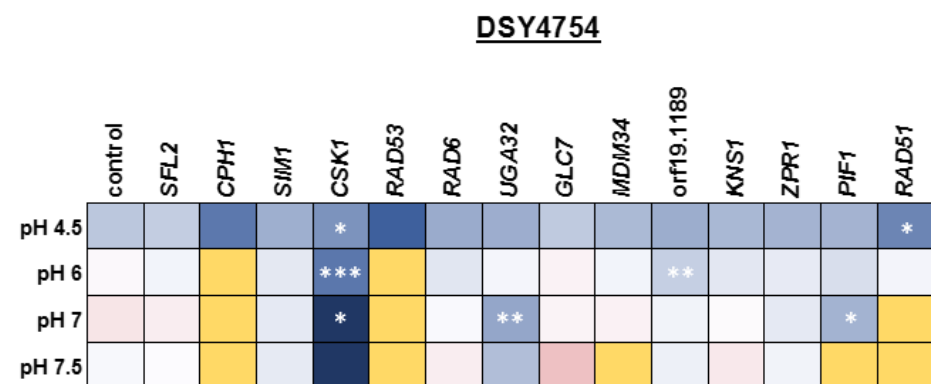
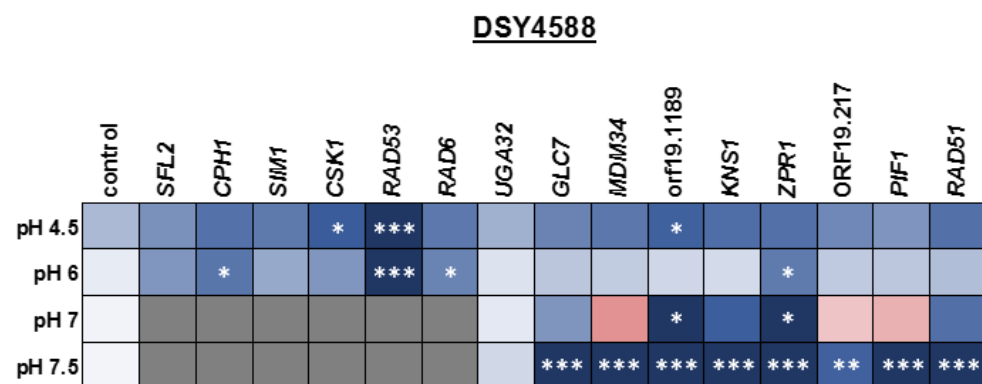
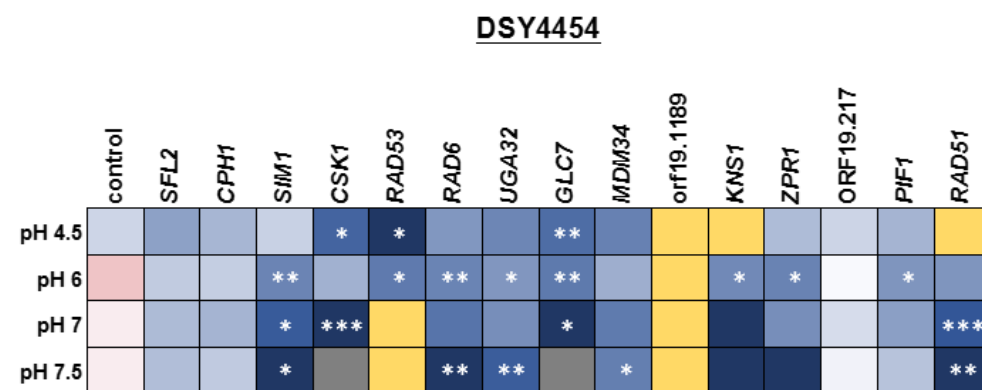
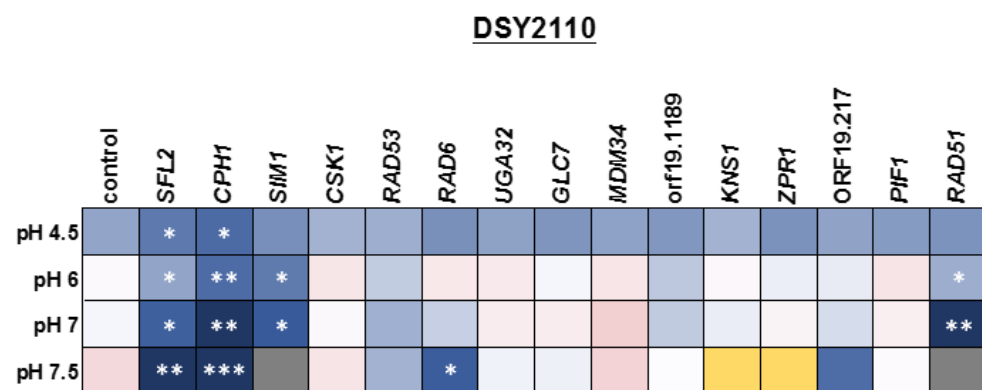


Figure 31: Tolerance of selected clinical isolates. TI levels of the WT strain (SC5314) and of 4 clinical isolates at 4 different pH conditions are shown. Horizontal dashed lines represent the lower and upper thresholds of tolerance (TI = 0.2 and 0.8, respectively), and the limit of susceptibility (TI = 0.5) as described by EUCAST. Each bar corresponds to the mean of at least biological duplicates.

The OE system for each selected gene was cloned into the strains (Table 12, Supplementary Table 1) as described by Chauvel *et al.* [56]. Unfortunately, the plasmid overexpressing orf19.2097 (*i.e.* the gene resulting in the most depleted strain of the enrichment when OE) could not be linearized using any available restriction enzymes for genome integration. In addition to the genes tested in the calcium tolerance induction assay (*i.e.* *SFL2*, *CPH1*, *SIM1*, *RAD53*, orf19.1189, *ZPR1*, orf19.217, *PIF1*, *RAD51*, *MDM34*, *GLC7* and *UGA32*), the plasmids overexpressing *CSK1*, *RAD6* and *KNS1* were also transformed (Supplementary Table 1 and 3). Each clinical isolate and its respective OE-clones were then tested in tolerance assays in presence or absence of Dox to observe any potential alteration of tolerance upon overexpression of the selected genes (Figure 32). To quantify the modification of tolerance upon Dox addition, we defined a tolerance ratio (TR), which compares growth in presence of FLC in

presence/absence of Dox. Thus, a TR = 1 indicated no growth difference between both conditions. A TR < 1 reflects that the overexpressed gene could be a suppressor of FLC tolerance whereas a TR > 1 will indicate that the GOI could be a positive regulator of tolerance. When growth was absent in the presence of FLC in both conditions, a TR could not be calculated (Figure 32).

Overall, the TR at pH 4.5 were below a value of 1. This tendency was also observed in control strains bearing an empty OE plasmid (Figure 32). Therefore, this effect could not be attributed to specific genes or specific strains and could be resulting from an effect of the pH upon tolerance in the tested conditions. In addition, the strains derived from DSY4454 exhibited a surprisingly high number of positive scores (*i.e.* a significant decrease of TR compared with the respective control strain). It is likely that the DSY4454 background is more susceptible to the OE system than other clinical strains. Thus, the results obtained by this strain were not further evaluated. Another global finding was that strains derived from DSY4588, including the control strain, showed growth deficiencies at pH 7 and pH 7.5 in the presence of FLC as if the OE system drastically increases FLC susceptibility. This susceptibility was not observed in the initial clinical isolates (Figure 32). Comparisons of TR at these pH values were thus more difficult. Growth at pH 6 appeared the most optimal condition when considering the entire set of mutants. Overall, we observed several conditions in which TRs were significantly decreased relative to the control strain at a specific pH. Interestingly, the overexpression of *SFL2* and *CPH1* (in DSY2110) as well as *CSK1* (in DSY4754) significantly decreased tolerance at all pH (TR < 1) on a strain-specific manner (Figure 32), thus making them interesting putative repressors of FLC tolerance. However, none of the tested genes could be clearly identified as a general repressor of FLC tolerance when comparing all the different strains. This underscored a strain-specific behavior of these genes in the presence of FLC and is certainly due to the different genetic backgrounds of the tested clinical isolates.



Tolerance ratio (-)

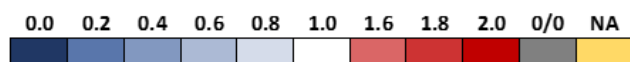


Figure 32: Tolerance ratio of selected Tet-inducible clinical isolates. Heatmaps correspond to the comparisons of the TIs at pHs 7.5, 7, 6 and 4.5 under FLC pressure (8 µg/ml) between growth in presence and absence of 5 µg/ml Dox. FeCl₃ (0.5 mM) was added to avoid the synergistic FLC-Dox effect. Each square corresponds to the mean tolerance ratio (TR) (Dox+/Dox-) of biological triplicates. Briefly, a TR = 1 indicates that the specified gene OE has no effect upon tolerance, a TR > 1 indicates that the gene OE results in a better growth in presence of the drug and Dox and a TR < 1 indicates a loss of tolerance upon the selected genes Dox induction. Grey and yellow squares indicate samples with no detectable growth in presence of FLC (no TR could be defined) and samples which could not be analyzed, respectively. Statistical significance was determined using Kruskal-Wallis non-parametric tests (Dunn's correction). P-values: (ns) ≤ 0.1235, (*) ≤ 0.0332, (**) ≤ 0.0021, (***) ≤ 0.0002, (****) ≤ 0.0001. A table with the corresponding strains name can be found in Supplementary table 1.

Putative positive regulators of tolerance

FLC susceptibility profile of putative positive mediators

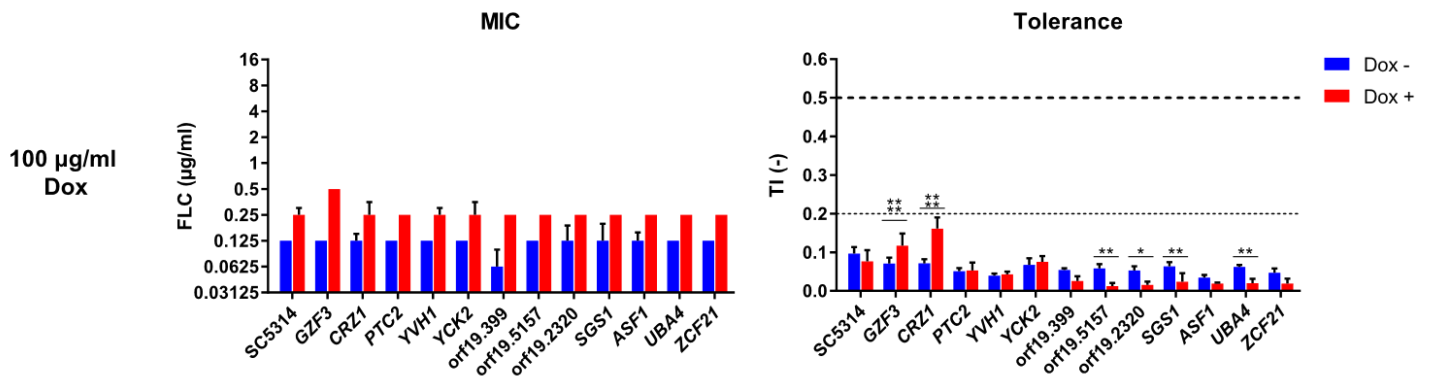
In opposite to the identification of negative regulators of FLC tolerance, the identification of positive regulators was not impaired by the low basal tolerance level of the BWP17-derived parental strain CEC161 used to construct the OE collection. Thus, strains selected from both the pool enrichment and the single strain assays (Figure 26 and Figure 27) were tested individually to establish their FLC susceptibility profiles at pH 6 in the presence of Dox. Only pH 6 was tested to remain consistent with the pool enrichment assay. A total of 12 strains of the OE collection were tested, including strains overexpressing *GZF3*, *CRZ1*, *PTC2*, *YVH1*, *YCK2*, orf19.399, orf19.5157, orf19.2320, *SGS1*, *ASF1*, *UBA4* and *ZCF21* (Supplementary File 2), in addition to the WT SC5314 which was used as a susceptibility control.

Overall, no strains could be considered as tolerant as defined earlier for clinical isolates (*i.e.* $TI \geq 0.2$) at 100 $\mu\text{g/ml}$ Dox. However, all strains showed a two-fold dilution increase in MIC under Dox induction conditions (0.125 $\mu\text{g/ml}$ FLC to 0.25 $\mu\text{g/ml}$ FLC), except for the strain overexpressing *GZF3* which reached a MIC of 0.5 $\mu\text{g/ml}$ in presence of Dox. Nevertheless, MIC values remained below the FLC CBP (*i.e.* 4 $\mu\text{g/ml}$ FLC) (Figure 33A, left panel). With regards to the tolerance level, all strains had an equal or lower TI in the presence of Dox, except for the *GZF3* and *CRZ1* OE strains that exhibited a significantly higher TI (from $TI = 0.07$ to 0.12 and 0.16, respectively). However, all TI levels remained under the tolerance threshold defined earlier for clinical isolates (*i.e.* $TI < 0.2$) (Figure 33A, right panel).

Due to a global increase in MIC values at 100 $\mu\text{g/ml}$ Dox, strains were also tested at 10 $\mu\text{g/ml}$ Dox to test whether this increase was concentration-dependent. At this Dox concentration, every strain presented a similar MIC independently of Dox induction, with all MICs remaining at around 0.125 $\mu\text{g/ml}$ FLC except for the *GZF3* OE strain which reached a MIC of 0.25 $\mu\text{g/ml}$ FLC (Figure 33B, left panel). Here again, no increases in tolerance levels could be observed for most of the strains under Dox induction, except for the strains overexpressing *GZF3* ($TI = 0.048$ to 0.2), *CRZ1* ($TI = 0.07$ to 0.21) and

YCK2 (TI = 0.06 to 0.14). However, only *GZF3* and *CRZ1* OE allowed a tolerance increase above the lower tolerance threshold of TI = 0.2 (Figure 33B, right panel).

A



B

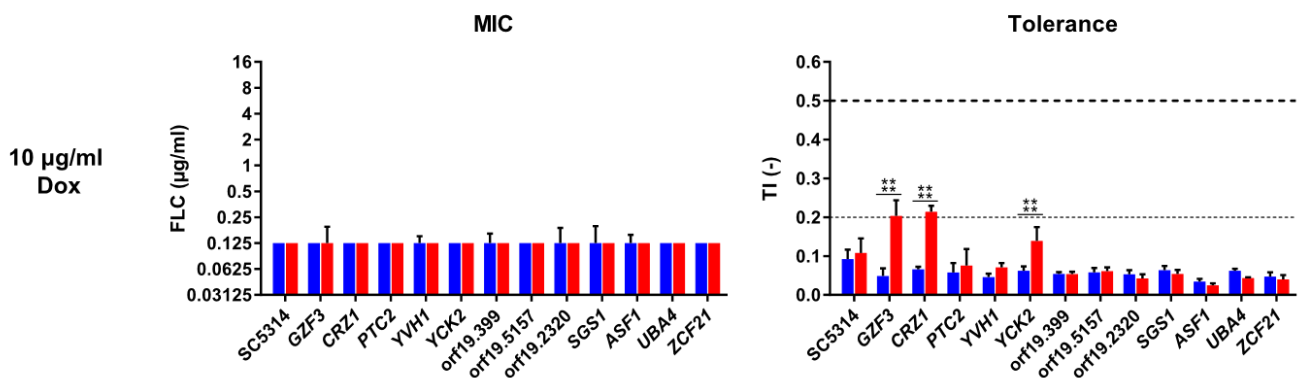


Figure 33: Susceptibility profiles of selected Tet-inducible strains in the presence Dox. Susceptibility profiles were performed at pH 6, in a range of FLC concentrations (0-16 µg/ml), in the presence (Dox+) or absence (Dox-) of doxycycline and complemented with 1 mM FeCl₃. FLC susceptibility at 100 µg/ml (A) and 10 µg/ml (B) Dox represented by their modal MIC value (left panel) and TI at 8 µg/ml FLC (right panel). Standard deviations of the MIC values were calculated based on the mean MIC of each sample. The horizontal dashed line represents the lower threshold of tolerance (TI = 0.2) and the limit of susceptibility (TI = 0.5) as defined by EUCAST. Each bar is representative of biological triplicates. Statistical significance was determined using Sidak's multiple comparison tests (Two-way ANOVA, Confidence interval = 95 %). P-values: (*) ≤ 0.05, (**) ≤ 0.01, (***) ≤ 0.0001.

CRZ1 and GZF3 OE in deletion mutants

In order to better understand the mechanisms behind tolerance and the potential relation between *CRZ1* and *GZF3*, each gene was overexpressed in simple and double mutants. For this purpose, a *crz1Δ/Δ*, *gzf3Δ/Δ* double mutant (EDY28-2, Table 13) was constructed using the *crz1Δ/Δ* mutant from the Homann's deletion mutant collection [57]. The OE system for either *CRZ1* or *GZF3* was then transformed in this double mutant, in both Homann's *crz1Δ/Δ* and *gzf3Δ/Δ* single mutants as well as in the parental WT strain of the Homann's collection (Table 13). The plasmid overexpressing an empty overexpression plasmid (*i.e.* Clp10-P_{TET}-GTW, Supplementary Table 3) was also transformed in each strain as control of the OE system (Table 13). The FLC susceptibility profiles of these strains were then established in presence or absence of Dox and FLC to assess their respective MICs and TIs (Figure 34). FeCl₃ was once again used to avoid the synergistic effect between FLC and Dox. These susceptibility assays were performed at pHs 7 and 6 to avoid the growth defect observed at pH 7.5 and the iron precipitation observed at pH 4.5.

Overall, all strains had similar MIC values in presence or absence of Dox. The MIC for all tested strains at pH 7 was equal to 0.0625 µg/ml FLC with negligible variability (*i.e.* MIC = 0.125 µg/ml FLC). The *gzf3Δ/Δ* mutant overexpressing *CRZ1* showed the highest increase in MIC value, reaching 0.25 µg/ml FLC in presence of Dox (Figure 34A). Globally, the susceptibility profile remained the same at pH 6, with only the MIC values of all WT and *crz1Δ/Δ*-derived strains increasing at pH 7 from 0.0625 µg/ml to 0.125 µg/ml FLC (Figure 34C). However, the MICs of all strains in all the tested conditions remained well below the CBP of 4 µg/ml FLC. With regards to FLC tolerance, all strains showed a basal TI under the lower tolerance threshold (*i.e.* TI = 0.2) at both pH values in absence of Dox, with TIs ranging from 0.04 to 0.17 (Figure 34B and D). As expected, no significant fluctuation of the TI could be observed for the Clp10-P_{TET}-GTW overexpressing control strains at both tested pH values, with their TIs remaining below the lower tolerance threshold (TI values between 0.04 and 0.08, Figure 34B and D). Consistently with observations of the pool enrichment assay, *CRZ1* and *GZF3* OE resulted in a significant increase of the TI in a WT background. The TI increased from 0.08 to 0.2 for both the *CRZ1* and *GZF3* OE strain at

pH 7 and from 0.09 to 0.18 for the *CRZ1* OE strain and 0.09 to 0.14 for the *GZF3* OE strain at pH 6 (Figure 34B and D, respectively). Despite a significant increase in tolerance, only *CRZ1* OE at pH 7 reached the lower tolerance threshold in the WT genetic background. Looking at the deletion mutants, significant increase in TI could be observed at both pHs in the *gzf3Δ/Δ* mutant under *CRZ1* and *GZF3* OE. Indeed, TI increased from 0.17 to 0.28 and 0.16 to 0.31 at pH 7 and from 0.07 to 0.13 and 0.07 to 0.14 at pH 6 for *CRZ1* and *GZF3* OE, respectively (Figure 34B and D), thus reaching the lower threshold of tolerance at pH 7. On the other hand, only *CRZ1* OE resulted in an increased in tolerance in the double *crz1Δ/Δ*, *gzf3Δ/Δ* mutant, but significantly at pH 7 only with a TI increasing from 0.09 to 0.21 and with a tendency at pH 6 with an increase from 0.04 to 0.09. No effect of *GZF3* OE on the tolerance level could be observed in the double *crz1Δ/Δ*, *gzf3Δ/Δ* mutant with TI values of about 0.09 and 0.05 at pHs 7 and 6, respectively (Figure 34B and D). Interestingly, no effect of *GZF3* OE could be observed in the *crz1Δ/Δ* mutant, with TI fluctuation between 0.08 and 0.06 at pH 7 and about 0.05 at pH 6 (Figure 34B and D). However, *CRZ1* OE in this mutant background resulted under Dox induction in an increased tolerance from TI = 0.23 to 0.32 and from TI = 0.08 to 0.21 at pH 7 and 6, respectively (Figure 34B and D). To summarize, our results indicate that overexpressing *CRZ1* results in an increased FLC tolerance in all mutant backgrounds but, on the other hand, *GZF3* OE increases tolerance only when *CRZ1* was present (Figure 34B and D).

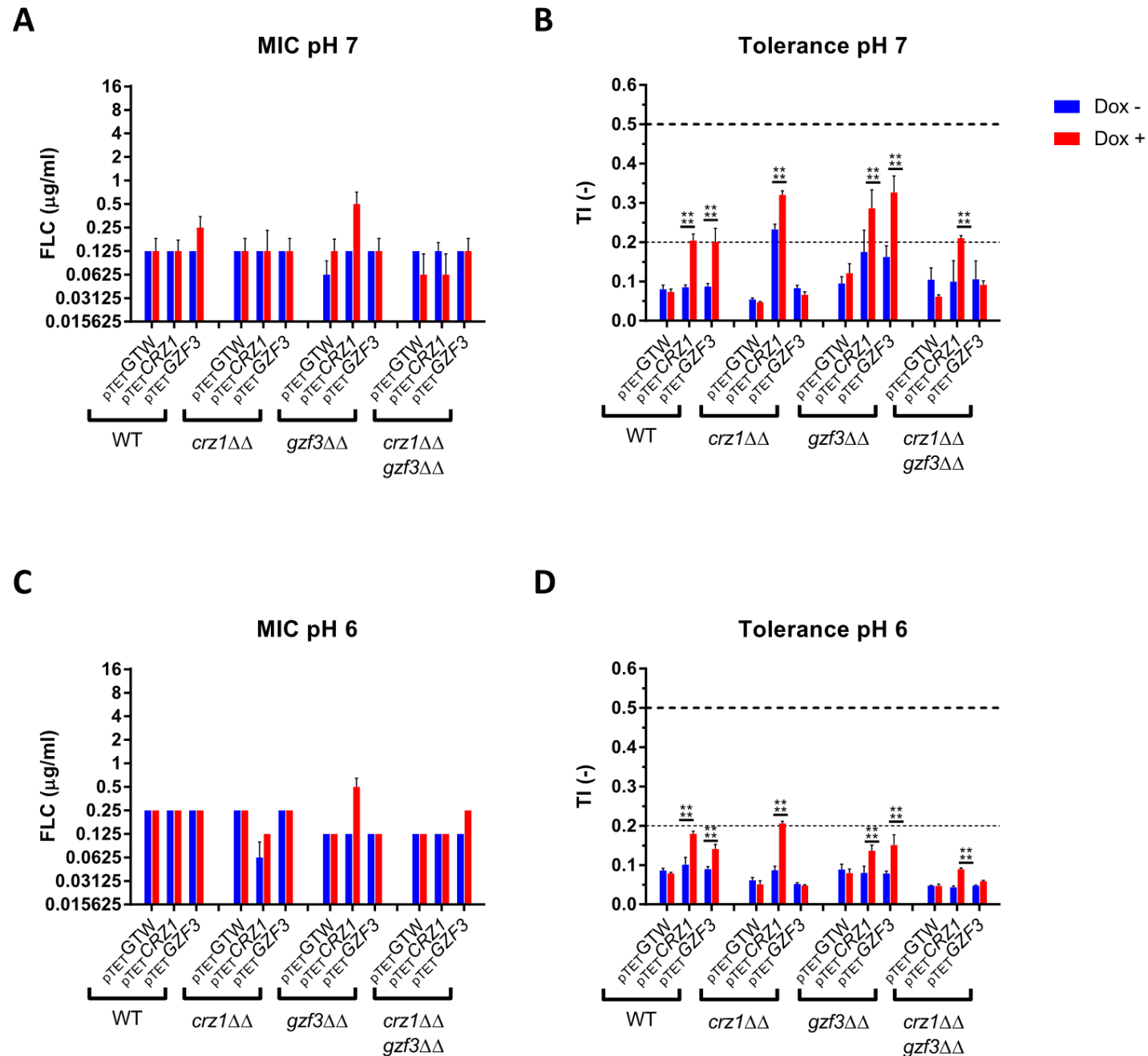


Figure 34: Susceptibility profile of the *CRZ1* and *GZF3* mutants overexpressing either *CRZ1*, *GZF3*. (A, C) Susceptibility to FLC is represented as the modal MIC value with standard deviation calculated on the mean MIC of all replicates. (B, D) Tolerance profile of the mutant strains. The mean TI and standard deviations are represented. Horizontal dashed lines represent the lower threshold of tolerance (TI = 2), and the upper limit of susceptibility (TI = 0.5) as described by EUCAST. Each data set represents the mean (or mode) of biological duplicates. Statistical significances (B, D) were estimated using Sidak's multiple comparison tests (2-way ANOVA, 95 % confidence interval) between Dox- and Dox + conditions in the same mutants set. P-values: (***) ≤ 0.0001 . A figure with the corresponding strains name can be found in Supplementary Figure 2.

CRZ1 and GZF3 deletions in tolerant clinical isolates

To confirm the role of *CRZ1* and *GZF3* in promoting tolerance to fluconazole not only in laboratory strains, either one or both allele of each gene were deleted in the *C. albicans* clinical isolates DSY2110, DSY4454, DSY4754 and DSY4588, already known to exhibit different level of FLC tolerance (Table 12, Table 14, Figure 31). Revertant strains were constructed by reinsertion of *CRZ1* and *GZF3* alleles from the reference isolate SC5314 as a control (Table 14). The FLC susceptibility profiles of each mutant and associated parental clinical isolates were assessed at pHs 7.5, 7, 6 and 4.5 and their MIC values and TIs extracted for comparisons (Figure 35 and Figure 36).

Globally, no differences could be observed between the MIC values of the original clinical isolates and their respective mutants, with all MICs standing below the FLC clinical breakpoint (CBP) of 4 µg/ml. In general, MICs slightly increased at more acidic pH (Figure 35). The isolate DSY2110 and its derived mutants showed mean MIC values of 0.5 µg/ml for the parental strain and 0.25 µg/ml for all the mutant strains at any pH (Figure 35A). DSY4454 and its derived mutants exhibited also similar MIC patterns as described in DSY2110 (ranging from 0.125 to 0.25 µg/ml FLC) which depended on the pH value. The mutants derived from DSY4454 were slightly more susceptible with MICs ranging from 0.0625 to 0.25 µg/ml (Figure 35B). The isolate DSY4588 and its derived mutants showed the same MIC levels than the previous strains, with MICs ranging from 0.125 to 0.25 µg/ml for the parental strains and from 0.0625 to 0.5 µg/ml for the mutants (Figure 35D). On the other hand, the isolate DSY4754 and its derived mutants exhibited an altered growth at pHs 7.5 and 7, resulting in aberrant MIC values reaching 16 µg/ml at pH 7.5 and ranging between 0.03125 and 0.25 µg/ml at pH 7 but with a high variability. The susceptibility results for DSY4754 and derivatives at these pH values should thus be carefully considered (Figure 35C).

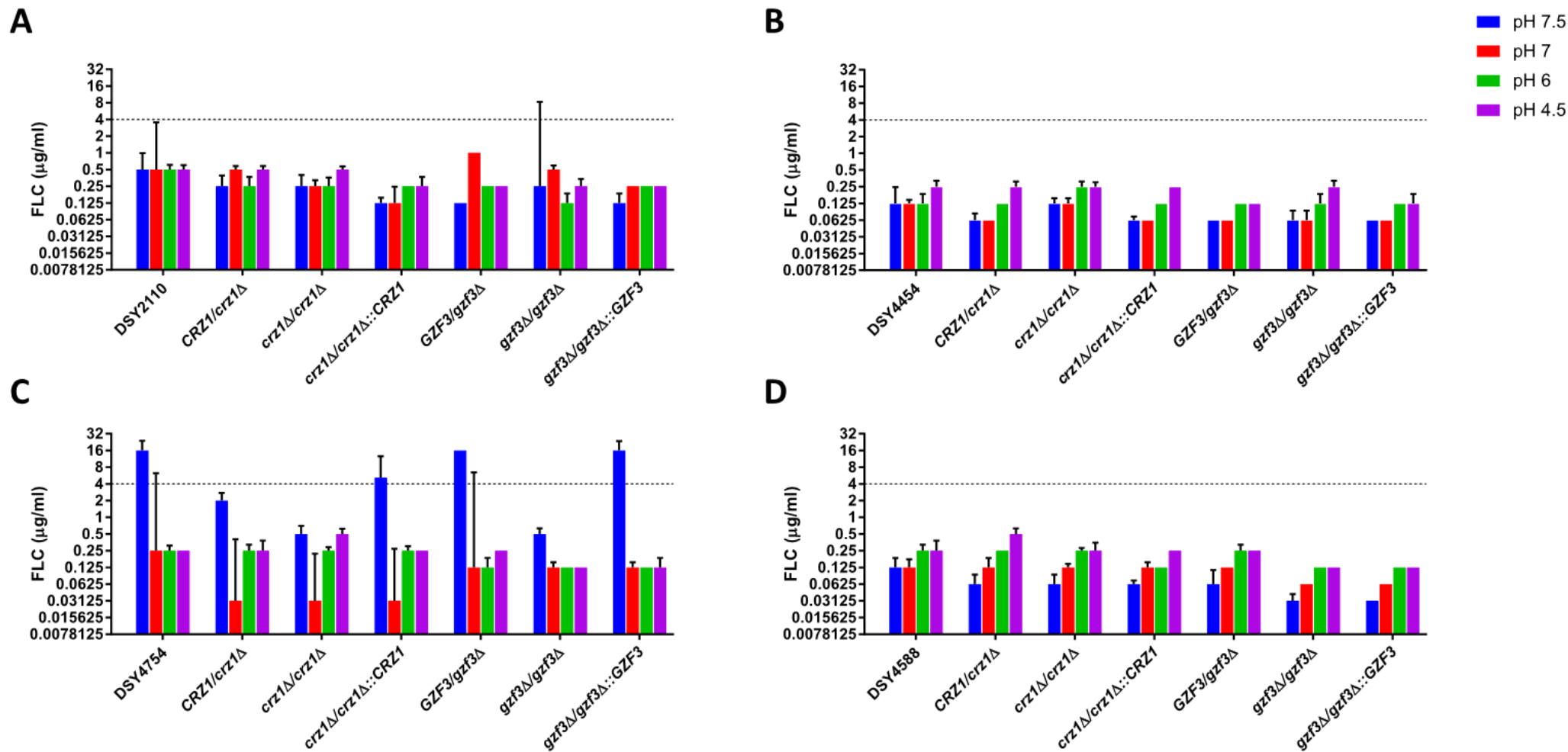


Figure 35: Fluconazole susceptibility profiles of the clinical isolates and their respective deletion mutants and revertant for *CRZ1* and *GZF3*. Susceptibility to FLC is represented as modal MIC values. Error bars indicate the standard deviation based on the mean MIC values. Dotted lines show the CBP for FLC (4 µg/ml). Each bar corresponds to biological duplicate.

When inspecting variations of FLC tolerance, a general reduction of tolerance levels was observed at acidic pH independently of the genetic background or of *CRZ1* and *GZF3* deletions (Figure 36). On the other hand, the effect of the deletion of *CRZ1* or *GZF3* upon tolerance seemed to be dependent on both the pH and the genetic background of the parental clinical isolate.

In the DSY2110 background, both heterozygous and homozygous *CRZ1* deletions as well as *CRZ1* complementation in the revertant strain resulted in a decreased FLC tolerance (Figure 36A). Unfortunately, no restoration of the initial tolerance level in the DSY2110 revertant strains could be observed. However, the homozygous *crz1Δ/Δ* mutant was consistently less tolerant than its heterozygous counterpart at all pHs, except pH 4.5 (Figure 36A, red bars). Regarding *GZF3* mutants in the DSY2110 background, deletion of only one allele did not have any effect upon tolerance. However, the deletion of both alleles resulted in reduced tolerance at pHs 6 and 4. Interestingly, the homozygous *GZF3* deletion resulted in increased tolerance level at pH 7.5. However, this was only observed in the DSY2110 background and at this pH condition. Complementation of *GZF3* consistently restored tolerance to the heterozygous mutant level, except at pH 7.5 (Figure 36A, green bars).

When inspecting DSY4454 and its derived mutants, a global reduction of tolerance could be observed for all mutants and revertant strains of both *CRZ1* and *GZF3* at any tested pH. Only *GZF3* mutants at pH 4.5 exhibited tolerance level similar to the parental isolate DSY4454. However, no differences could be observed between the heterozygous and homozygous mutants of both *CRZ1* and *GZF3*, and no effect of the complementation of both genes could be observed in this genetic background (Figure 36B).

Concerning DSY4754 and its derived mutant strains, all *CRZ1* mutants showed a reduced tolerance at pHs 7.5 and 7. At pHs 6 and 4.5, only the homozygous *CRZ1* mutant showed a significant tolerance reduction. The revertant strain restored tolerance to level similar to the DSY4754 parental strain at pH 7.5 but only to the heterozygous level at pHs 7 and 6. At pH 4.5, the revertant showed no difference with the homozygous mutant (Figure 36C, red bars). On the other hand, both *GZF3* mutant strains

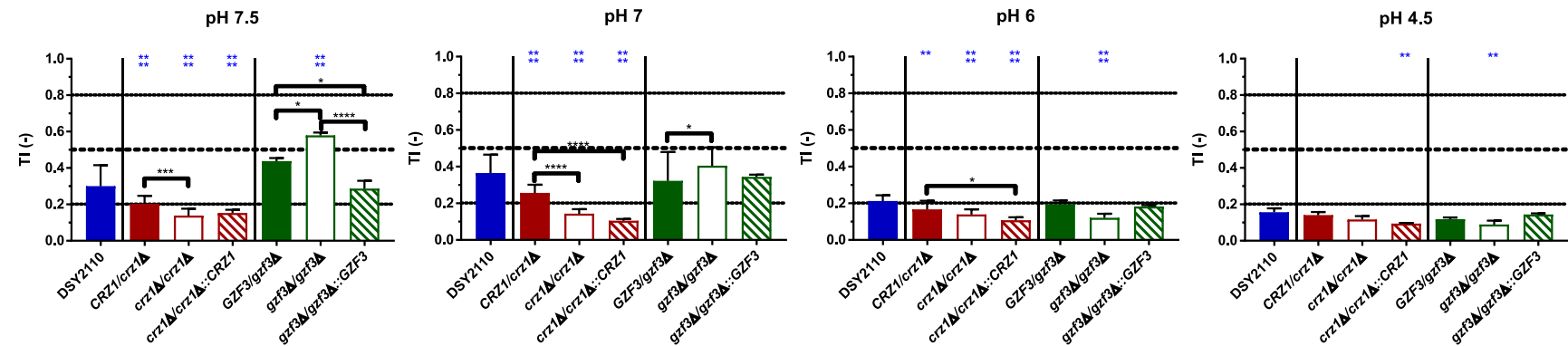
retained tolerance of DSY4754 at all tested conditions, except for the *GZF3* revertant at pH 7 in which a tolerance decrease could be measured as compared to DSY4754 (Figure 36C, green bars).

Finally, both *CRZ1* mutants derived from DSY4588 all showed reduced tolerance at any tested pH condition. However, the homozygous mutant had a significantly lower tolerance than the heterozygous mutant only at pH 7. *CRZ1* complementation restored tolerance to heterozygous levels at pH 7 and with a tendency at pH 7.5. However, no difference could be observed at pHs 6 and 4.5 with tolerance level similar the homozygous mutant (Figure 36D, red bars). With regards to *GZF3*, only the homozygous mutant and the revertant strain exhibited a reduced tolerance, and only at pHs 7 and 6. *GZF3* complementation did not restore tolerance in this genetic background and the heterozygous mutant did not show any loss of tolerance as compared to DSY4588. No reduction of tolerance could be observed for the *GZF3* mutant strains at pHs 7.5 and 4.5 (Figure 36D, green bars).

Taken together, the results of *CRZ1* and/or *GZF3* deletions and reversions revealed that *CRZ1* was the factor that most prominently altered FLC tolerance of the clinical stains. The results were dependent on the tested pHs and on the genetic background of the isolates.

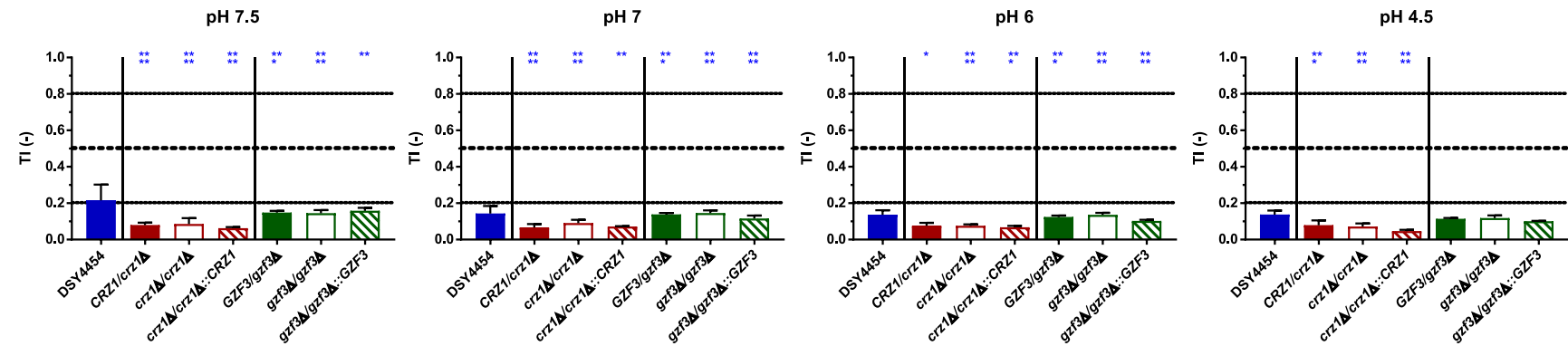
A

DSY2110 background



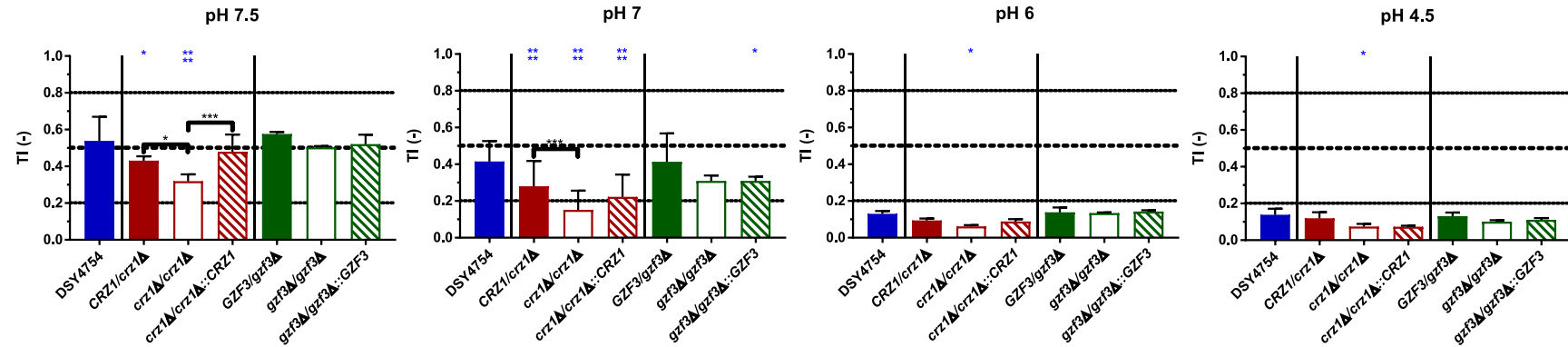
B

DSY4454 background



C

DSY4754 background



D

DSY4588 background

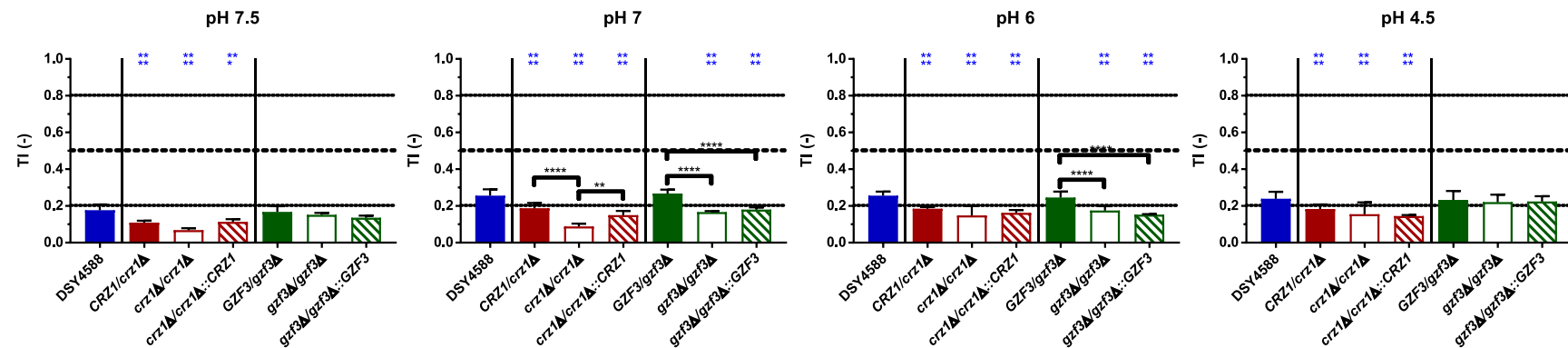


Figure 36: Tolerance levels of the different deletions mutants for both *CRZ1* and *GZF3* in the DSY2110 (A), DSY4454 (B), DSY4754 (C) and DSY4588 (D) genetic backgrounds. Each bar corresponds to at least biological duplicates. Statistical significance was calculated using Turkey multiple comparison tests (95 % confidence interval). P-values: 0.1234 (ns), ≤ 0.0332 (*), ≤ 0.0021 (**), ≤ 9.0002 (***), ≤ 0.0001 (****). Blue stars correspond to the comparison with the parental clinical isolates (blue bars). Black stars correspond to the comparisons between related mutant strains. A figure with the corresponding strains name can be found in Supplementary Figure 3.

Conclusions

Until now, tolerance to fluconazole has been an understudied research topic. Tolerance has been linked to an increased survival in the presence of FLC which may ultimately lead to the acquisition of genome mutations and/or may serve as a source of reinfection upon arrest of the treatment. Identifying genetic mediators of FLC tolerance could lead to the development of new treatment strategies which will increase FLC efficiency in patients. In this study, we developed a forward genetic screen with a pool enrichment approach using a collection of 579 barcoded strains. Each of these strains overexpressed a specific gene under the control of doxycycline [57, 66]. The same set of pooled strains was used by Znaidi *et al.* [65] in a genetic screen performed in a murine model of gastrointestinal colonization. In this study, the authors used the barcodes to identify strains of interest that were enriched and/or depleted in the animal model in the presence of Dox. Different from the barcode sequencing system used in the present study, Znaidi *et al.* [65] used a barcode detection system based on microarrays on which all barcode tags were deposited. In the animal model selection system, only one gene, *CRZ2*, was identified as conferring a selective growth advantage when overexpressed in the animal gut. *CRZ2* encodes a zinc finger transcription factor of the C2H2 family that is similar to the calcineurin target Crz1p, however it is not involved in calcium signaling [66]. The microarray detection approach to quantify the barcode population from recovered isolates could have been less sensitive than the barcode sequencing approach used here. Barcode sequencing provides the absolute counts of barcodes that occur in a given sample which can be compared to any other sample, while microarray analysis provides an indirect quantification through labelling with two different fluorescent dyes and calculating their ratios. This may provide an explanation as to why only *CRZ2* was identified in the work of Znaidi *et al.* [65]. By maintaining, in the present study, the pooled collection under strong FLC pressure for five days in the presence and absence of Dox, we were first able to identify enriched and depleted isolates in these conditions (78 strains at least 2-fold enriched and 39 strains at least 2-fold depleted). The susceptibility profiles of these candidate genes were further investigated in single strain assays to address potential pool effects in the enrichment assay. We applied here a threshold

definition of tolerance for clinical strains as described earlier in this thesis (Delarze *et al.*, unpublished, Thesis part 1). This allowed the discrimination between resistant ($TI > 0.8$), tolerant ($0.2 \leq TI \leq 0.8$) and non-tolerant susceptible strains ($TI < 0.2$). Unfortunately, this single-strain assay did not allow to identify isolates with decreased tolerance level under Dox induction, probably due to the already low basal tolerance level of the CEC161 parental strain used to build the collection. This basal tolerance level strongly impaired possible conclusions derived from the overexpression of the putative negative regulators of tolerance. Our attempt to increase the basal tolerance level with the addition of calcium in isolates derived from CEC161 (thus stimulating the calcineurin pathway) resulted in strong tolerance induction. This calcium-mediated induction probably masked the potential effects that could originate from tested putative negative regulators. However, using the overexpression system in known clinical isolates, we were finally able to observe reductions of the levels of tolerance, but these were dependent on both the genetic background and the pH condition tested. Three genes seemed to deplete FLC tolerance in all conditions and several genetic backgrounds: the transcription factors *CPH1* and *SFL2*, involved in cell morphology (formation of biofilm and filamentation, respectively) and the putative mitogen-activated protein (MAP) kinase *CSK1* which currently has an unknown role in *C. albicans* (the ortholog of *SMK1* in *S. cerevisiae* is involved in sporulation). The identification of these three putative negative regulators of FLC tolerance was part of a preliminary experiment and further investigations need to be performed to confirm them as true negative regulators. However, our experiments showed the limitation and the difficulties in identifying such regulators. Here we suggest that the use of tolerant clinical isolates can be a promising approach to identify and confirm additional candidate genes responsible for FLC tolerance.

On the other hand, from the initial 12 proposed and putative mediators of FLC tolerance, at least two could be linked to a significant increase of tolerance under Dox induction ($TI > 0.2$). One of these two genes was the calcineurin-regulated transcription factor *CRZ1*, already identified to play a role in FLC tolerance by Onyewu *et al.* [67] and Karababa *et al.* [66]. To act as a transcription factor, Crz1 needs to be translocated to the nucleus. This is achieved by dephosphorylation via calcineurin, which is known

to act as a protein phosphatase [66]. In this work, we showed that *CRZ1* overexpression is triggering FLC tolerance, which may be achieved by transcriptional activation and thus a shift in the balance towards dephosphorylated Crz1. The relationship between *CRZ1* overexpression and Crz1 dephosphorylation has not been tested here but needs to be addressed in future investigations. The other identified gene was the putative GATA-type transcription factor *GZF3*, of which the *S. cerevisiae* ortholog negatively regulates nitrogen catabolic gene expression [68]. Little is known about *GZF3* function in *C. albicans*, but it was shown to be induced, via Cap1, in oxidative stress conditions [69]. Most of the information on *GZF3* come from Homann's and Noble's phenotypic screens [58, 71]. In their works, they observed that the homozygous *gzf3Δ/Δ* mutant resulted in abnormal growth on Spider medium and decreased competitive fitness in a mice systemic infection model [58, 71]. Homann *et al.* also observed an increased susceptibility to heat, FLC, lithium chloride, copper and rapamycin [57]. However, no genetic clues could explain those phenotypes so far. To our knowledge, it is the first time here that *GZF3* has been linked to an increase of FLC tolerance when overexpressed in *C. albicans*. A third gene, *YCK2*, was also identified. This gene encodes a plasma membrane protein similar to the *S. cerevisiae* casein kinase I, which is required for the membrane trafficking of Pdr5 (the ortholog of the multidrug transporter *CDR1* in *S. cerevisiae*) to the cell surfaces [71]. *YCK2* overexpression significantly increased FLC tolerance. However, it did not reach the threshold of tolerance ($TI < 0.2$) defined for clinical isolates. This gene remains however a good candidate for future investigations on molecular mechanisms behind FLC tolerance. The single strain assay also confirmed our pool enrichment protocol to be a valuable approach for the identification of putative positive mediators of FLC tolerance. Additional enrichment experiments using extended OE collections might reveal novel insights into the mechanisms behind this phenotype.

To further characterize the possible interactions existing between *CRZ1* and *GZF3* (since both could mediate FLC tolerance), we observed that *GZF3* significantly increased tolerance when overexpressed, but only when at least a single copy of *CRZ1* was present. On the opposite, the overexpression of *CRZ1* resulted in increased tolerance in every condition tested, even in the absence of *GZF3*. This highlights

that *CRZ1* controls the expression of one or more intermediary proteins or cofactors necessary for *GZF3* activity, which in its turn could activate other regulators of tolerance. Taking the hypothesis that *CRZ1* and *GZF3* are part of a same pathway, our results suggest that *GZF3* acts downstream of *CRZ1*. Further investigation of *CRZ1* target genes via RNA sequencing or chromatin immunoprecipitation may reveal such proteins necessary to *GZF3* activity. In addition, using a Dox-free overexpression system would be more optimal in such investigations to avoid the synergistic effect between Dox and FLC. This negative effect was compensated here by the addition of iron in the culture media.

Both *CRZ1* and *GZF3* were also shown to play a role in FLC tolerance in clinically relevant isolates. *CRZ1* deletion significantly reduces FLC tolerance in the four tested strains to levels below the tolerance threshold ($TI < 0.2$) of clinical isolates. On the other hand, *GZF3* deletion was able to reduce tolerance levels but only when both alleles were deleted. The pH of the medium also had an visible influence on tolerance as already described by Marr *et al.* [42], but the reduction of tolerance by *CRZ1* and *GZF3* deletions was independent of the tested pH conditions, thus highlighting diverse additional pathways/mechanisms behind the development of tolerance.

Experiments aimed to re-introduce *CRZ1* and *GZF3* in the background of deletion mutants in clinical strains yielded different phenotypic complementation results (Figure 36). For example, revertant isolates from strains DSY2110 and DSY4454 did not revert to initial parent wild type levels. This apparent lack of phenotypic reversion may have several reasons. First, the *CRZ1* allele re-introduced in the mutant may not be functional. However, separate successful phenotypic revision of SDS (a cell wall destabilizing agent) susceptibility in these revertant strains argues against this hypothesis (Supplementary Figure 4). Second, the reversion of the full initial phenotype may require that two *CRZ1* copies are being re-introduced at their genomic loci. Third, the reversion of the initial phenotype requires the presence of *CRZ1* alleles originating from the clinical strains and not from SC5314. Since the *CZR1/crz1Δ* heterozygote mutants exhibit intermediate tolerance phenotypes (Figure 36), the third option may be a likely explanation. To confirm this hypothesis, future experiments should introduce the *CRZ1* alleles from the parental clinical strains in their respective homozygote mutants. This last

hypothesis suggests that *CRZ1* alleles from these clinical strains could exhibit polymorphisms responsible for the gain of FLC tolerance.

In a recent study published by the group of J. Berman, some mechanistic insights into the basis of FLC tolerance were given [51]. As suggested by our results, this study highlighted that, using chemically-induced phenotypes, the calcineurin pathway was implicated in the development of azole tolerance. One major difference between the present study and Berman's results was that tolerance assays were carried out in static growth conditions on agar plates (*i.e.* disk diffusion assays), whereas here liquid media were used. The study of Rosenberg *et al.* used mutants constructed in laboratory strains (for example *crz1*, *cnb1*) and reduction of trailing growth on disk diffusion assays to support their hypothesis [51]. In addition, this study indicated that the development of tolerance in clinical strains still susceptible to FLC was attributed to distinct subpopulations [51]. This was inferred by growth assays showing that isolates with high tolerance profiles were growing better in the presence of FLC than isolates with low tolerance profiles. The subpopulation argument seems therefore questionable since single cell analysis was not performed. An interesting approach from the work of Rosenberg *et al.* was the estimation of FLC accumulation in several isolates using a fluorescent FLC derivative [51]. The general trend of their results showed that high tolerance was correlated with decreased accumulation of the fluorescent probe, thus probably contributing to the final tolerance phenotype [51]. Among other interesting observations, Rosenberg *et al.* observed that tolerant strains were more likely to be isolated from FLC-treated patients than others, which suggested that *C. albicans* may adapt to this drug [51]. If azole treatment is prolonged, tolerant isolates may persist and, thus, may cause more severe damage to the host. However, the relationship between occurrence of FLC tolerance and FLC efficacy is still not clearly established in *C. albicans*. A study from Astvad *et al.* undertaken with *C. tropicalis* isolates exhibiting different tolerance profiles tested FLC efficacy in systemic mice infection models [72]. The data of this study established that high FLC tolerance compromised the efficacy of FLC in the mice, thus suggesting a clinical relevance of the tolerance phenomenon [72].

To conclude, the enrichment approach developed here can easily be adapted to test other antifungal drugs and to different *Candida* species. Optimistically, one can imagine performing this type of enrichment in a collection representing the whole *C. albicans* transcriptome to uncover novel mediators involved in the response to FLC and to highlight additional mechanisms. By analysis of the mechanisms and identification of mediators, it may be possible to develop inhibitors which may lead to optimized treatments against clinically challenging *C. albicans* isolates.

Part three: Transcriptomic imprints of fluconazole response in the wild type strain SC5314 and tolerant clinical isolates.

Abstract

Fungal infections are challenging to treat, mainly due to the limited number of antifungal drugs available. Among them, the azole fluconazole (FLC) has been widely used for the treatment of *Candida albicans* infections. Acquired resistance to fluconazole has been extensively studied in the past. However, another phenomenon called antifungal tolerance, characterized by an extended survival in presence of the drug without acquiring mutations linked to resistance might also play a role in FLC treatment failures of *C. albicans* infections. Little is known about FLC tolerance, and most of the observations were made in laboratory conditions. Some genetic clues have been linked to FLC tolerance, but no clear mechanisms could explain the extended survival under high FLC concentrations yet. In addition, the link between tolerance and therapeutic failure still need to be addressed.

In this study, we used a transcriptomic approach to further investigate the response of *C. albicans* to FLC in standardized antifungal susceptibility assay conditions. This was first carried out in the laboratory strain SC5314 and next in known tolerant clinical isolates sampled from the same patient over an 8 years period which exhibited increased FLC tolerance over time. The data of this work showed that the SC5314 transcriptome highlighted not only known drug-induced responses but also the participation of several calcineurin-dependent genes. This suggested that FLC recruits this pathway known to be critical for *C. albicans* survival in presence of drugs. The clinical isolates showed also a corresponding classical drug-induced transcriptional response along with calcineurin-dependent genes. Interestingly, *CRZ1*, that codes for a transcriptional factor activated by calcineurin, was more expressed in the clinical tolerant isolates than parent wild types. This result mimics artificial *CRZ1* overexpression and resulting FLC tolerance of laboratory isolates and suggests that *CRZ1* could be the critical mediator of tolerance in the clinical isolates. The targets of *CRZ1* may therefore be critical for

tolerance and their identification could reveal the molecular mechanisms behind the development of tolerance in *C. albicans*.

Introduction

Transcriptomics is a powerful technology to address gene function and to get insights in circuits activated upon environmental perturbations. Chemical stress can induce transcriptional changes reflecting both general (*e.g.* detoxification pathways) and specific responses of the organism to alteration of one or more biological pathways that are affected by treatment with the chemical. When transcriptional signatures are compared to comprehensive transcript profiling data of gene deletions, drug-gene associations can be established. One nice example reflecting this concept is the study by Hughes *et al.* in which gene expression profiles of yeast cells treated with both known and unknown drugs were compared with a compendium of transcript profiles from an array of yeast deletion mutants [73]. Several transcriptional studies have shown that inhibition of an antifungal drug target leads to increased expression of genes that function in the same pathway. This is a compensatory response to the reduced activity of the target gene. A clear example reflecting this hypothesis is the study conducted by Rogers and coworkers, which characterized the transcriptional profiles of *C. albicans* cells treated with different antifungal agents including azoles, polyenes, echinocandins [74] and ciclopirox [75]. Strong induction of most of the genes involved in ergosterol biosynthesis, including *ERG11* encoding the target of azoles, was observed upon treatment with ketoconazole [74]. Similarly, cell-wall maintenance-encoding genes were induced upon caspofungin treatment, and, interestingly, down-regulation of *ERG3* and *ERG11* were detected following incubation with amphotericin B [74]. Consistent with the notion that ciclopirox olamine acts as an iron chelator, alteration of the expression of iron uptake genes was observed [75], which was in agreement with data from a similar study that used qRT-PCR [76].

While drug exposed conditions can be helpful in revealing biological meaningful data, the use of clinical strains with specific phenotypes is also useful to identify the mechanisms that control these phenotypes. For example, azole-resistant isolates from different origins that were investigated by transcriptional profiling were used to predict expression patterns resulting from transcription factor alterations. For example, Morschhäuser *et al.* used clinical strains overexpressing *MDR1*, a major

facilitator superfamily transporter responsible for azole resistance to identify *MRR1*, the transcriptional regulator of *MDR1* [77]. It turned out that *MRR1* was upregulated in the azole-resistant strains, which facilitated its identification as a regulator of azole resistance.

In this work, we used transcriptional profiling of clinical strains with known FLC tolerance indexes (TI). These strains, known as FLC-susceptible, were exposed to FLC under conditions defined to establish tolerance profiles. The results were compared with a wild type isolate (SC5314) known as FLC-susceptible and with low FLC tolerance. Our results highlight that the calcineurin pathway can be stimulated in the presence of FLC and that tolerant clinical strains exhibit increased transcriptional activity of calcineurin-dependent genes.

Material and methods

Strains used in this study

All clinical *C. albicans* isolates used for the RNA extraction are listed in Table 17 and were sequentially isolated from a same patient with a *C. albicans* endocarditis. The wild type strain SC5314 was used to identify the basal response to supra-MIC concentration of FLC (8 µg/ml).

Table 17: Clinical isolates used for RNAseq with their MIC values for different antifungal drugs.

Isolate ^a	MIC (µg/ml)				
	FLC	VRC	CAS	5-FC	AMB
DSY4454 (<u>0</u> 526-6020)	0.25	0.0078	0.25	0.0315	0.125
DSY4452 (<u>1</u> 101-334)	0.5	0.015	0.25	0.0625	0.25
DSY4588 (<u>1</u> 3 0420 0673)	0.25	0.015	0.25	0.015	0.25

¹For each isolate, a code originating from the diagnostic laboratory of the CHUV is provided in parentheses with underscored numbers indicating the year of sampling

²(FLC) Fluconazole, (VRC) Voriconazole, (CAS) Caspofungin, (5-FC) Flucytosine, (AMB) Amphotericin B

Media and growth conditions

All strains were stored in 20 % glycerol at -80°C and routinely grown at 30°C under constant shaking (220 rpm) in complete Yeast Extract Peptone Dextrose (YEPD) medium (1 % Bacto peptone, Difco Laboratories, Basel, Switzerland), 0.5 % Yeast extract (Difco) and 2 % glucose (Fluka, Buchs, Switzerland). When grown on solid YEPD plates (YEPDA), 2 % agar (Difco) was added and plates were incubated at 35°C.

For culture in presence of supra-MIC concentrations of FLC, strains were grown according to the EUCAST “Method for the determination of broth dilution minimum Inhibitory concentrations of antifungal agents for yeasts” (E.DEF 7.3.1) [38], with slight modifications. Cultures were done in RPMI1640 medium with phenol-red (Sigma-Aldrich) complemented with 2 % glucose (Fluka, Buchs, Switzerland) and buffered with 0.33 M morpholinepropanesulfonic acid (MOPS). The pH was adjusted to pH 7 using NaOH. Stock solutions were prepared as 2x concentrated RPMI as recommended by

EUCAST [38]. Cells were grown in presence or absence of a fixed FLC concentration of 8 µg/ml as used for the identification of FLC tolerance (Delarze *et al.*, unpublished, Thesis part 1 and 2).

Briefly, individual colonies of each tested strain were grown overnight in YEPD medium at 30°C under constant shaking (220 rpm). Cultures were centrifuged (5 min, 4600 rpm, 4°C) and washed twice with PBS (137 mM NaCl, 10 mM Phosphate, 2.7 mM KCl, and pH 7.4). Cell concentration was estimated by spectrophotometry (OD_{540 nm}) and cells were resuspended at 5 x 10⁵ cells/ml in distilled water. Then, 100 µl of this suspension were transferred into the wells of flat-bottom 96-well plates (Costar) containing 100 µl of 2x RPMI (2 % glucose) complemented or not with 16 µg/ml FLC to obtain a final cell concentration of 2.5 x 10⁵ cells/ml and 8 µg/ml FLC per well. Each tested condition corresponded to a whole 96-well plate (with two contamination control wells) and represented approximately 18.8 ml of culture in total. Plates were incubated at 35°C without shaking for 24 h. The next day, plates were centrifuged (5 min, 3700 rpm, 35°C) and the supernatant discarded. To preserve the RNA before RNA extraction, 25 µl of RNA*later* (Ambion) was added per well and the plates were incubated at 4°C for at least an hour. Plates were then stored at -80°C prior to RNA extraction.

RNA extraction

All nucleic acids were extracted by mechanical disruption using glass beads and phenol-chloroform separation as described previously with slight modifications [78]. Briefly, the culture plates preserved in RNA*later* were thawed on ice and cells from each plate recovered by addition of 150 µl diethyl pyrocarbonate (DEPC)-treated distilled water in wells of the first column and pooled progressively toward the last column of the plates. These cell suspensions were collected in RNase-free micro-centrifuge tubes (Eppendorf) kept on ice. The RNA*later* was removed after centrifugation (5 min, 14000 rpm, 4°C) and cell pellets were resuspended in 300 µl RNA buffer (0.5M EDTA [pH 8], 20 % SDS, 1 M LiCl, 1 M Tris-HCl [pH 7.5]) and transferred to 2 ml screw cap tubes (Sarstedt). Approximately 0.3 g of acid washed glass beads (0.5 mm) (SIGMA) were added in addition to 300 µl of phenol-chloroform-isoamylalcohol (24:24:1). Cells were mechanically disrupted (1 pulse, 5 sec, 5000 rpm, 4°C) in a Precellys Evolution tissue homogenizer (Bertin instruments, Montigny-le-Bretonneux, France). Tubes

were centrifuged (10 min, 14000 rpm, 4°C) and 300 µl of the aqueous phase was transferred into new screw-cap tubes containing 300 µl phenol-chloroform-isoamylalcohol. Tubes were vortexed (10 sec, full speed) and centrifuged once more (10 min, 14000 rpm, 4°C) before transferring 250 µl of the aqueous phase into RNA-free micro-centrifuge tubes. To ensure the complete removal of phenol, a last centrifugation (5 min, 14000 rpm, 4°C) was performed and 200 µl transferred in new RNA-free micro-centrifuge tubes. Nucleic acids were then precipitated with 600 µl 100 % EtOH (-20°C) for 15 min on dry-ice, and the pellets were finally washed with 800 µl 70 % EtOH (-20°C) and air-dried before resuspension in 50 µl H₂O DEPC (4°C). Nucleic acid concentration and quality was verified by spectrophotometry (NanoDrop 1000 Spectrophotometer) and adjusted to 10 µg/45 µl in DEPC-treated water. The nucleic acids were stored at -80°C prior to DNase treatment.

DNase treatment

Genomic DNA was removed by DNase treatment using the DNA-free DNA Removal Kit (Invitrogen) following manufacturer's recommendation and samples were stored at -80°C.

Determination of RNA quality

RNA concentration was measured with a Nanodrop-1000 (Witec AG, Switzerland). Tubes were stored at -80°C until analysis. RNA quality was analyzed using a Fragment Analyzer (Advanced Analytical Technologies, Ankeny, IA, USA) according to manufacturer's instructions. The Lausanne Genomic Technologies Facility (LGTF) which performed the RNA sequencing recommended a $A_{260/280}$ ratio > 1.9, $A_{260/230}$ ratio > 1.8 and an RNA Integrity Number (RIN) > 7.0 to perform RNAseq.

RNA sequencing and RNAseq data mining

Library preparation and sequencing were carried out by the LGTF and the sequencing was performed on an Illumina HiSeq 2500 system (Illumina, San Diego, CA, USA), using the TruSeq Stranded RNA, 125 bp single read protocol. The analysis was performed with three biological replicates for each condition. RNAseq data were processed using CLC Genomic Workbench Version 10.1.1 (Qiagen). Reads were

aligned to the *C. albicans* SC5314 genome and read counts were normalized using the quantile approach method. All conditions were compared with each other and filtered according to a specific statistical cut-off as explained in the Results section.

Results

Transcriptional profile of SC5314 in the presence of FLC

The *C. albicans* strain SC5314 is the classical laboratory strain that is commonly used by the research community and from which the genome has been annotated.

As shown in earlier chapters of this thesis, SC5314 is a strain exhibiting a relatively low level of FLC tolerance (generally below the TI threshold of 0.2). It was therefore of interest to address the transcriptional profile of this strain in the presence of FLC under the conditions where tolerance is tested and to compare the obtained profile with those of clinical strains exhibiting high FLC tolerance. RNAseq data were obtained as described in Material and Methods and were analyzed with the help of a dedicated software package (CLC Genomics Workbench, V 10.1.1). Genes that were significantly differentially regulated by the presence of FLC ($\text{FDR} \leq 0.05$) leading to an expression change of at least 2-fold were first selected (Supplementary File 5). A total of 1641 genes followed these selection criteria.

These expression data were first analyzed by Gene Ontology term enrichment. Enriched GO terms of genes up- and downregulated in the presence of FLC are shown in Figure 37. FLC is known to perturb the expression of genes involved in sterol biosynthesis and those mediating azole efflux [79]. The data of Figure 37 are consistent with these observations since processes involving ergosterol biosynthesis, azole transport and response to stress are enriched in FLC-upregulated genes. Interestingly, processes related to vesicle-mediated transport and azole transport were closely clustered, thus indicating a functional relationship between both processes. Another relevant enriched process derived from upregulated genes includes the glyoxylate cycle, which suggests that FLC mediates a change in the metabolic state in *C. albicans*. Since processes involving cell wall organization and hyphal growth are enriched in FLC-upregulated genes, this suggests that this drug may alter cell wall composition as well as morphogenesis in *C. albicans*. Consistent with these observations, it has been reported in *C. albicans* that FLC is able to induce a switch from the yeast form to elongated growth reminiscent of hyphal growth [80]. Lastly, our data indicate an enrichment for multi-organism processes, which correspond

to genes involved in biofilm formation. This suggests that the growth conditions chosen here to address FLC tolerance may favor biofilm formation.

With regards downregulated genes in the presence of FLC, the data of Figure 37 show that processes related to glucose catabolism are enriched. This suggests a rewiring of glucose metabolism induced by FLC. These data are consistent with the upregulation of genes involved in the glyoxylate cycle as above-

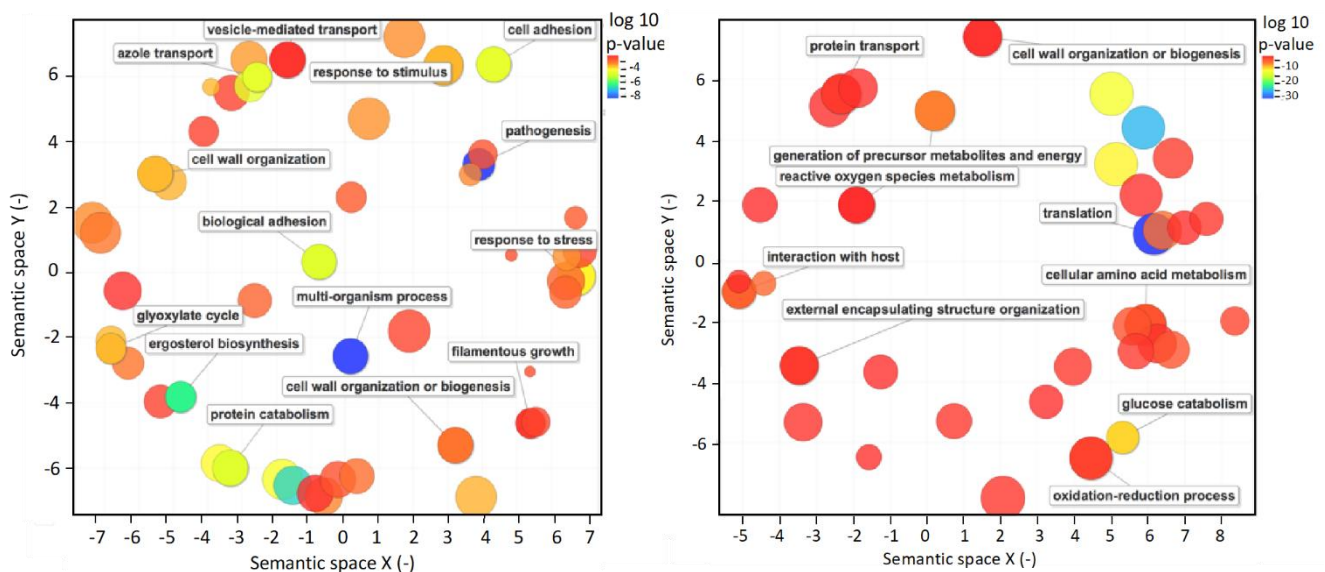


Figure 37: Schematic representation of GO terms enriched in genes up- (left panel) and down-regulated (right panel) by FLC in *C. albicans*. Go term enrichments were performed with the online tool Fungifun (<https://elbe.hki-jena.de/fungifun/>). Enriched GO categories were next visualized with the online tool Revigo (<http://revigo.irb.hr>) which groups redundant GO terms according to semantic similarity-based scatterplots.

mentioned. Oxidation-reduction processes as well as processes involving reactive oxygen species (ROS) metabolism are identified in the data of Figure 37 and thus indicate an impact of FLC on oxidative processes. Lastly, processes related to translation are among the enriched processes in FLC-downregulated genes. FLC has a growth inhibitory function and this is reflected by down-regulation of genes of the translation machinery.

To compare the genes up- and downregulated by FLC in SC5314 with transcriptional profiles published in the literature, a gene set enrichment approach (GSEA, for Gene Set Enrichment Analysis) was used. The list of transcriptional profiles that was used here comprises 307 different conditions (Supplementary File 6) in which (i) *C. albicans* was exposed to different antifungal agents, (ii) *C. albicans* mutants were exposed to different growth conditions, (iii) *C. albicans* was exposed to host cells and

(iv) *C. albicans* was grown *in vitro* under conditions mimicking host environments. The GSEA list also contains *C. albicans* genes with binding sites for several transcription factors. In general, the used conditions are divided into lists of up- and down-regulated genes. The software compares a query list of up- and down-regulated genes with existing gene lists and identifies those that overlap through statistical evaluation. A network of associated gene lists can be formed using visualization software such as Cytoscape (GSEA enrichment map) depending on the overlaps between conditions.

Figure 38 shows the GSEA enrichment map of genes up- and downregulated by FLC in SC5314. One can observe three major networks, two containing blue nodes and one with red nodes, which indicates a separation between genes down- and upregulated, respectively, in the presence of FLC. On the other hand, several other nodes, in which down- and upregulated genes could be found, were not overlapping with existing datasets.

The GSEA map highlights several features. First, the genes regulated by FLC in SC5314 overlap well with published datasets in which *C. albicans* was exposed to FLC in different growth conditions. The connected nodes “FLUCONAZOLE_UP”, “KETCONAZOLE_UP”, “FLC3H_UP” were overlapping with most FLC-upregulated genes in SC5314. FLUCONAZOLE_UP data originate from a study [81] in which *C. albicans* was exposed for 6 h in the presence of 10 µg/ml FLC in YEPD at 30°C. FLC3H_UP data are from a study [82] in which *C. albicans* was treated with 0.5 µg/ml FLC for 3 h in RPMI medium at 37 °C. KETCONAZOLE_UP data are from a study [83] in which *C. albicans* was exposed to 0.04 µg/ml ketoconazole for 3.5 h in YEPD at 30°C. All these experiments were performed under agitation in liquid cultures. The growth conditions used here were different from the 96-well microtiter plate format of the EUCAST. Even though these conditions were quite different from the published studies, the GSEA could identify significant overlaps between these conditions (Figure 39). A core group of 29 genes could be found in all the data sets (Figure 39). Considering that most FLC-downregulated genes are also found in the nodes “KETOCONAZOLE_DN”, “FLC3H-DN” and “FLUCONAZOLE_DN”, the results obtained here are consistent with already published transcriptional data of FLC-exposed cells.

When inspecting other nodes overlapping with the FLC-regulated genes of SC5314, it was of interest to identify those labelled as “CALCINEURIN”, “CNA_CRZ1” and “CNA 20 min_up”. The gene lists from these nodes originate from a study published by Karababa *et al.* [66] in which calcineurin- and *CRZ1*-dependent genes were identified. The overlaps between these different nodes are shown in Figure 40 and show that most of the FLC-regulated genes are upregulated in these nodes. A common set of 20 genes was present among these different nodes, in which *CRZ1*, a critical gene of the calcineurin pathway [66], was present.

These nodes were connected to those assembling FLC-exposure data as above-mentioned. “CALCINEURIN” and “CNA 20 MIN_UP” were connected with the node “UPC2_UP”, which comprises genes upregulated in the absence of *UPC2* under anaerobic conditions [83]. *UPC2* is known to regulate several genes involved in sterol biosynthesis [83], a pathway affected by FLC. “UPC2_UP” is next connected to the FLC response nodes. Inspection of the genes on the edges between “CALCINEURIN” and “CNA 20 MIN_UP” and “UPC2_UP” revealed 20 and 18 genes, respectively (Supplementary File 7). Among these genes, *CRZ1* was again identified. As a matter of fact, *CRZ1* was 2.5-fold upregulated by FLC in SC5314 (Supplementary File 5), which corroborates with the effect of *CRZ1* overexpression on FLC tolerance that was demonstrated earlier in this work. Interestingly, *GZF3*, which was another gene conferring FLC tolerance when overexpressed, was also upregulated (2.5-fold) by FLC in SC5314. Taken together, these data highlight a relationship between calcineurin signaling and response of *C. albicans* to FLC.

Several other nodes were identified by GSEA and contain genes that are upregulated in response to drugs, including FLC, yet not connected to the calcineurin pathway. These nodes include for example “MILBE_UP”, “FLUODIOXONIL_UP”, “FR59_15MIN_UP”, “FLUPHENAZINE294_UP” and indicate that FLC invokes a response shared by other drugs. In some cases the drug response is mirrored by FLC-downregulated genes in nodes reflecting gene down-regulation by drug response (Figure 38, “MILBE_DN”, “FLUODIOXONIL_DN”, “FLUPHENAZINE294_DN”).

When scrutinizing nodes that matched down-regulated genes in the presence of FLC (blue nodes), two major clusters were identified. In one of them, nodes related to hyphal growth (“HYPHAE_LEE_UP”, “HYPHAE_SPIDER_UP”, “HYPHAE_FBS37B_UP”) were present. These gene lists include genes that are upregulated when *C. albicans* switches from the yeast form to the hyphal form. Therefore, our data suggests that genes involved in hyphal formation tend to be downregulated by FLC in *C. albicans*. These results are consistent with some studies showing that azoles can modify the dynamics of the switch between the yeast and hyphal phase [84].

The other cluster of nodes connects several processes related to the response of *C. albicans* to host conditions or to host cells (“IN VIVO_DN”, “CAECUM_DN”, “RNASEQ120MIN_DN”). The data of these nodes comprises genes down-regulated under host conditions. FLC-downregulated genes are enriched in these conditions thus suggesting that the response of *C. albicans* to FLC can also modify *C. albicans* host response. The significance of these results is not clear yet.

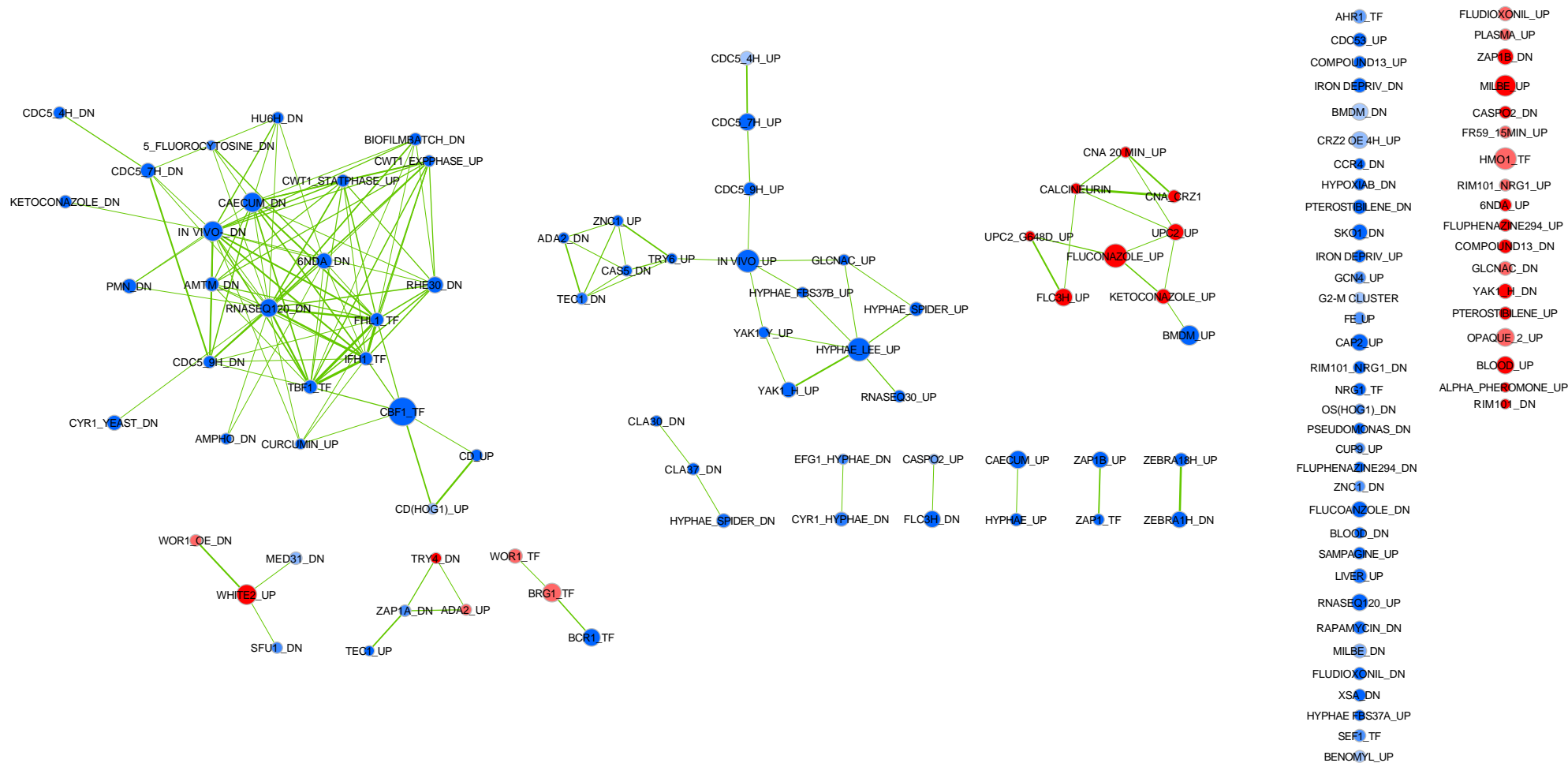


Figure 38: GSEA enrichment map of FLC regulated genes in *C. albicans* SC5314. Analysis parameters were as follows: norm, meandiv; scoring_scheme, weighted; set_min, 15; nperm, 1000; set_max, 500. GSEA results were uploaded into Cytoscape 3.0 with the following parameters: P value cutoff, 0.01; FDR q value, 0.05. Red nodes represent enriched gene lists in upregulated genes from the GSEA. Blue nodes represent enriched gene lists in downregulated genes from the GSEA. Nodes are connected by edges when overlaps exist between nodes. The size of nodes reflects the total number of genes that are connected by edges to neighboring nodes. Edge thickness reflects the level of confidence between nodes.

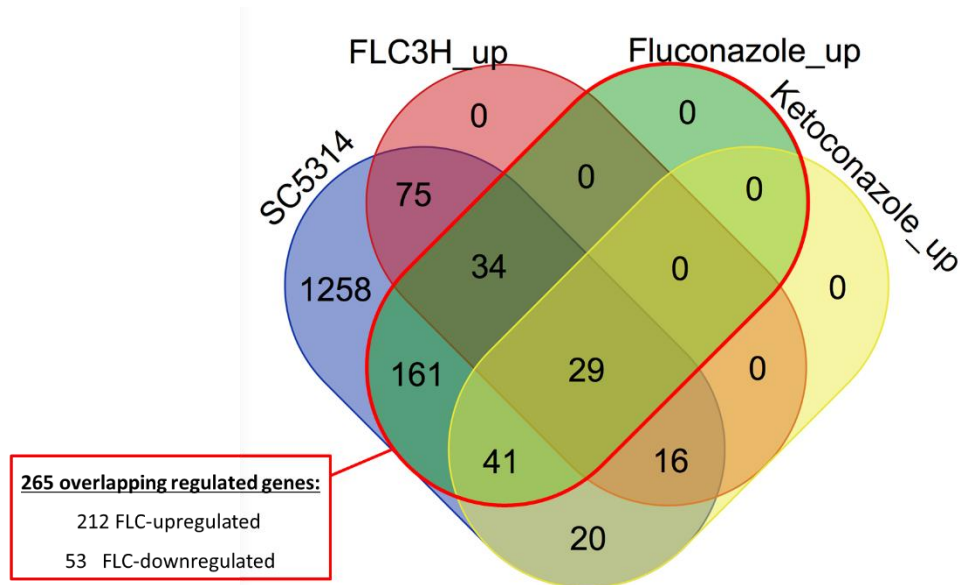


Figure 39: Venn diagram of FLC-regulated genes in *C. albicans*. Gene lists derived from the GSEA plot of Figure 38 (Supplementary File 6) were used in the online tool available at <http://bioinformatics.psb.ugent.be/webtools/Venn/>. From 265 genes overlapping between the gene list “FLUCONAZOLE_UP” and the SC5314 data (1641 regulated genes), 212 were FLC-upregulated.

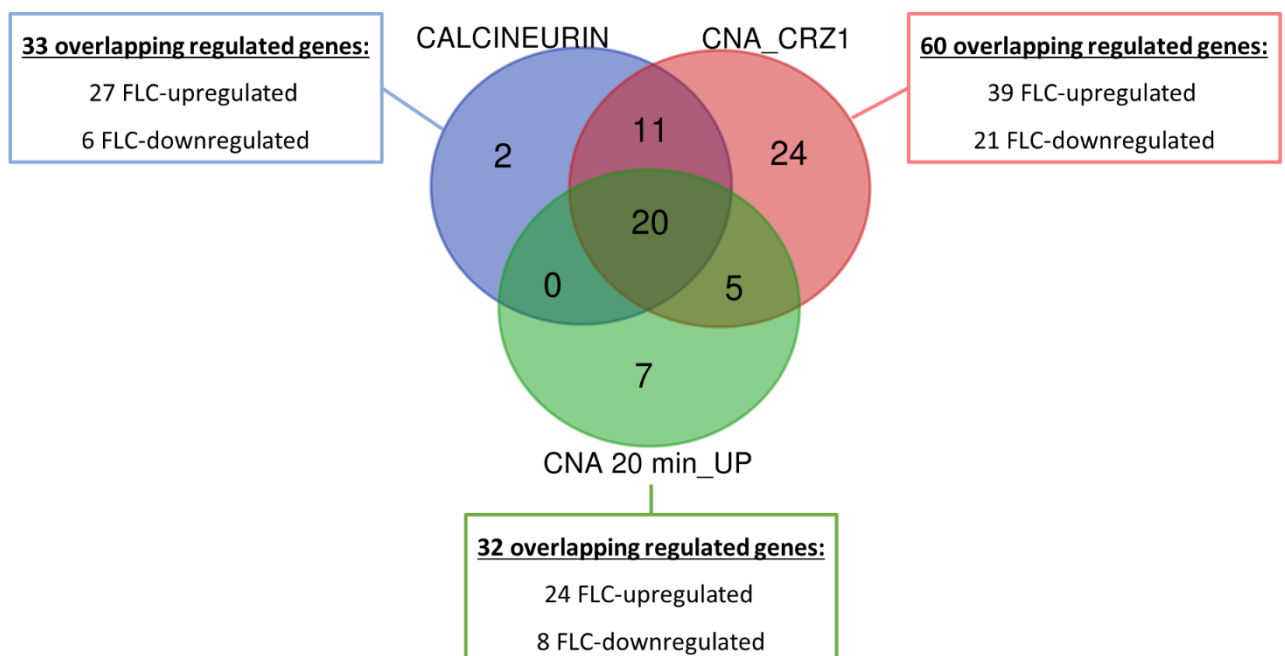


Figure 40: Venn diagram of genes within the calcineurin-CRZ1 cluster of the GSEA. The gene lists of each node were extracted from the GSEA analysis (Supplementary File 7) and a Venn Diagram was constructed with the online tool available at <http://bioinformatics.psb.ugent.be/webtools/Venn/>. For each node the number of up- and downregulated genes by FLC is indicated.

Transcriptional profiles of clinical strains in the presence of FLC

After the analysis of the transcriptional response of SC5314 to FLC, it was of interest to address the same type of response using *C. albicans* clinical isolates with known high FLC TIs. The chosen strains were originating from a group of related strains including DSY4454, DSY4452 and DSY4588. These strains were recovered from a patient suffering of endocarditis which was treated for an extensive period with FLC (8 years). DSY4454 was the earliest strain recovered (2005) from the patient, while DSY4588 was the latest (2013) (Table 17). Patient and sampling details are given in Table 18.

The relationship between strains was investigated with Multi Locus Sequence Typing (MLST, Supplementary File 8) [85]. A single loss of heterozygosity (LOH) event was detected in the *SYA1* allele of isolate DSY4588 as compared to the other strains, thus suggesting that micro-evolution between the strains could have occurred. However, the MLST results indicated that the strains were from the same type, thus suggesting a strong genetic relationship between them.

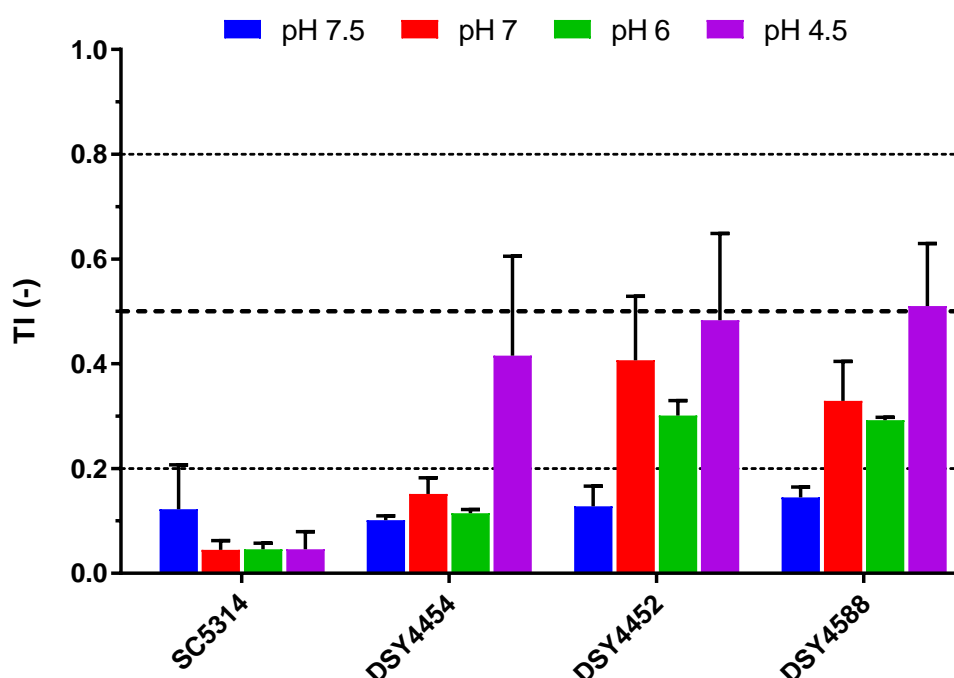


Figure 41: Tolerance profile of the *C. albicans* clinical isolates.

Table 18: Details on the endocarditis patient and the collected isolates.

Year of Record	2004	2005	2010	2012	2013
Isolated strain	DSY4454		DSY4452	DSY4588	
Symptoms/intervention	- Aortic valve replacement for stenosis	- <i>C. albicans</i> prosthetic valve endocarditis	- <i>C. albicans</i> prosthetic valve endocarditis	- <i>C. albicans</i> prosthetic valve endocarditis - Valvuloplasty - Abscess resection between aortic and mitral valve	- <i>C. albicans</i> prosthetic valve endocarditis - Aortic valve replacement (homograft)
Treatments		1) AMB ¹ (5 mg/kg/day IV ²) for 4 weeks 2) Suppressive therapy with FLC ¹ (200 mg/day <i>p.o.</i> ²)	1) CSP ¹ (70 mg/day IV) for 3 months 2) Suppressive therapy with FLC (200 mg/day <i>p.o.</i>)	1) CSP 70 mg/day for 1 week IV 2) CSP 50 mg/day for 5 weeks IV c	1) AMB (5 mg/kg/day IV) for 5 weeks + 5FC ¹ (25mg/kg/day IV) for 2 weeks 2) CSP 100 mg/day IV for 6 weeks 3) Suppressive therapy with CSP 3x/week (200-200-250 mg IV)

¹(AMB) Amphotericin B, (FLC) Fluconazole, (CSP) Caspofungin, (5FC) Flucytosine

²(IV) Intravenous, (*p.o.*) Per os

The strains were subjected to RNA extraction in conditions identical to SC5314 and RNAseq analysis was carried out. The data were treated and analyzed in a manner similar to SC5314 and expression changes were extracted by pairwise comparison between conditions with and without FLC. The data were filtered for significance ($FDR \leq 0.05$) and for expression change (≥ 2 -fold) between drug-exposed and non-exposed conditions (Supplementary File 5). Data are summarized in Table 19.

Table 19: Genes regulated by FLC in the clinical strains.

Isolate	FLC upregulated genes	FLC downregulated genes
DSY4454	484	579
DSY4452	370	471
DSY4588	451	262

The FLC-regulated genes from the clinical strains DSY4452, DSY4454 and DSY4588 were also subjected to GSEA as was performed for SC5314. These data are summarized in Figure 42.

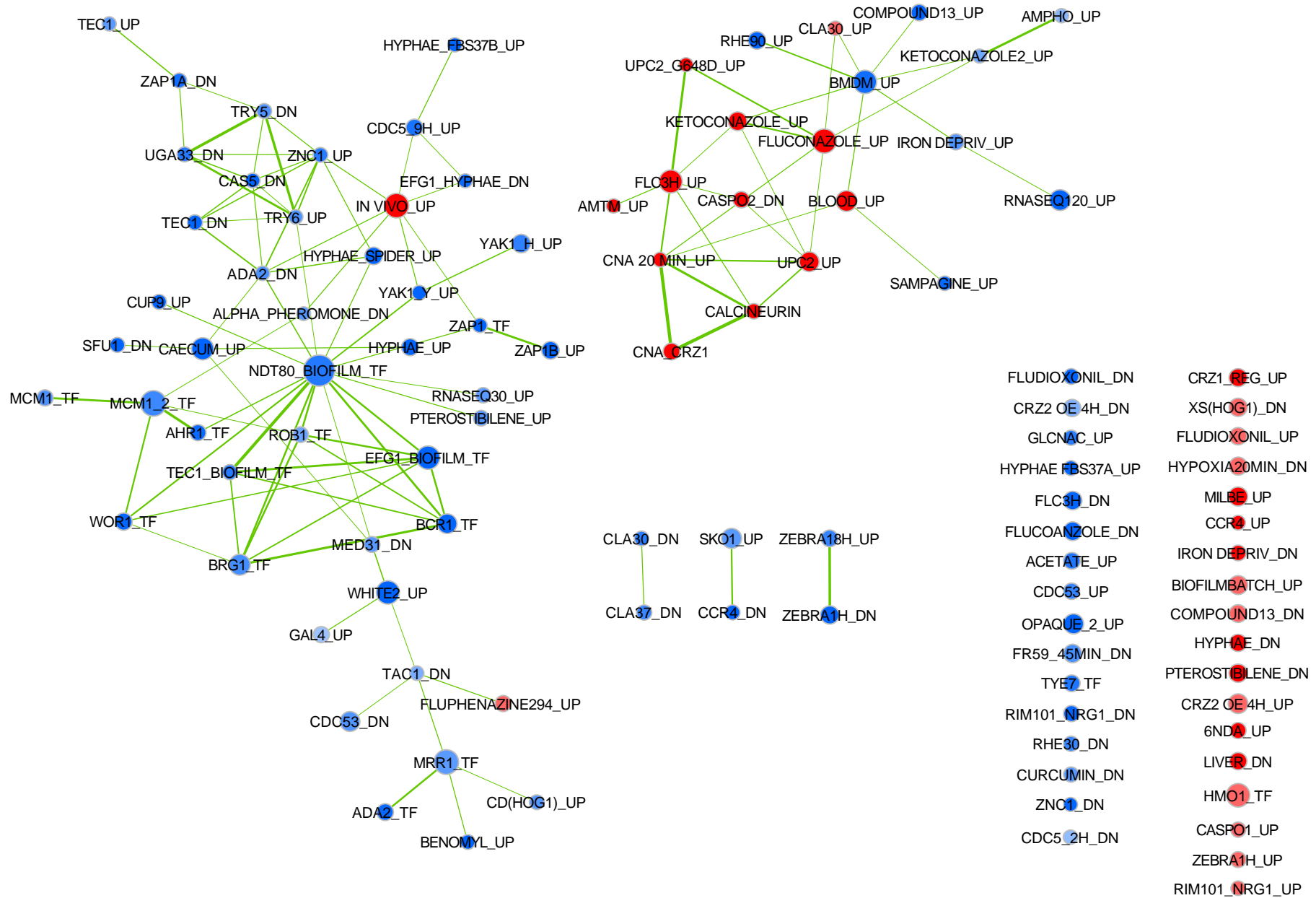
When looking at FLC-upregulated genes, the GSEA data of the clinical isolates contained in common clusters of nodes related to the calcineurin pathway (CALCINEURIN", "CNA_CRZ1" and "CNA 20 min_up"). Strikingly, these nodes were connected to those originating from FLC-exposed conditions ("FLUCONAZOLE_UP", "KETCONAZOLE_UP", "FLC3H_UP") and from nodes of transcription factors controlling sterol homeostasis ("UPC2_UP"). These networks, containing genes positively regulated by FLC, were also associated with a node comprising genes upregulated by *UPC2* with a gain of function mutation ("UPC2_G648D_UP") [86]. This underlines the importance of this transcription factor in azole response. Taken together, these data suggest that the calcineurin pathway is connected to the response of *C. albicans* to FLC and this confirms the observations made above in SC5314.

When looking at clusters matching with down-regulated genes, a central node assembling list of genes with transcription factor (TF) binding sites could be identified ("NDT80_BIOFILM_TF") which in some cases was itself connected to other nodes of the same type ("BRG1_TF", "BRC1_TF", "EFG1_BIOFILM_TF", "TEC1_BIOFILM_TF", "WOR1_TF"). The data of these gene lists originates from a

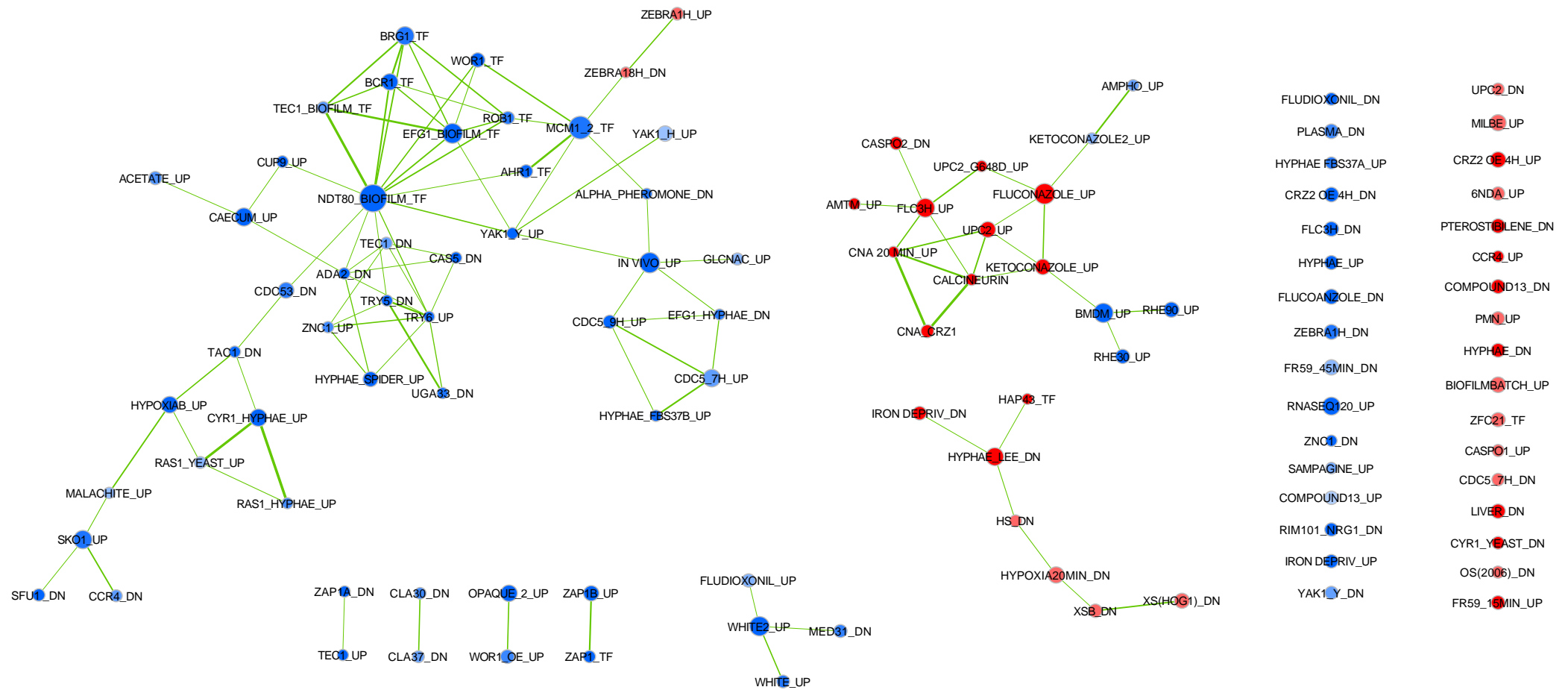
study that identified a hub of transcription factors controlling biofilm formation [87]. The connections between these nodes suggest that most genes down-regulated by FLC are controlled by these transcription factors and indicates that biofilm formation is affected by the presence of FLC. One can observe the occurrence of nodes of FLC-downregulated genes containing data of hyphal-regulated genes. Since biofilm formation is closely associated with hyphal formation [88], the data of the present work are consistent with this assumption.

In the data of the clinical strains, other interesting nodes related to drug resistance, were found in the cluster of down-regulated genes. For example, the nodes “TAC1-DN”, “MRR1_TF” and BENOMYL_UP” were connected with each other and the remaining clusters of down-regulated genes (data from DSY4452). The node “TAC1-DN” assembles data of genes downregulated by the absence of *TAC1* in *C. albicans*. Since *TAC1* is a major transcription factor in drug-induced response [89], it can be expected that several regulated genes will be controlled by this factor. This is reflected by the occurrence of FLC-downregulated genes in this specific node. The node “MRR1_TF” and “BENOMYL_UP” include genes with binding sites of the TF Mrr1 [90] and genes upregulated by the presence of benomyl [91], respectively. *MRR1* is another TF playing an important role in drug response in *C. albicans* and especially in the response to benomyl [90]. Interestingly, the data presented here show that FLC regulates genes in the opposite way compared to benomyl. Therefore, since *MRR1* is positively controlling benomyl-induced genes, it not surprising that FLC-downregulated genes can be found in the node “MRR1_TF”.

A



B



C

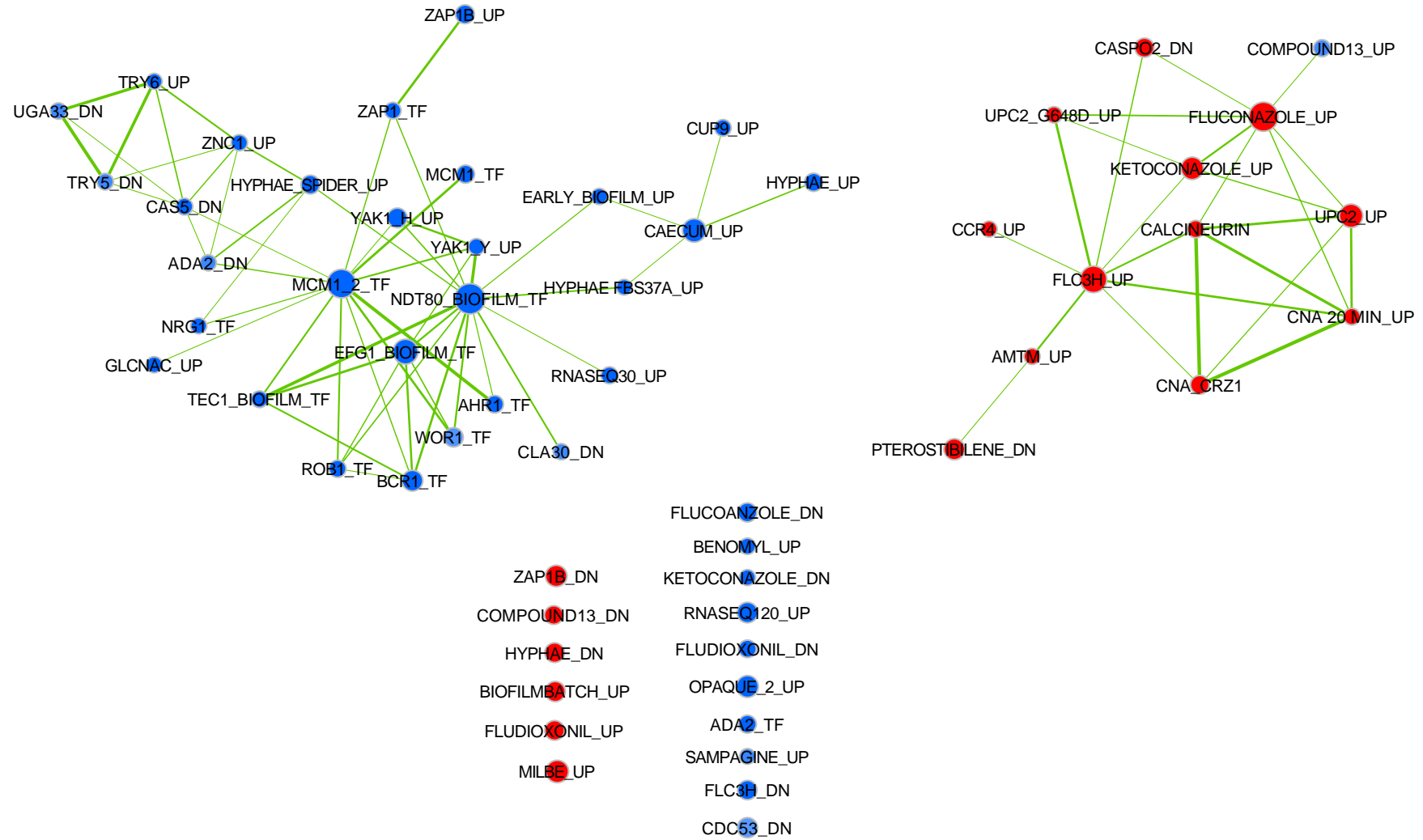


Figure 42: GSEA enrichment map of FLC regulated genes in clinical isolates DSY4454 (A), DSY4452 (B) and DSY4588 (C). Analysis parameters were as follows: norm, meandiv; scoring_scheme, weighted; set_min, 15; nperm, 1000; set_max, 500. GSEA results were uploaded into Cytoscape 3.0 with the following parameters: P value cutoff, 0.01; FDR q value, 0.05. Red nodes represent enriched gene lists in upregulated genes from the GSEA. Blue nodes represent enriched gene lists in downregulated genes from the GSEA. Nodes are connected by edges when overlaps exist between nodes. The size of nodes reflects the total number of genes that are connected by edges to neighboring nodes. Edge thickness reflects the level of confidence between nodes.

In order to identify potential mediators of tolerance in the set of clinical strains, the expression of which could vary between wild type (DSY4454) and FLC-tolerant isolates (DSY4452 and DSY4588), the ratios of FLC-regulated genes were determined between pairs of isolates. Expression ratios were first calculated between DSY4452 and DSY4454 and between DSY4588 and DSY4454 (Supplementary file 9). Significant fold-changes were selected between these conditions (p -values ≤ 0.05) and the data were filtered with a 2-fold change as a cut-off. The expression ratio between DSY4452 and DSY4454 was changed by more than 1.5-fold for 41 genes. Interestingly, 12 out of these 41 genes were regulated by calcineurin and/or *CRZ1*. Moreover, the expression ratios of these 41 genes between DSY4588 and DSY4454 were above the 1.5-fold threshold. These results suggest a conservation of the FLC response between the tolerant strains DSY4452 and DSY4588 as compared to DSY4454. Intriguingly, most of the ratios of the 41 above-mentioned genes between DSY4454 and SC5314, both of which could be considered as “wild type” in term of FLC tolerance, were below the 1.5-fold threshold. Taken together, the data presented here suggest that the expression of genes that are known to be calcineurin- and/or *CRZ1*-dependent is increased in the FLC-tolerant clinical strains and this indicates that the calcineurin pathway is modified by still uncharacterized factors in these strains.

Conclusions

In this work, we addressed the transcript profiling of several isolates in the presence of FLC, some of which exhibit FLC tolerance. The major difference in these experiments as compared to similar published results was that the incubation conditions were mimicking standard susceptibility assays performed under EUCAST recommendations. In these conditions, the first investigated isolate was SC53145 and showed a typical drug-induced transcriptional response. In addition, we showed here that FLC induced a response that included several calcineurin-dependent genes. Such a response profile has not yet been clearly demonstrated in published profiling studies. Such an association strongly suggests that FLC recruits the calcineurin pathway, which was already showed to be critical

for survival of *C. albicans* exposed to FLC [44]. The same relationship could be established in the clinical isolates when inspecting their response to FLC.

The clinical isolates used here were related to each other, which was expected to reduce transcriptional noise that can arise from strains exhibiting different genetic backgrounds. In these sequential isolates, DSY4454 was the first recovered isolate from a patient suffering from endocarditis. DSY4454 exhibited relative low TI as compared to the other isolates (DSY4452 and DSY4588). The patient had been treated for several years with FLC until blood cultures were positive for DSY4452 and DSY4588 about 7 and 9 years after the isolation of DSY4454. It is likely that the duration of FLC treatment along these years selected for isolates with genome modifications favoring, among other phenotypes, the development of azole tolerance. Our data revealed that several genes of the calcineurin pathway were upregulated as compared to the initial isolate as well as SC5314. Currently the genetic basis for this modification is unknown. In the transcript profiling, *CRZ1* was upregulated in the tolerant isolates. As mentioned earlier in this work, *CRZ1* overexpression mediated by an artificial regulatable promoter is enough to induce FLC tolerance in *C. albicans*. *CRZ1* expression changes could therefore be taken as a candidate marker for azole tolerance. How *CRZ1* overexpression mediates azole tolerance is still unknown. *CRZ1* needs to localize into the nucleus to target genes and this process is known to involve phosphorylation/dephosphorylation steps [44]. *CRZ1* overexpression could change the protein homeostasis and perturb the ratio between phosphorylation/dephosphorylation states, which will result in the upregulation of target genes. No detailed information currently exists on *CRZ1* target genes that could ultimately be responsible for azole tolerance. As mentioned earlier, identification of *CRZ1* target genes that could mediate azole tolerance needs to be systematically performed. Another approach that could lead to resolve the molecular basis of azole tolerance in the clinical isolates could consist of comparative genomics. Such an approach could be undertaken in order to reveal nucleotide changes between the isolates and thus to identify the molecular basis behind the occurrence of FLC tolerance. This type of approach may be rendered difficult due to the likely genome divergence that evolved during the years of persistence of the strains in the host. Preliminary data

from the isolates' whole genome sequencing support this hypothesis. In conclusion, even if the present results converge to the involvement of the calcineurin pathway in the development of azole tolerance, additional studies are needed to resolve the molecular details behind this phenomenon.

General discussion and future perspectives:

C. albicans is a major human pathogen and can develop resistance to antifungal drugs leading to therapeutic failures. Antifungal tolerance, characterized by an increased survival in presence of drug without acquiring mutations leading to resistance, is also thought to be involved at least in part of these therapeutic failures. Antifungal tolerance has mainly been described for the fungistatic drug fluconazole (FLC). However, mechanisms behind FLC tolerance have remained little understood, mainly due to a lack of clear definition and approaches to identify and quantify tolerance. The work described in this thesis contributed to better define FLC tolerance and to give novel insights behind this phenomenon.

Defining FLC tolerance

First, a clearer definition of FLC tolerance as well as a tolerance index (TI) and tolerance thresholds, allowing tolerance quantification, were established and used to better identify tolerant clinical isolates. Using the standard antifungal susceptibility assays protocols proposed by EUCAST and CLSI, tolerance was defined as a residual growth between 20 and 80 % of a drug-free control above the clinical breakpoint of FLC. By establishing the TI as the residual growth at a fixed antifungal concentration, this allowed an easy way to assess tolerance in large strains collection in so-called tolerance assays, as showed with the 182 strains used here. The upper threshold of tolerance (TI = 0.8) was also further confirmed as most isolates above this threshold were exhibiting known mutations linked to FLC resistance. The lower threshold of tolerance (TI = 0.2) was established on a more empirical basis but was useful to distinguish between wild type and tolerant isolates. The method and definition developed here gave, in addition to the method based on disk diffusion assay developed by Gerstein *et al.* [51] and applied by Rosenberg *et al.* [52, 94], an alternative to better understand tolerance and identify mechanisms responsible for this phenotype. However, our methods may be more efficient for large scale tolerance screenings and may be more easily implemented as a routine laboratory method as it only used a microplate reader. In addition, culture in liquid and in RPMI medium might better

reflect the environmental conditions of the host, as opposed to static growth on solid phases. This method can also be used to assess tolerance to other antifungal drugs in *C. albicans* but also in other pathogenic fungi.

Discovery of novel FLC tolerance mediators

Using the definition and TI established in the first part of this work, the transcription factors *CRZ1* and *GZF3* were identified in a pool enrichment approach using a collection of doxycycline (Dox)-dependent overexpression strains with each a specific barcode and an overexpressed gene. A third gene, encoding the plasma membrane protein Yck2, was also observed to increase tolerance when overexpressed but with less effect than *CRZ1* and *GZF3*. This gene was not further investigated in the current study but remains of interest since its ortholog in *S. cerevisiae* is critical for the trafficking of Pdr5. This protein is functionally similar to the multidrug transporter Cdr1 of *C. albicans*. *CDR1* is already known to be involved in acquired FLC resistance [32]. *YCK2*-induced FLC tolerance may lead to stabilized localization of Cdr1 in the plasma membrane, thus resulting in a decreased intracellular FLC concentration.

CRZ1 was already known to be part of the calcineurin pathway which was reported as involved in FLC tolerance. When calcineurin is activated, it dephosphorylates its downstream targets, including Crz1, which in turn will translocate into the nucleus. The identification of *CRZ1* in this work therefore consolidated our approach and highlighted the crucial role of the calcineurin pathway in FLC tolerance. On the other hand, little is known from *GZF3* in *C. albicans*. Most information about *GZF3* originate from the works of Homann *et al.* and Noble *et al.* [58, 71], where they linked the absence of *GZF3* with abnormal growth on Spider medium and decreased competitive fitness in mice, but also with an increased susceptibility to heat, FLC, lithium chloride, copper and rapamycin [58, 71]. *GZF3* ortholog in *S. cerevisiae* is involved in nitrogen homeostasis but was never linked to any antifungal drug response. In the present study, *GZF3* was shown for the first time to be linked to Crz1 activity and, more interestingly, to be situated downstream of this transcription factor. Indeed, using overexpression of each factor in *CRZ1* and *GZF3* deletion mutants, it was observed that *CRZ1* overexpression was enough

to promote tolerance, even in absence of *GZF3*. However, it seems that the effect of *GZF3* overexpression on tolerance needs the presence of at least a single *CRZ1* allele. This highlights that, somehow, Crz1 regulates *GZF3* expression either directly via binding to the *GZF3* promoter, or indirectly via regulation of intermediate factors. These factors can either regulate *GZF3* expression or be cofactors of Gzf3 necessary for its activity in the nucleus. Further characterization of the link between both factors will reinforce the knowledge on FLC tolerance. More importantly, the present study highlighted the role played by both *CRZ1* and *GZF3* in the FLC tolerance of clinical isolates. Their deletions resulted in decreased FLC tolerance, but did not impact the FLC susceptibility, thus showing that the cellular processes controlling these phenotypes can be separated.

Next steps in understanding of FLC tolerance

It is important to note here that only approximately 1/10th of *C. albicans* ORFome was covered by the overexpression collection used for the identification of tolerance mediators. In addition, the collection used was enriched in genes encoding for transcription factors, protein involved in DNA replication/repair/recombination, protein kinases/phosphatases and cell wall proteins. Due to the limited representation of the *C. albicans* ORFome, only a fraction of potential FLC tolerance mediators could be therefore identified. In order to perform a more comprehensive analysis of potential FLC tolerance mediators, it will be necessary to include, in the future, an overexpression collection representing the whole *C. albicans* ORFome.

With regards to the involvement of *CRZ1* in tolerance, the next step will be to further characterize its role on FLC tolerance in clinical isolates. Crz1 needs to be dephosphorylated by calcineurin to translocate into the nucleus and binds to promoters of target genes. It is possible that, in FLC-tolerant clinical isolates, Crz1 is constitutively dephosphorylated due to calcineurin in an activate state, thus resulting in increased Crz1 nuclear localization and transcription of target genes. It could be possible to tag Crz1 with a fluorescent marker to observe its cellular localization upon FLC treatment as compared to a drug-free control. As it was shown that *CRZ1* overexpression increased tolerance, a first

approach would be to address Crz1 localization in the overexpression system used here. To avoid problems with correct localization and/or function of the tagged protein, construction of both N- and C- terminal tagged Crz1 would be necessary.

As both *CRZ1* and *GZF3* encodes transcription factors, they are indirect mediators of FLC tolerance. It is thus of primary interest to identify their targets genes since they might be direct effectors of FLC tolerance. In addition, this would reveal other pathways involved in increased FLC tolerance. An elegant approach to identify these target genes would be to perform chromatin immunoprecipitation sequencing (ChIP-Seq), using the *CRZ1* and *GZF3* overexpression strains used in this study in order to directly identify their DNA binding sites. Another approach would be comparative transcriptomic analyses in presence and absence of Dox. However, in this case, it would be more convenient to construct a Dox-free overexpression system rather than the one used in this study, in order to avoid observing a transcriptomic imprint of the adjunction of Dox and FeCl₃. The construction of constitutive *CRZ1* and *GZF3* overexpression strains under the control of a strong constitutive promoter (*e.g.* *ACT1* or *TDH3* promoters) would not only be useful for such transcriptomic comparisons, but also to develop “tolerant laboratory strains” which could then be used to assess the effect of tolerance in a mice infection model, and also for the identification and characterization of negative mediators of FLC tolerance.

Transcriptomic imprints of FLC response in tolerant clinical isolates

In the last part of this work, we demonstrated, using a transcriptomic approach, for the first time to our knowledge, the imprint of the FLC response in conditions similar to the EUCAST’s standard antifungal susceptibility assay protocol. Using the WT strain SC5314, we were able to demonstrate that FLC seems to recruit the calcineurin pathway. This pathway is already known to be essential for *C. albicans* survival in presence of the drug [89]. The recruitment of this pathway was also confirmed using genetically related tolerant clinical isolates that were isolated from the same patient over a time lapse of about 9 years. These sequential isolates were known to show an increased tolerance over

time, with the initial DSY4454 isolate considered as having a “wild-type” susceptibility profile and the following DSY4452 and DSY4588 isolates characterized by a clear increased of FLC tolerance. Interestingly, several genes of the calcineurin pathway, including *CRZ1*, were overexpressed in these clinical isolates as compared to the reference strain SC5314, in the presence of FLC. This overexpression could at least partially explain the increased FLC tolerance in these clinical isolates. Indeed, members of the calcineurin pathway were clearly overexpressed in presence of FLC in the two tolerant isolates DSY4452 and DSY4588 in comparison to their parental “wild type” isolate DSY4454 and the SC5314 control strain. The next step will be to investigate the differentially expressed genes between the tolerant clinical isolates and the SC5314 strain. Overexpressing or deleting such genes in the SC5314 susceptible strain (for putative positive mediators) or in tolerant clinical isolates (for putative negative mediators) will confirm their role in the increased tolerance to FLC and give new insights of the mechanisms behind this phenotype. In complement to this transcriptomic approach, genome data mining could be implemented in the future to help deciphering the molecular basis of FLC tolerance in these isolates. Likely candidate genes could be in the calcineurin pathway for examples. In agreement with this hypothesis, a study published by Hill *et al.* reported that the calcineurin subunit A (*CNA1/CMP1*) exhibited a truncation in a *C. albicans* FLC-resistant isolate [93]. *CNA1* truncations were already known to increase FLC tolerance to high levels through hyperactivation of calcineurin [44]. Therefore, it is possible that such mutations could be found in clinical isolates as those used in this study.

To conclude, this study, focusing on FLC tolerance and its mechanisms, allowed a better understanding of *C. albicans* response to FLC. The identification of mediators of FLC tolerance, specific to *C. albicans*, might potentially serve as novel drug targets. By targeting such mediators in co-treatment with FLC, activity of FLC in *C. albicans* may be potentiated, or may convert FLC to a fungicidal drug as already observed with the inhibition of the calcineurin pathway by cyclosporin A [66]. These new treatment strategies may broaden the range of treatment options and help to decrease treatment failures caused by *C. albicans* infections.

Bibliography

- [1] J. Guinea, "Global trends in the distribution of *Candida* species causing candidemia," *Clin. Microbiol. Infect.*, vol. 20, no. 6, pp. 5–10, Jun. 2014.
- [2] B. J. Kullberg and M. C. Arendrup, "Invasive Candidiasis," *N. Engl. J. Med.*, vol. 373, no. 15, pp. 1445–1456, Oct. 2015.
- [3] H. Wisplinghoff *et al.*, "Nosocomial Bloodstream Infections in US Hospitals : Analysis of 24 , 179 Cases from a Prospective Nationwide Surveillance Study," vol. 0019, no. April 2003, pp. 309–317, 2004.
- [4] J. C. O. Sardi, L. Scorzoni, T. Bernardi, A. M. Fusco-Almeida, and M. J. S. Mendes Giannini, "Candida species: Current epidemiology, pathogenicity, biofilm formation, natural antifungal products and new therapeutic options," *Journal of Medical Microbiology*. 2013.
- [5] P. G. Pappas, M. S. Lionakis, M. C. Arendrup, L. Ostrosky-Zeichner, and B. J. Kullberg, "Invasive candidiasis," *Nat. Rev. Dis. Prim.*, vol. 4, no. May, pp. 1–20, 2018.
- [6] A. Jeffery-Smith *et al.*, "Candida auris : a Review of the Literature," *Clin. Microbiol. Rev.*, vol. 31, no. 1, pp. 1–18, Nov. 2017.
- [7] D. S. Thompson, P. L. Carlisle, and D. Kadosh, "Coevolution of morphology and virulence in *Candida* species," *Eukaryotic Cell*, vol. 10, no. 9. pp. 1173–1182, 2011.
- [8] P. Sudbery, N. Gow, and J. Berman, "The distinct morphogenic states of *Candida albicans*," *Trends Microbiol.*, vol. 12, no. 7, pp. 317–324, 2004.
- [9] F. C. Odds, *The ecology of Candida and epidemiology of Candidosis. Candida and Candidosis: a review and bibliography.*, 2nd ed. London, UK: Balliere Tindall, 1988.
- [10] D. M. MacCallum, "Hosting Infection: Experimental Models to Assay *Candida* Virulence," *Int. J. Microbiol.*, vol. 2012, pp. 1–12, 2012.
- [11] J. D. Sobel, "Recurrent vulvovaginal candidiasis," *American Journal of Obstetrics and Gynecology*, vol. 214, no. 1. pp. 15–21, 2016.
- [12] A. J. P. Brown *et al.*, "Stress adaptation in a pathogenic fungus," *J. Exp. Biol.*, vol. 217, no. 1, pp. 144–155, 2013.

- [13] J. Kim and P. Sudbery, "Candida albicans, a major human fungal pathogen.," *J. Microbiol.*, vol. 49, no. 2, pp. 171–177, 2011.
- [14] F. L. Mayer, D. Wilson, and B. Hube, "Candida albicans pathogenicity mechanisms.," *Virulence*, vol. 4, no. 2, pp. 119–28, 2013.
- [15] M. A. Pfaller and D. J. Diekema, "Epidemiology of invasive mycoses in North America.," *Crit. Rev. Microbiol.*, vol. 36, no. 1, pp. 1–53, Feb. 2010.
- [16] S. S. Magill *et al.*, "Multistate Point-Prevalence Survey of Health Care–Associated Infections," *N. Engl. J. Med.*, vol. 370, no. 13, p. 1198, Mar. 2014.
- [17] M. A. Pfaller *et al.*, "Results from the artemis disk global antifungal surveillance study, 1997 to 2007: A 10.5-year analysis of susceptibilities of candida species to fluconazole and voriconazole as determined by CLSI standardized disk diffusion," *J. Clin. Microbiol.*, vol. 48, no. 4, pp. 1366–1377, 2010.
- [18] M. Bondaryk, W. Kurzatkowski, and M. Staniszewska, "Antifungal agents commonly used in the superficial and mucosal candidiasis treatment: Mode of action and resistance development," *Postep. Dermatologii i Alergol.*, vol. 30, no. 5, pp. 293–301, 2013.
- [19] S. Campoy and J. L. L. Adrio, "Antifungals," *Biochem. Pharmacol.*, vol. 133, pp. 86–96, Jun. 2017.
- [20] E. Delarze and D. Sanglard, "Defining the frontiers between antifungal resistance, tolerance and the concept of persistence," *Drug Resist. Updat.*, 2015.
- [21] C. Spampinato, D. Leonardi, S. C., and L. D., "Candida Infections, Causes, Targets, and Resistance Mechanisms: Traditional and Alternative Antifungal Agents," *Biomed Res. Int.*, vol. 2013, pp. 1–13, 2013.
- [22] A. Vermes, "Flucytosine: a review of its pharmacology, clinical indications, pharmacokinetics, toxicity and drug interactions," *J. Antimicrob. Chemother.*, vol. 46, no. 2, pp. 171–179, 2002.
- [23] G. S. Hisao *et al.*, "Amphotericin forms an extramembranous and fungicidal sterol sponge," *Nat. Chem. Biol.*, vol. 10, no. 5, pp. 400–406, 2014.
- [24] D. Sanglard, F. Ischer, T. Parkinson, J. Bille, and D. Falconer, "Candida albicans Mutations in the Ergosterol Biosynthetic Pathway and Resistance to Several Antifungal Agents Candida albicans Mutations in the Ergosterol Biosynthetic Pathway and Resistance to Several Antifungal Agents," *Antimicrob. Agents Chemother.*, vol. 47, no. 8, pp. 2404–2412, 2003.

- [25] M. A. Pfaller, S. A. Messer, P. R. Rhomberg, R. N. Jones, and M. Castanheira, "Activity of a long-acting echinocandin, CD101, determined using CLSI and EUCAST reference methods, against *Candida* and *Aspergillus* spp., including echinocandin- and azole-resistant isolates," *J. Antimicrob. Chemother.*, 2016.
- [26] D. Sanglard, "Emerging Threats in Antifungal-Resistant Fungal Pathogens," *Front. Med.*, vol. 3, no. March, pp. 1–10, Mar. 2016.
- [27] L. E. Cowen, "The evolution of fungal drug resistance: modulating the trajectory from genotype to phenotype," *Nat. Rev. Microbiol.*, vol. 6, no. 3, pp. 187–198, Mar. 2008.
- [28] G. Giusiano, P. A. Ezkurra, and G. Quindós, "MOA yeast review.pdf," *Rev Esp Quimioter.*, vol. 19, no. June, pp. 130–139, 2006.
- [29] S. G. Revankar, M. D. Nailor, and J. D. Sobel, "Use of terbinafine in rare and refractory mycoses," *Future Microbiology*, vol. 3, no. 1, pp. 9–17, 2008.
- [30] T. C. White, K. A. Marr, and R. A. Bowden, "Clinical, cellular, and molecular factors that contribute to antifungal drug resistance.," *Clin. Microbiol. Rev.*, vol. 11, no. 2, pp. 382–402, Apr. 1998.
- [31] M. V. Martin, "The use of fluconazole and itraconazole in the treatment of *Candida albicans* infections: A review," *Journal of Antimicrobial Chemotherapy*. 1999.
- [32] J. Morschhäuser, "The development of fluconazole resistance in *Candida albicans* – an example of microevolution of a fungal pathogen," *Journal of Microbiology*, vol. 54, no. 3, pp. 192–201, 2016.
- [33] D. Sanglard, "Resistance and tolerance mechanisms to antifungal drugs in fungal pathogens," *Mycologist*, vol. 17, 2003.
- [34] V.-S. Luís A., "Molecular Mecganisms of Resistance of *Candida* spp. to Membrane-targeting Antifungals," in *Antifungals - From Genomics to Resistance and the Development of Novel Agents*, A. T. Coste and P. Vandeputte, Eds. Caister Academic Press, Norfolk, UK, 2014, pp. 1–25.
- [35] D. Sanglard, F. Ischer, D. Calabrese, M. de Micheli, and J. Bille, "Multiple resistance mechanisms to azole antifungals in yeast clinical isolates," *Drug Resist. Updat.*, vol. 1, no. 4, pp. 255–265, Jan. 1998.
- [36] R. A. Akins, "An update on antifungal targets and mechanisms of resistance in *Candida albicans*," *Med. Mycol.*, vol. 43, no. 4, pp. 285–318, 2005.
- [37] Clinical and Laboratory Standards Institute, *Reference Method for Broth Dilution Antifungal Susceptibility Testing of Yeasts; Approved Standard—Third Edition*. Wayne, PA, 2008.

- [38] European Committee on Antimicrobial Susceptibility Testing, "EUCAST DEFINITIVE DOCUMENT E.DEF 7.3.1 - Method for the determination of broth dilution minimum inhibitory concentrations of antifungal agents for yeasts," 2017.
- [39] M. A. Pfaller, M. Castanheira, S. A. Messer, P. R. Rhomberg, and R. N. Jones, "Comparison of EUCAST and CLSI broth microdilution methods for the susceptibility testing of 10 Systemically active antifungal agents when tested against *Candida* spp.," *Diagn. Microbiol. Infect. Dis.*, 2014.
- [40] O. Fridman, A. Goldberg, I. Ronin, N. Shores, and N. Q. Balaban, "Optimization of lag time underlies antibiotic tolerance in evolved bacterial populations," *Nature*, vol. 513, no. 7518, pp. 418–421, Sep. 2014.
- [41] K. Lewis, "Persister cells, dormancy and infectious disease," *Nat. Rev. Microbiol.*, vol. 5, no. 1, pp. 48–56, 2007.
- [42] K. A. Marr *et al.*, "The Trailing End Point Phenotype in Antifungal Susceptibility Testing Is pH Dependent," *Antimicrob. Agents Chemother.*, vol. 43, no. 6, pp. 1383–1386, Jun. 1999.
- [43] B. Micota *et al.*, "Saponins of *Trifolium* spp. Aerial Parts as Modulators of *Candida Albicans* Virulence Attributes," *Molecules*, vol. 19, no. 7, pp. 10601–10617, 2014.
- [44] D. Sanglard, F. Ischer, O. Marchetti, J. Entenza, and J. Bille, "Calcineurin A of *Candida albicans*: Involvement in antifungal tolerance, cell morphogenesis and virulence," *Mol. Microbiol.*, vol. 48, no. 4, pp. 959–976, 2003.
- [45] L. E. Cowen, "The fungal Achilles' heel: targeting Hsp90 to cripple fungal pathogens.," *Curr. Opin. Microbiol.*, vol. 16, no. 4, pp. 377–84, Aug. 2013.
- [46] A. Luna-Tapia, M. E. Kerns, K. E. Eberle, B. S. Jursic, and G. E. Palmer, "Trafficking through the Late Endosome Significantly Impacts *Candida albicans* Tolerance of the Azole Antifungals," *Antimicrob. Agents Chemother.*, vol. 59, no. 4, pp. 2410–2420, Apr. 2015.
- [47] S. G. Whaley *et al.*, "The RTA3 Gene, Encoding a Putative Lipid Translocase, Influences the Susceptibility of *Candida albicans* to Fluconazole," *Antimicrob. Agents Chemother.*, vol. 60, no. 10, pp. 6060–6066, Oct. 2016.
- [48] J. Gao *et al.*, "*Candida albicans* gains azole resistance by altering sphingolipid composition," *Nat. Commun.*, vol. 9, no. 1, pp. 1–14, Dec. 2018.

- [49] C. Garnaud *et al.*, "The Rim Pathway Mediates Antifungal Tolerance in *Candida albicans* through Newly Identified Rim101 Transcriptional Targets, Including Hsp90 and Ipt1," *Antimicrob. Agents Chemother.*, vol. 62, no. 3, Jan. 2018.
- [50] A. C. Gerstein, A. Rosenberg, I. Hecht, and J. Berman, "DiskimageR: Quantification of resistance and tolerance to antimicrobial drugs using disk diffusion assays," *Microbiol. (United Kingdom)*, vol. 162, no. 7, pp. 1059–1068, 2016.
- [51] A. Rosenberg *et al.*, "Antifungal tolerance is a subpopulation effect distinct from resistance and is associated with persistent candidemia," *Nat. Commun.*, vol. 9, no. 1, 2018.
- [52] W. A. A. Fonzi and M. Y. Y. Irwin, "Isogenic strain construction and gene mapping in *Candida albicans*," *Genetics*, vol. 134, no. 3, pp. 717–28, Jul. 1993.
- [53] K. M. T. T. Astvad *et al.*, "Update from a 12-Year Nationwide Fungemia Surveillance: Increasing Intrinsic and Acquired Resistance Causes Concern," *J. Clin. Microbiol.*, vol. 56, no. 4, pp. 1–15, Dec. 2017.
- [54] S. Matuszewski, M. E. Hildebrandt, A. H. Ghenu, J. D. Jensen, and C. Bank, "A statistical guide to the design of deep mutational scanning experiments," *Genetics*, vol. 204, no. 1, pp. 77–87, 2016.
- [55] C. Rueda *et al.*, "Evaluation of the possible influence of trailing and paradoxical effects on the clinical outcome of patients with candidemia," *Clin. Microbiol. Infect.*, vol. 23, no. 1, p. 49.e1-49.e8, Jan. 2017.
- [56] M. Chauvel *et al.*, "A Versatile Overexpression Strategy in the Pathogenic Yeast *Candida albicans*: Identification of Regulators of Morphogenesis and Fitness," *PLoS One*, 2012.
- [57] O. R. Homann, J. Dea, S. M. Noble, and A. D. Johnson, "A phenotypic profile of the *Candida albicans* regulatory network," *PLoS Genet.*, vol. 5, no. 12, 2009.
- [58] R. B. Wilson, D. Davis, and A. P. Mitchell, "Rapid hypothesis testing with *Candida albicans* through gene disruption with short homology regions," *J. Bacteriol.*, vol. 181, no. 6, pp. 1868–74, Mar. 1999.
- [59] S. M. Noble and A. D. Johnson, "Strains and Strategies for Large-Scale Gene Deletion Studies of the Diploid Human Fungal Pathogen *Candida albicans*," *Eukaryot. Cell*, vol. 4, no. 2, pp. 298–309, 2005.
- [60] A. Firon *et al.*, "The SUN41 and SUN42 genes are essential for cell separation in *Candida albicans*," *Mol. Microbiol.*, vol. 66, no. 5, pp. 1256–1275, 2007.
- [61] A. Fiori and P. Van Dijck, "Potent synergistic effect of doxycycline with fluconazole against *Candida albicans* is mediated by interference with iron homeostasis," *Antimicrob. Agents Chemother.*, vol. 56,

- no. 7, pp. 3785–96, Jul. 2012.
- [62] D. Sanglard, F. Ischer, M. Monod, and J. Bille, “Susceptibilities of *Candida albicans* multidrug transporter mutants to various antifungal agents and other metabolic inhibitors,” *Antimicrob. Agents Chemother.*, vol. 40, no. 10, pp. 2300–5, Oct. 1996.
 - [63] O. Reuss, A. Vik, R. Kolter, and J. Morschhäuser, “The SAT1 flipper, an optimized tool for gene disruption in *Candida albicans*,” *Gene*, vol. 341, no. 1–2, pp. 119–27, Oct. 2004.
 - [64] M. Wellington and E. Rustchenko, “5-Fluoro-orotic acid induces chromosome alterations in *Candida albicans*,” *Yeast*, vol. 22, no. 1, pp. 57–70, 2005.
 - [65] S. Znaidi *et al.*, “Systematic gene overexpression in *Candida albicans* identifies a regulator of early adaptation to the mammalian gut,” *Cell. Microbiol.*, vol. 20, no. 11, pp. 1–21, 2018.
 - [66] M. Karababa, E. Valentino, G. Pardini, A. T. Coste, J. Bille, and D. Sanglard, “CRZ1, a target of the calcineurin pathway in *Candida albicans*,” *Mol. Microbiol.*, vol. 59, no. 5, pp. 1429–1451, Mar. 2006.
 - [67] C. Onyewu, F. L. Wormley, J. R. Perfect, and J. Heitman, “The calcineurin target, Crz1, functions in azole tolerance but is not required for virulence of *Candida albicans*,” *Infect. Immun.*, vol. 72, no. 12, pp. 7330–7333, Dec. 2004.
 - [68] S. S. Soussi-Boudekou, S. Vissers, A. Urrestarazu, J.-C. C. Jauniaux, B. André, and B. Andre, “Gzf3P, a fourth GATA factor involved in nitrogen-regulated transcription in *Saccharomyces cerevisiae*,” *Mol. Microbiol.*, vol. 23, no. 6, pp. 1157–1168, Mar. 1997.
 - [69] Y. Wang *et al.*, “Cap1p is involved in multiple pathways of oxidative stress response in *Candida albicans*,” *Free Radic. Biol. Med.*, vol. 40, no. 7, pp. 1201–1209, Apr. 2006.
 - [70] S. M. Noble, S. French, L. A. Kohn, V. Chen, and A. D. Johnson, “Systematic screens of a *Candida albicans* homozygous deletion library decouple morphogenetic switching and pathogenicity,” *Nat. Genet.*, vol. 42, no. 7, pp. 590–598, Jul. 2010.
 - [71] A. Decottignies, G. Owsianik, and M. Ghislain, “Casein Kinase I-dependent Phosphorylation and Stability of the Yeast Multidrug Transporter Pdr5p,” *J. Biol. Chem.*, vol. 274, no. 52, pp. 37139–37146, Dec. 1999.
 - [72] K. M. T. Astvad, D. Sanglard, E. Delarze, R. K. Hare, and M. C. Arendrup, “Implications of the EUCAST trailing phenomenon in *Candida tropicalis* for the in vivo susceptibility in invertebrate and murine models,” *Antimicrob. Agents Chemother.*, vol. 62, no. 12, 2018.

- [73] T. R. Hughes *et al.*, "Functional Discovery via a Compendium of Expression Profiles," *Cell*, vol. 102, no. 1, pp. 109–126, Jul. 2000.
- [74] T. T. Liu *et al.*, "Genome-Wide Expression Profiling of the Response to Azole, Polyene, Echinocandin, and Pyrimidine Antifungal Agents in *Candida albicans*," *Antimicrob. Agents Chemother.*, vol. 49, no. 6, pp. 2226–2236, Jun. 2005.
- [75] R. E. B. Lee, T. T. Liu, K. S. Barker, R. E. Lee, and P. D. Rogers, "Genome-wide expression profiling of the response to ciclopirox olamine in *Candida albicans*," *J. Antimicrob. Chemother.*, vol. 55, no. 5, pp. 655–662, May 2005.
- [76] M. Niewerth, D. Kunze, M. Seibold, M. Schaller, H. C. C. Korting, and B. Hube, "Ciclopirox olamine treatment affects the expression pattern of *Candida albicans* genes encoding virulence factors, iron metabolism proteins, and drug resistance factors," *Antimicrob. Agents Chemother.*, vol. 47, no. 6, pp. 1805–1817, 2003.
- [77] J. Morschhäuser, K. S. Barker, T. T. Liu, J. Blaß-Warmuth, R. Homayouni, and P. D. Rogers, "The transcription factor Mrr1p controls expression of the MDR1 efflux pump and mediates multidrug resistance in *Candida albicans*," *PLoS Pathog.*, vol. 3, no. 11, pp. 1603–1616, 2007.
- [78] M. Martin, "Cutadapt removes adapter sequences from high-throughput sequencing reads," *EMBnet.journal*, vol. 17, no. 1, p. 10, May 2011.
- [79] K. S. Barker *et al.*, "Genome-wide expression profiling reveals genes associated with amphotericin B and fluconazole resistance in experimentally induced antifungal resistant isolates of *Candida albicans*," *J. Antimicrob. Chemother.*, vol. 54, no. 2, pp. 376–385, 2004.
- [80] B. D. Harrison *et al.*, "A Tetraploid Intermediate Precedes Aneuploid Formation in Yeasts Exposed to Fluconazole," *PLoS Biol.*, vol. 12, no. 3, p. e1001815, Mar. 2014.
- [81] E. M. Vasicek *et al.*, "Disruption of the transcriptional regulator Cas5 results in enhanced killing of *Candida albicans* by fluconazole," *Antimicrob. Agents Chemother.*, vol. 58, no. 11, pp. 6807–6818, 2014.
- [82] P. Keller *et al.*, "An Antifungal Benzimidazole Derivative Inhibits Ergosterol Biosynthesis and Reveals Novel Sterols," *Antimicrob. Agents Chemother.*, vol. 59, no. 10, pp. 6296–6307, Oct. 2015.
- [83] J. M. Synnott, A. Guida, S. Mulhern-Haughey, D. G. Higgins, and G. Butler, "Regulation of the hypoxic response in *Candida albicans*," *Eukaryot. Cell*, vol. 9, no. 11, pp. 1734–1746, 2010.

- [84] K. C. Ha and T. C. White, "Effects of azole antifungal drugs on the transition from yeast cells to hyphae in susceptible and resistant isolates of the pathogenic yeast *Candida albicans*," *Antimicrob. Agents Chemother.*, vol. 43, no. 4, pp. 763–768, 1999.
- [85] N. A. R. Gow *et al.*, "Collaborative Consensus for Optimized Multilocus Sequence Typing of *Candida albicans*," *J. Clin. Microbiol.*, vol. 41, no. 11, pp. 5265–5266, 2003.
- [86] N. Dunkel, J. Blaß, P. D. Rogers, and J. Morschhäuser, "Mutations in the multi-drug resistance regulator MRR1, followed by loss of heterozygosity, are the main cause of MDR1 overexpression in fluconazole-resistant *Candida albicans* strains," *Mol. Microbiol.*, vol. 69, no. 4, pp. 827–840, 2008.
- [87] C. J. Nobile *et al.*, "A recently evolved transcriptional network controls biofilm development in *Candida albicans*," *Cell*, vol. 148, no. 1–2, pp. 126–138, 2012.
- [88] E. Paramonova, B. P. Krom, H. C. van der Mei, H. J. Busscher, and P. K. Sharma, "Hyphal content determines the compression strength of *Candida albicans* biofilms," *Microbiology*, vol. 155, no. 6, pp. 1997–2003, Jun. 2009.
- [89] A. T. Coste, M. Karababa, J. Bille, and D. Sanglard, "TAC1 , Transcriptional Activator of CDR Genes , Is a New Transcription Factor Involved in the Regulation of *Candida albicans* ABC Transporters," *Eukaryot. Cell*, vol. 3, no. 6, pp. 1639–1652, 2004.
- [90] S. Schubert *et al.*, "Regulation of efflux pump expression and drug resistance by the transcription factors Mrr1, Upc2, and Cap1 in *Candida albicans*," *Antimicrob. Agents Chemother.*, vol. 55, no. 5, pp. 2212–2223, 2011.
- [91] M. Karababa, A. T. Coste, B. Rognon, J. Bille, and D. Sanglard, "Comparison of Gene Expression Profiles of *Candida albicans* Azole-Resistant Clinical Isolates and Laboratory Strains Exposed to Drugs Inducing Multidrug Transporters," *Antimicrob. Agents Chemother.*, vol. 48, no. 8, pp. 3064–3079, Aug. 2004.
- [92] A. Rosenberg *et al.*, "Clearing the Fungal FoG: Perseverance, a property distinct from resistance, is associated with clinical persistence," *BioRxiv Prepr.*, 2017.
- [93] J. A. Hill, T. R. O'Meara, and L. E. Cowen, "Fitness trade-offs associated with the evolution of resistance to antifungal drug combinations," *Cell Rep.*, vol. 10, no. 5, pp. 809–819, 2015.